Modeling of Hydrogen Consumption and Process Optimization for Hydrotreating of Light Gas Oils

A Thesis Submitted to the College of
Graduate and Postdoctoral Studies
in Partial Fulfilment of the Requirements
for the Degree of Master of Science
in the Department of Chemical and Biological Engineering
University of Saskatchewan
Saskatoon

By

Adrian A. Rodriguez Pinos

PERMISSION TO USE

It is my consent that the libraries of the University of Saskatchewan may make this thesis freely available for inspection. Besides, I agree that permission for copying of this thesis in any manner, either in whole or in part, for scholarly purposes be granted primarily by the professor(s) who supervised this thesis work or in their absence by the Head of the Department of Chemical Engineering or the Dean of the College of Graduate Studies. Duplication or publication or any use of this thesis, in part or in whole, for financial gain without prior written approval by the University of Saskatchewan is prohibited. It is also understood that due recognition shall be given the author of this thesis and to the University of Saskatchewan in any use of the material therein.

Request for permission to copy or to make any other use of the material in this thesis in whole or in part should be addressed to:

Head of the Department of Chemical and Biological Engineering
57 Campus Drive
University of Saskatchewan
Saskatoon, Saskatchewan, Canada
S7N 5A9

ABSTRACT

The main objective of this work was to develop a regression model for hydrogen consumption during hydrotreating of several gas oils such as virgin light gas oil (VLGO), hydrocracker light gas oil (HLGO), coker light gas oil (KLGO), and a partially hydrotreated heavy gas oil (PHTHGO) stream over commercial NiMo/ɣ-Al_2O_3 in a micro-trickle bed reactor. The experiments covered a temperature range of 353-387 °C, pressure range of 8.27-10.12 MPa, LHSV range of 0.7-2.3 h^{-1}, and H_2/oil ratio = 600 N m^3/m^3. H_2 consumption can be determined by different approaches; therefore, the best approach was selected by comparing the following: analysis of H_2 content in gas streams, analysis of H_2 content in liquid streams, and an approach reported in literature that is based on the decrease of the aromatics content. The comparison showed better agreement between the analysis of H_2 content in gas streams and the method reported in the literature. For this reason, the analysis of gas streams was selected to build a regression model by performing statistical analysis of the effects of process conditions on H_2 consumption data at the conditions mentioned above. H_2 consumption based on gas analysis decreased in the following order: KLGO>VLGO>HLGO>PHTHGO. The H_2 consumption regression model developed in this work was then tested with a new batch of experimental data, and the model performed better than similar correlations available in the literature.

The secondary objective of this work was to study the effects of process conditions indicated above on hydrodesulfurization (HDS), hydrodenitrogenation (HDN), and hydrodearomatization (HDA) conversions by statistical analysis. The experimental data of hydrotreating conversions were then used to build regression models and carry out the optimization of process conditions for each feedstock. The optimum sets of conditions for the hydrotreating of each feedstock are the following: VLGO (T = 353 °C, P = 9.37 MPa, LHSV = 0.9 h^{-1}), HLGO (T = 383 °C, P = 10.12 MPa, LHSV = 0.9 h^{-1}), KLGO (T = 372 °C, P = 7.79 MPa, LHSV = 0.7 h^{-1}), PHTHGO (T = 379 °C, P = 9.44 MPa, LHSV = 0.7 h^{-1}). In summary, the optimum hydrogen consumption as well as hydroprocessing conditions for all the four different feedstocks are substantially different. This information is critical in operating a commercial hydrotreater efficiently.

ACKNOWLEDGEMENT

I would like to thank my supervisors Dr. A.K. Dalai and Dr. John Adjaye for their valuable input and guidance to take the project forward. Also, I appreciate the time and help provided by my advisory committee members: Dr. Catherine Niu and Dr. Hui Wang.

I am greatly thankful to all the members of the Catalysis and Chemical Reaction Engineering Laboratory (CCREL) at the University of Saskatchewan for always being open to cooperate and assist with any inquiry related to this research project.

Last but not least, I would like to appreciate the support provided by the technical and laboratory staff of the Department of Chemical and Biological Engineering.

DEDICATION

This thesis is dedicated to my parents,
Rosa Elena and Fernando, and my brother Luis
for their support and motivation
throughout the realization of this project.

TABLE OF CONTENTS

LIST OF TABLES

LIST OF FIGURES

NOMENCLATURE AND ABBREVIATIONS

Nomenclature

Adj R^2	Modification of R^2 based on significant factors only
°API	American Petroleum Insitute gravity
C_{Ar}	Aromatics content (wt %)
cP	Centipoise
Cx	Concentration of x species (ppm)
G_1	Inlet gas stream flowrate (m^3/h)
G_2	Outlet gas stream flowrate (m^3/h)
G/O	Gas to oil ratio (Nm^3 H_2/m^3 oil)
H/C	Hydrogen to carbon ratio
H_{2G_1}	Concentration of hydrogen in gas inlet stream (mol %)
H_{2G_2}	Concentration of hydrogen in gas outlet stream (mol %)
H_{2L_1}	Concentration of hydrogen in liquid feedstocks (mol %)
H_{2L_2}	Concentration of hydrogen in liquid products (mol %)
H_2pp	Hydrogen partial pressure (MPa)
L_1	Inlet liquid stream flowrate (m^3/h)
L_2	Outlet liquid stream flowrate (m^3/h)
LHSV	Liquid hourly space velocity (h^{-1})
N	Normal laboratory conditions (P=101.35 kPa and T=20°C)
P	Pressure (MPa)
R^2	Statistical measure that represents the goodness fit of a model
T	Temperature (°C)
V	Volumetric flow (m^3/h)

Abbreviations

CCD	Central composite design
HDA	Hydrodearomatization
HDN	Hydrodenitrogenation
HDS	Hydrodesulfurization
HLGO	Hydrocracker light gas oil
KLGO	Coker light gas oil
LGOs	Light gas oils
PHTHGO	Partially hydrotreated heavy gas oil
VLE	Vapor-liquid equilibrium
VLGO	Virgin light gas oil

1 INTRODUCTION

The use of bitumen-derived gas oils is indispensable because of the increasing demand for oil and the limited availability of conventional oil sources. Conventional oil sources are expected to decrease to 60 % in 2040 as compared to 80 % in 2010 (World Energy Outlook, 2011). Hydrotreating is one of the essential processes to upgrade bitumen derived gas oils by lowering sulfur, nitrogen and aromatic contents. An oil market forecast performed in the year 2010 predicted that by 2013, hydrotreating units would produce 49.24 million bbl oil/day out of 90.8 million bbl oil/day produced worldwide (Silvy, 2010). The production capacity of this process implies its significant contribution to the global hydrogen mass balance of refineries

During primary upgrading of bitumen, light gas oils (LGOs) can be obtained from various processing units. Virgin light gas oil (VLGO) is obtained from the atmospheric distillation of bitumen dissolved in naphtha, vacuum distillation of the atmospheric distillation unit residue produces vacuum LGO (LVGO). Coker LGO (KLGO) and hydrocracker LGO (HLGO) are obtained from the conversion of vacuum residue in coking and hydrocracking units, respectively (Jones & Pujado, 2006). Because of the varying composition and properties of hydrotreating feedstocks, special attention has to be paid to study the variability in H_2 consumption during the processing of each feed for technical and economical purposes.

1.1 Background of the project

Hydrogen is one of the most important elements in refinery operations due to its high demand and price. Gas oil hydrotreaters use hydrogen in excess to prevent the formation of coke and provide an optimal liquid-solid contact (Ancheyta & Speight, 2007).These units consume about 50.7-135 N m^3 H_2/m^3 oil (Ramachandran & Menon, 1998). The outlet gas stream from hydrotreaters is composed of H_2S, NH_3, C_1-C_6, and H_2 with a concentration of 78-85 mol. % (Peramanu et al., 1999). In the industry, this stream is purified to recover the excess of H_2 and

then it is recycled and mixed with pure H_2 to achieve the required hydrogen partial pressure (H_2pp) in the hydrotreater and make up for the hydrogen consumed in the different hydrotreating reactions.

Hydrogen consumption is dependent on feedstock properties. Feedstocks with lower hydrogen-carbon ratio (H/C) such as KLGO (H/C = 0.13) in comparison with VLGO (H/C = 0.15), will demand more hydrogen to improve the degree of unsaturation (Yui, 2008). Similarly, higher amounts of sulfur and nitrogen impurities will also translate into more H_2 demand. The total H_2 consumption in the industry not only involves the amount of H_2 consumed in hydrotreating reactions, but also considers mechanical losses due to the use of compressors, venting losses during gas purging, and solution losses (dissolved H_2) in the final product (Hisamitsu et al., 1976). In the case of experimental studies, dissolved H_2 and chemical H_2 consumption should be considered; dissolved H_2 may affect total H_2 consumption by a factor of 6 % (Castañeda et al., 2011). Dissolved H_2 in hydrotreated products can be calculated in HYSYS software by performing VLE (vapor-liquid equilibrium) simulations (Mapiour et al., 2010).

Two important issues may arise to determine H_2 consumption in hydrotreating processes. First, developing hydrogen mass balances and the use of methods to determine chemical H_2 consumption based on reaction stoichiometry require the use of different analytical techniques such as gas chromatography (GC), GC coupled to mass spectroscopy, elemental analysis (measures C, H, N, and S content) and ^{13}C nuclear magnetic resonance (Castañeda et al., 2011). Second, values and models available in literature have limited application. For instance, Castañeda et al. (2011) found out that Edgar's approach (Edgar, 1993) presented an error higher than 50 % for the determination of H_2 consumption during hydrotreating of naphtha and gas oils. Jones & Pujado (2006), reported values of 17-25 and 34-59 N m^3 H_2/m^3 oil for each wt. % change in sulfur or nitrogen content, respectively. Meanwhile, Gary et al. (2007), reported values of 12.5 and 57 N m^3 H_2/m^3 oil for each wt. % change in sulfur or nitrogen content, respectively.

1.2 Knowledge gaps

The amount of hydrogen consumption during hydrotreating is important for refineries to determine and calculate the overall hydrogen mass balance. Problems may arise when these hydroprocessing units process feedstocks with varying composition and properties, which may

require different amounts of hydrogen. The overestimation of hydrogen may cause economic losses, and underestimating the amount of this reactant may cause operational problems and possible shutdown of the unit. It is well known that modern refineries treat numerous feedstocks including fractions from residues to maximize the output from crude petroleum feedstock. Therefore, the knowledge to determine hydrogen consumption for different feedstocks in essential.

There are several models in the literature to determine H_2 consumption during hydrotreating; however, these models may present disadvantages such as the following: the models are feed dependent and therefore cannot be used for all petroleum fractions, models developed based on reaction stoichiometry require detailed characterization of feedstocks and products, and these models omit dissolved H_2. In addition, the values of H_2 consumption from these models are too general for specific application. Based on these arguments, there is the need to carry a comparative study for hydrogen consumption between common hydrotreating feedstocks considering two main purposes: (i) provide scientific explanation on the behavior of each feedstock towards hydrogen consumption at industrial operating conditions during hydrotreating, and (ii) develop simple models to calculate H_2 consumption based on processing conditions.

1.3 Hypotheses

- Hydrogen consumption is dependent on process parameters; thus, statistical models based on process conditions can provide an accurate and simple prediction of this dependent variable.
- Each feedstock has a different set of optimum conditions of temperature, pressure, and LHSV to maximize HDS (hydrodesulfurization), HDN (hydrodenitrogenation), and HDA (hydrodearomatization) conversions, which can provide data for the development of statistical models to predict HDS, HDN and HDA for these gas oils.

1.4 Objectives

The main objective of this work was to develop a H_2 consumption regression model applicable to the hydrotreating of light gas oils such as KLGO from coking, HLGO from hydrocracking, VLGO from atmospheric distillation, and PHTHGO from a hydrotreating unit

based on temperature, pressure, and LHSV. The developed model was compared with other models and data available in the literature.

The second objective of this work was to study the effects of process conditions on hydrotreating conversions for the light gas oils mentioned above and find the best sets of conditions to process each feedstock.

Based on these two objectives, this work was divided into two phases.

1.4.1 Phase I - Development of hydrogen consumption regression models for hydrotreating of gas oils

Hydrogen consumption was measured by liquid and gas stream analysis and the best method was selected to build regression models based on process conditions. The experiments were designed by central composite design (CCD). Based on the data for each experimental run and feedstock, a composite regression model of H_2 consumption was built and then the model was tested with a new batch of experimental data. The response of model was compared with other models and data available in the literature.The models available in the literature calculate chemical H_2 consumption only; therefore, dissolved H_2 was added to the chemical H_2 consumption. Dissolved H_2 was calculated in HYSYS software by performing VLE (vapor-liquid equilibria) calculations. Data of H_2pp and feed vaporization can also be obtained from the simulation; therefore, this work also studied the effects of process conditions on H_2 inlet pp, H_2 outlet pp, and feed vaporization.

1.4.2 Phase II – Development of the statistical models for HDS, HDN, and HDA conversions based on the process parameters and perform the optimization of process conditions during hydrotreating of gas oils

Hydrotreating conversions were determined for the experiments given by the CCD to examine the single and combined effects of process conditions on HDS, HDN, and HDA. Consequently, the conversion data were analyzed statistically to develop regression models and optimize process conditions for each feedstock.

1.5 Organization of the thesis

In addition to the Introduction chapter, this thesis contains the following chapters. Chapter 2 explains the concepts and principles of the processing route to convert bitumen into hydrotreated oil and the challenges to determine H_2 consumption during hydrotreating. Chapter 3 describes the materials and experimental methods which were used to carry out each of the phases proposed in this thesis. Chapter 4 presents a comprehensive and detailed discussion of the results obtained in this research work. Chapter 5 provides a summary of the main findings of this research as well as conclusions and recommendations for the future work.

2 LITERATURE REVIEW

This chapter describes the principles and concepts for extracting hydrotreated oil from bitumen. Major emphasis was placed on describing the methods to determine H_2 consumption in hydrotreating and the challenges associated with the usage of the various models and data available in the literature. Also, this chapter describes the process optimization studies of various gas oils for HDS, HDN, and HDA.

2.1 Bitumen recovery

The components of oils sands are bitumen (organic components), quartz/clay particles, and water. Oil sands are produced by surface mining when the reservoirs are located at maximum of 75 m of depth. Then, bitumen is recovered by treating oil sands with alkaline hot water. When the reservoirs of oil sands are situated below 75 m, bitumen is recovered by in-situ methods such as steam assisted gravity drainage (SAGD) and cyclic steam simulation (CCS) (Banerkke, 2012). Bitumen has a viscosity greater than 10,000 cP and API gravity less than 10 in comparison with other unconventional oils (1,000-10,000 cP and < 10 °API) and conventional oil sources (1-1,000 cP and 10-20 °API) (Banerkke, 2012). The typical composition of bitumen in the Canadian Athabasca deposits is presented in Table 2.1.

Table 2.1 Typical composition of Athabasca bitumen (Banerkke, 2012)

Carbon	82-83 wt. %
Hydrogen	10.1-10.2 wt. %
Nitrogen	3,000-5,000 ppm
Sulfur	4.5-6.0 wt. %
Oxygen	< 1.0 wt. %
Vanadium	180-250 ppm
Nickel	60-90 ppm

2.2 Bitumen upgrading

2.2.1 Atmospheric distillation

Bitumen dissolved in naphtha is distilled in a pressure range of 5-10 psig to obtain the products shown in Table 2.2 (Jones & Pujado, 2006). The residue can be processed either by vacuum distillation or thermal cracking.

Table 2.2 Atmospheric distillation cuts (Jones & Pujado, 2006)

Products	Temperature range (°C)
Naphtha	35-193.3
Kerosene	193.3-248.9
VLGO	248.9- 321.1
Virgin heavy gas oil (VHGO)	321.1- 365.6
Residue (Fuel oil)	> 365.6

2.2.2 Vacuum distillation

The residue of the atmospheric distillation unit is processed by vacuum distillation at approximately 1.3 kPa to obtain light vacuum gas oil (LVGO), heavy vacuum gas oil (HVGO), and topped bitumen as shown in Table 2.3. Vacuum is used to prevent cracking of the feed (Jones & Pujado, 2006).

Table 2.3 Vacuum distillation cuts (Jones & Pujado, 2006)

Products	Temperature range (°C)
LVGO	365.6- 398.9
HVGO	398.9 -529.4
Topped bitumen	>529.4

2.2.3 Hydrocracking

Hydrocracking is a high pressure (13.79 MPa) catalytic process used for cracking long chain hydrocarbons in the presence of hydrogen. It also performs HDA, HDS, HDN and HDM (hydrodemetallization) function to prevent the poisoning of the cracking catalyst. Hydrocracking can process several feeds such as vacuum gas oils, straight run gas oils, thermally cracked gas oils, and vacuum distillation bottoms. (Ancheyta & Speight, 2007). Usually, the products from hydrocracking do not require further upgrading. Hydrocrackers consume approximately 200–420 N m^3 H_2/m^3 oil (Jones & Pujado, 2006).

LC-fining is a type of hydrocracking process that has HDS (60-90 %), and HDM (50-98 %) function. This process features an expanded catalyst bed which is in constant movement due to the up-flow of oil stream. Moreover, the catalyst is added and removed from the reactor after certain periods of time allowing the process to run continuously. The main advantages of this process are the following: low operating and investment costs, greater recovery of light fractions, and high yield of liquid products. The operating conditions of the process are the following: T = 385-450 °C, and P = 7.0-18.9 MPa. Moreover, the LC-fining process consumes about 240.4 N m^3 H_2/m^3 oil (Rana et al., 2007).

2.2.4 Coking

Coking uses only heat to crack heavy oil fractions or residues and convert them into lighter products such as naphtha, coker light gas oil (KLGO), and coker heavy gas oil gas oils (KHGO). There are two major coking processes: delayed coking and fluid coking. In the delayed coking process, the feed is preheated in a heat exchanger. Then, the furnace heats the feed which is retained in a coil for a determined period of time (up to 24 h) to temperatures higher than its cracking temperature (493 °C). The product that leaves the furnace is then directed to several coker drums in which the coking temperature is maintained. Then, the cracked oil is separated from the coke by cooling it down below the cracking temperature. Finally, the oil is sent to a fractionator (Jones & Pujado, 2006).

In the case of fluid coking, the feed is cracked using the heat generated by a coke bed fluidized by steam. The advantages of fluid coking over delayed coking are a higher yield of products and less consumption of energy and utilities; however, the products are of low quality. An important type of fluid coking process in the industry is Flexicoking. The latter uses a gasifier

to convert some fraction of the coke into syngas; however, the coke cannot be converted completely into oil fractions even at temperatures as high as 1000°C (Jones & Pujado, 2006; Rana et al., 2007). Since coking processes operate at high temperatures, the paraffins and cyclic paraffins that are usually found in crude oil are transformed into olefins due to unsaturation (Rana et al., 2007). Moreover, the products from coking contain a high percentage of aromatic compounds (Aoyagi et al., 2003).

2.3 Hydrotreating

Petroleum fractions obtained from unconventional oil sources contain high amounts of impurities such as sulfur, nitrogen, oxygen and in some cases metalloporphyrins. In addition, large amounts of aromatic compounds are present in gas oils. The reaction between oil and hydrogen takes place in a catalyst bed at high temperatures and pressures in a process called hydrotreating. Hydrotreating is capable of reducing sulfur, nitrogen, and aromatic contents to comply with environmental regulations and improve the quality of the final product (Papayannakos & Georgiou, 1988). Hydrotreating is dependent on the feed properties, the catalyst type and the operating conditions of the process (Ancheyta et al., 2005).

Hydrotreating is performed in a continuous trickle bed reactor operating close to a plug-flow in which the reactants (gas oil and hydrogen) are introduced from the top of the reactor. The reactants come in contact with the catalyst bed and HDS, HDN and HDA reactions take place.The gas and liquid products pass through a water scrubber to remove ammonia before going to a high-pressure separator. The liquid is collected and fractioned to obtain the final products; meanwhile, the gas stream proceeds to a series of units for purification (Gary et al., 2007).

The non-condensable gases are composed of 78-83 mol. % H_2, C_1-C_5, NH_3 and H_2S; the light ends (C_1-C_5) are produced due to cracking of the feed (< 20 vol. % of the feedstock) (Jones & Pujado, 2006). This stream is then taken to a sour water plant unit (amine contactor) to separate H_2S with the purpose of enhancing H_2 purity and preventing the release of H_2S to the environment. Following this step, 10-15 % of the gas stream is purged to the fuel gas system or to a H_2 purification process and the rest of the gas stream rich in H_2 (80-85 mol. % H_2) is compressed and mixed with make-up H_2 (96-99.9 mol. % H_2) (Peramanu et al., 1999; Jones & Pujado, 2006). Figure 2.1 shows the cycle of H_2 in the industry after hydrotreating.

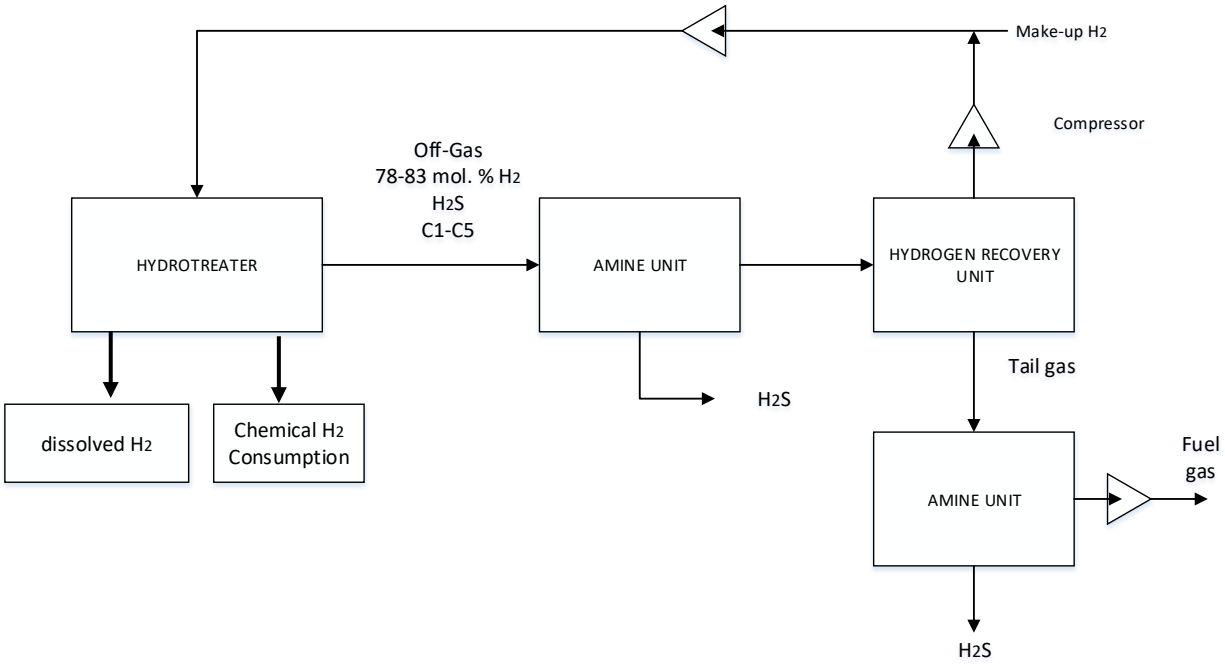

Figure 2.1 H_2 cycle during hydrotreating (Peramanu et al., 1999)

2.4 Hydrotreating process variables

The main independent process variables of hydrotreating are liquid hourly space velocity (LHSV), temperature, H_2 partial pressure and H_2/oil ratio. Table 2.4 provides a summary of the operating conditions used for hydrotreating of different petroleum fractions.

2.4.1 Liquid hourly space velocity

This variable is defined as the ratio between the volumetric flow rate of the feedstock and the volume of the catalyst used for the operation. Lower LHSV implies an increase in the residence time of the gas oil in the catalyst bed and it generally improves hydrotreating activities. LHSV can be set to maintain optimal conversion levels at high temperatures. However; the temperature cannot be increased to the point at which coke is formed. This will result in catalyst deactivation and consequently, the catalyst life will be reduced (Ancheyta & Speight, 2007).

2.4.2 H_2 partial pressure

Hydrogen partial pressure is the product of process pressure and H_2 purity. High H_2pp enhances the performance of the hydrotreating process by increasing the catalyst life and the throughput capability. Also, it allows the process to handle heavier feeds, increase the quality of the distillate, and promotes the elimination of the purged gas (Jones & Pujado, 2006). More details about H_2 partial pressure will be mentioned in the vapor-liquid equilibrium section.

2.4.3 Temperature

High temperature increases the removal of impurities; however, a temperature higher than 410°C promotes thermal cracking of the feed and produces hydrocarbons of low molecular weight. Moreover, high temperatures also deactivate the catalyst by coke formation (Ancheyta & Speight, 2007).

2.4.4 H_2/oil ratio

Hydrogen is used in excess (4 times more than the chemical H_2 consumption) to maintain an adequate contact between the feed and the catalyst which promotes the conversion of the reactants, removal of impurities and at the same time reduces the possibility of coke formation (Ancheyta & Speight, 2007). To optimize the use of H_2 which is costly, the use of recycled gas with addition of high purity H_2 is essential to maintain the hydrogen partial pressure. Hydrotreating units consume around 50.7-135 N m^3 H_2/m^3 oil (Ramachandran & Menon, 1998).

Table 2.4 Summary of operating conditions on hydrotreating of oil fractions

Study	Catalysts and operating conditions	Summary
Kinetics of hydrodesulfurization of heavy gas oil derived from oil-sands bitumen. (Bej et al., 2007)	Commercial $NiMo/Al_2O_3$ T = 365-415 °C P = 8.8 MPa LHSV = 0.5-1.9 h^{-1} H_2/oil = 400-800 m^3/m^3 Feedstock: Heavy gas oil	At higher residence time, HDS activities increased. HDS conversion of 96 wt% was obtained at LHSV = 0.5 h^{-1}. Temperature had a positive effect on HDS activities. This effect started to plateau at a temperature range of 400-415 °C. HDS activities did not show any significant improvement at H_2/oil ratio higher than 800 m^3/m^3.
Hydrogenation of coker naphtha with NiMo catalyst. (Yui & Chan, 1992)	Three NiMo catalysts T = 140-280 °C P = 3-5 MPa LHSV 1.0 and 2.0 h^{-1} H_2/oil = 600 m^3/m^3 Feedstock: Coker Naphtha	The three catalysts did not show any significant difference in terms of activities. Temperatures higher than 220 °C had a positive effect on HDS and HDN activities, while HDA conversions improved at values higher than 200 °C. Pressure did not show any significant effect on any of the hydrotreating conversions. Residence time had a significant effect for HDS, HDN, and HDA.
Product Selectivity during Hydrotreating and Mild Hydrocracking of Bitumen-Derived Gas Oil	Commercial $NiMo/Al_2O_3$ T = 340-420 °C P = 6.5-11.0 MPa LHSV = 0.5-2.0 h^{-1}	Temperature had a positive effect on HDS and HDN conversions. Sulfur contents reached lower values than nitrogen contents; however, temperature was more significant on HDN conversions.

(Botchwey et al., 2003)	H_2/oil = 600 m^3/m^3 Feedstock: Heavy gas oil	Pressure improved HDN activities more significantly than HDS activities. As LHSV increased, HDS and HDN conversions decreased. Higher values of LHSV improved the selectivity of sulfur removal over nitrogen removal. Temperature and pressure improved HDA conversions. Pressure was more significant on HDA conversions at lower temperatures due to equilibrium limitations.
Catalytic hydrorefining of heavy gas oil. (Mann et al., 1987)	Ni-Mo, Ni-W, and Co-Mo catalysts supported on alumina T = 300-450 °C LHSV = 0.5-4 h^{-1} P = 4.24-12.51 MPa	HDN and HDS conversions increased linearly with temperature. Ni-Mo catalyst had a better performance at temperatures lower than 350 °C; meanwhile, Ni-W was better at temperatures higher than 350 °C. Pressure had a positive effect on HDS and HDN conversions. This process condition was more significant on HDN conversions. Higher residence time improved HDS and HDN conversions. Changes in residence time were more significant on HDN. C/H ratio was not affected by LHSV for experiments using NiMo catalyst at T = 450 °C and LHSV of 2 h^{-1}. This means HDA conversions were independent of changes in the residence time due to equilibrium limitations.

		C/H ratio was not improved significantly with increasing temperature. On the other hand, pressure had a positive effect on C/H ratio.
Hydrotreating of straight run gas oil–light cycle oil blends (Ancheyta-Juárez et al., 1999)	Co–Mo/γ-Al_2O_3 T = 350, 360,370, 380 °C LHSV = 1, 1.5, 2 h^{-1} P = 5.29,6.86,8.82 MPa H_2/oil = 356.21 ml/ml Feeds: -Blend A: 80 vol. % straight-run gas oil (SRGO), and 20 vol. % light cycle oil (LCO). -Blend B: 50 vol.% SRGO, and 50 vol.% LCO.	LCO has lower cetane index (CI) and higher contents of S, and N than SRGO. Blend B needed higher reaction temperature to achieve the desired S content (<500 wppm) due to higher initial S content. At higher temperatures S, N, and aromatics content decreased. Consequently, °API and CI increased. Lower LHSV enhanced the product quality. Increasing pressure enhanced the product quality and the HDS and HDA rate.
Two stage aromatics hydrogenation of bitumen-derived light gas oil (Owusu-Boakye, 2005)	Single stage study summary: NiMo/Al_2O_3 T = 340-390 °C P = 6.9-12.4 MPa LHSV = 0.5-2 h^{-1} H_2/oil = 550 ml/ml	Maximum HDA conversion of 69 % at T = 379°C, P = 11.0 MPa, and LHSV= 0.6 h^{-1} HDA was affected primarily by temperature. HDS and HDN conversions were affected by temperature and also by pressure. Increasing temperature and pressure improved the CI. In the case of temperature, CI reached an equilibrium.

	Feed: light gas oil blend composed of vacuum light gas oil (VLGO), atmospheric light gas oil (ALGO), and hydrocracker light gas oil (HLGO).	
HDS reactivities of dibenzothiophenic compounds in an LC-finer LGO and H_2S/NH_3 inhibition effect (Chen & Ring, 2004)	$NiMo/Al_2O_3$ Catalyst volume = 150 ml T = 320-385 °C P =5-11 MPa LHSV = 0.54-2.31 h^{-1} Gas rate = 120-210 NL/h	HDS activities increased with increasing temperature. 4, 6- DMDBT and 4-MDBT had the lowest and highest HDS activity of all the sulfur compounds studied, respectively. 1, 4, 6-TMDBT and 2, 4, 6-TMDT had higher activity than 4, 6-DMDBT showing that methyl groups at carbon positions 1 or 2 may increase HDS activities due to possible contributions of the hydrogenation mechanism.

2.5 Hydrotreating chemistry

The reactions that are of greater concern during hydrotreating of oils are HDS, HDN, and HDA. The H_2 consumption in each reaction is shown in Table 2.5. The ease of carrying each reaction follows the next order: HDS>HDN>HDA (Jones & Pujado, 2006). Olefins saturation may also be present, especially during hydrotreating of feedstocks produced in thermal processes.

Table 2.5 H_2 consumption reported on literature

Reaction	**H_2 consumption / wt. % change (N m^3 H_2/m^3 oil)**	**Reference**
HDS	17-25 12.5 16.9-17.8 13.4	Jones & Pujado, 2006 Gary et al., 2007 Ancheyta & Speight, 2007 Edgar,1993
HDN	34-59 57 44.7-52.2 57.9	Jones & Pujado, 2006 Gary et al., 2007 Ancheyta & Speight, 2007 Edgar, 1993
HDA	4.0(per vol. %) 4.81	Ancheyta & Speight, 2007 Edgar, 1993

2.5.1 Hydrodesulphurization

Hydrodesulphurization (HDS) is an exothermic and generally irreversible reaction under industrial operating conditions (340-425 °C and 5.57-17.22 MPa) (Girgis & Gates, 1991).

There are six types of sulfur compounds and its derivatives that can be present in different distillate products. These are mercaptans, sulfides, disulfides, thiophenes, benzothiophenes, and dibenzothiophenes. In the case of gas oils, most of the sulfur compounds are present as benzothiophenes and dibenzothiophenes (Jones & Pujado, 2006; Ancheyta & Speight, 2007). Some examples of sulfur compounds found in oil are shown in Figure 2.2.

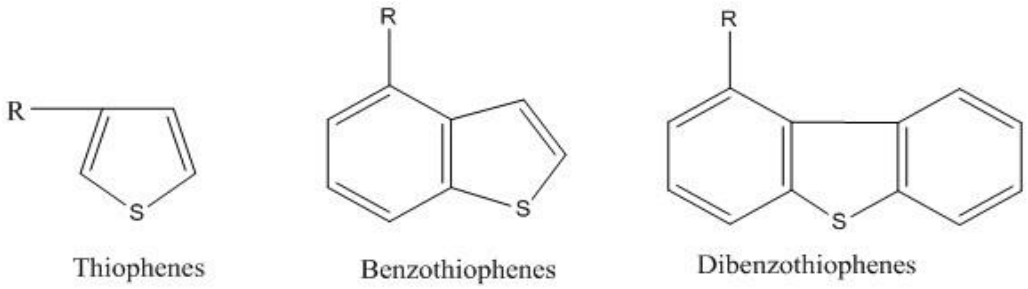

Figure 2.2 Examples of sulfur compounds found in gas oils

HDS can proceed by two possible mechanisms: direct hydrogenolysis of the C-S bond or hydrogenation of an unsaturated bond followed by hydrogenolysis which will consume more hydrogen than the first mechanism. In contrast to hydrogenolysis, hydrogenation is dependent on hydrogen partial pressure (Girgis & Gates, 1991). Both mechanisms are illustrated in Figure 2.3. Furthermore, the reactivity of benzothiophenes decreases with increasing molecular weight e.g. BT (benzothiophenes) are less reactive than DBT (dibenzothiophenes) (Stanislaus et al., 2010). When methyl groups are connected to the benzenoid ring in positions 4 and 6, the reactivity also decreases. In contrast, methyl groups in positions 2, 8, 3, or 7 do not show any significant change in the reactivity (Girgis & Gates, 1991). Sulfur compounds in oil fractions are numerous e.g. light gas oil from an Arabian crude oil was found to have at least 42 alkyl-substituted benzothiophenes and 29 alkyl-substituted dibenzothiophenes (Ishihara et al., 2005).

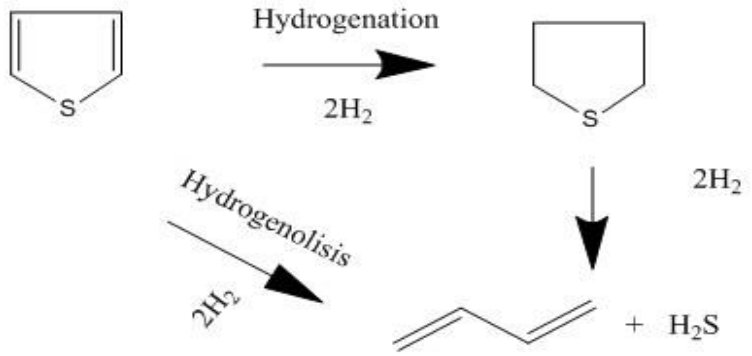

Figure 2.3 Schematic illustration of the hydrodesulphurization of thiophene

2.5.2 Hydrodenitrogenation

The removal of nitrogen is an exothermic reaction which is generally irreversible under industrial operating conditions (Jones & Pujado, 2006). The nitrogen compounds found in oil are

generally formed of five to six unsaturated rings and are classified as non-heterocyclic and heterocyclic compounds. Non-heterocyclic compounds (anilines, aliphatic amines, and nitriles) are de-nitrogenated more rapidly than heterocyclic compounds (basic: quinoline, acridine; non-basic: indole, carbazole) However, non-heterocyclic compounds are present in oil in small quantities (Girgis & Gates, 1991; Ancheyta & Speight, 2007).

The reactivity of heterocyclic nitrogen compounds seems to be independent of the number of benzenoid rings in the molecule. This means that the effect of the steric hindrance caused by the presence of various aromatic rings is independent of the molecular size for the C-N scission (Girgis & Gates, 1991). Furthermore, non-basic compounds are less reactive than basic compounds found in real oil feedstocks when temperature and pressure increases. This could be due to the prevailing effect of pre-hydrogenation reactions during the process which transforms non-basic into basic compounds (Bej et al., 2001).

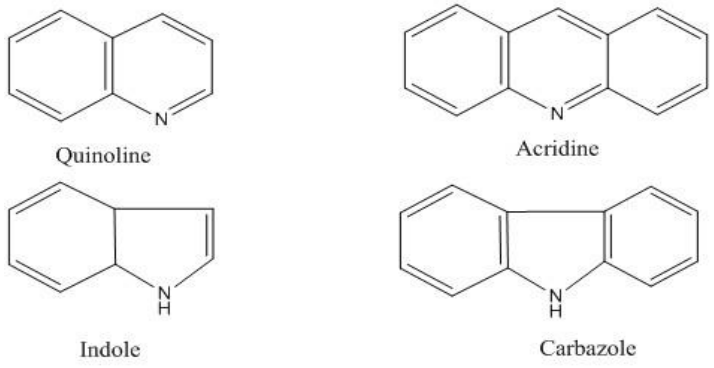

Figure 2.4 Examples of basic and non-basic nitrogen compounds found in gas oils

HDN mechanism proceeds in three steps: hydrogenation, hydrogenolisis, and denitrogenation. Hydrogenation is required to facilitate the removal of nitrogen because the amount of energy to break the -N=C bond (147 kcal/mol) is higher than the energy required to break the C-N- bond (73 kcal/mol) (Girgis & Gates, 1991; Jones & Pujado, 2006). The removal of nitrogen from pyridine is shown in Figure 2.5.

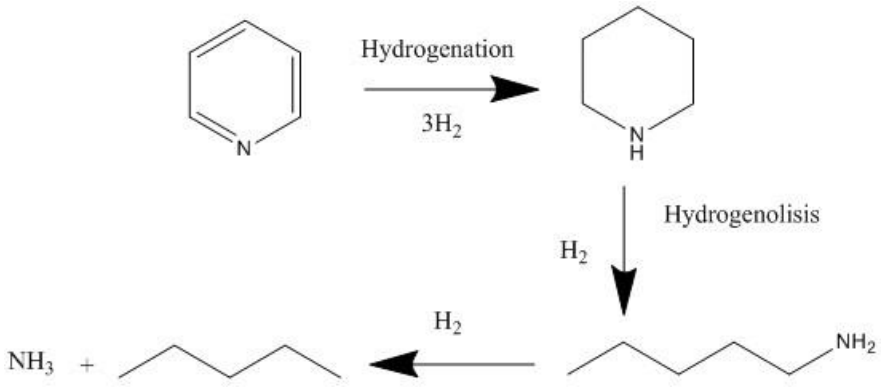

Figure 2.5 Schematic illustration of the hydrodenitrogenation of pyridine

2.5.3 Hydrodearomatization

Hydrodearomatization is an exothermic reaction and it can be reversible under normal industrial operating conditions as shown in Figure 2.6. Hydrogen partial pressure favors this reaction and high temperatures limit it (Girgis & Gates, 1991). According to Mapiour et al. (2010), the conversion of aromatics reaches its maximum activity at 360-400 °C. The compounds found in gas oils may contain a maximum of three aromatic rings. Most of the aromatic compounds are not completely saturated under normal hydrotreating conditions but converted to naphthenic rings.

The saturation of aromatics improves the properties of oil products such as cetane index and smoke point (Jones & Pujado, 2006).The reactivity of aromatic compounds increases with the presence of more aromatic rings while the methyl substituents do not affect the reactivity to a great extent. The greater reactivity of polyaromatics might be due to greater resonance stability of the π bond between naphthalene fractions and the active sites of the catalysts (Girgis & Gates, 1991). A simple illustration of hydrodearomatization reaction is shown in Figure 2.6.

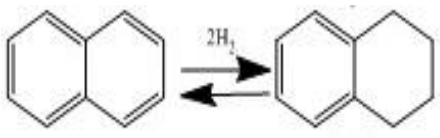

Figure 2.6 Schematic illustration of the hydrodearomatization of naphthalene

2.5.4 Saturation of olefins

Olefins are not found naturally in petroleum; however, they can be formed during thermal or catalytic processes such as coking, ethylene manufacturing, among others. Olefins saturation is an exothermic reaction (Jones & Pujado, 2006).

2.6 Hydrotreating catalysts

Catalysts used for hydrotreating of heavy oils require an optimal balance between high activities and proper physical properties. High surface area and moderate pore volume improve HDS activities due to high dispersion of the active phases. However, feeds with high metal contents will require catalysts with higher pore volume to prevent mouth plugging (Ancheyta et al., 2005). Also, due to processing at high temperatures, coke can be formed and dispersed between the pores of the catalyst causing deactivation (Ancheyta & Speight, 2007).

The most widely used catalyst in the industry is composed of molybdenum supported on gamma alumina (γ-Al_2O_3) and promoted by either nickel or cobalt (Papayannakos & Georgiou, 1988). The promoters' function is to enhance the selectivity and activity of the catalysts by decreasing the metal-sulfur interaction in MoS_2. Ni prefers to be attached to the Mo edge providing higher hydrogenation activities, while Co prefers the S-edge providing higher sulfur removal activities (Sun et al., 2005).

The active phases (Co-Mo-S or Ni-Mo-S) of the catalyst are produced during sulfidation. When interactions between active phases and the support are weak, the active phases form a stack of 2-4 layers defined as Type II Co-Mo-S or Ni-Mo-S (Topsøe, 2007). From this species, the sulfur ion is expelled as H_2S forming sulfur vacancies commonly known as coordinatively unsaturated sites (CUS) with Lewis acid nature. This property allows the adsorption of molecules with unpaired electrons such as pyridine and DBT. On the neighboring site, the heterocyclic and homocyclic splitting of hydrogen form Mo-H and –SH groups which are the sources of hydrogen for the hydrotreating reactions to occur. These groups have Bronsted acid character (Ancheyta et al., 2005). The reaction completes by the re-formation of the original active phases and it is known as sulfur-breathing. Mochida & Choi (2006 described the sulfur-breathing mechanism graphically.

Alumina is the support of choice due to characteristics such as metal oxides from group VI, and VIII oxides are highly dispersed forming inactive compounds, stabilization of the operating

phases, high purity, physical properties can be tailored easily, thermal stability and regeneration conditions, malleable into different forms, and low cost (Luck, 1991). Supports can either be modified chemically or physically to improve their characteristics; additives such as phosphate have shown improvement on activity, and the addition of TiO_2 to alumina allowed control of pore volume and mean pore diameter. Research has also been focused on testing other types of supports such as mixed oxides, and carbon-based supports for improving acidic sites distribution for a better hydrocracking activity, and improving the resistance to N bases, respectively (Ancheyta et al., 2005).

Other physical properties of concern are mechanical strength, and sizes and shapes of catalysts particles. Sufficient mechanical strength is required to prevent breakage during the process, and specific sizes are required to prevent diffusion problems; large particles may present problem of underutilization while small particles (under 0.8 mm) may cause pressure drop in the reactor. The most common shapes are sphere, pellet, cylinder, bilobular, trilobular and teralobular respectively (Ancheyta et al., 2005; Rana et al., 2007).

2.7 Hydrogen consumption

The catalyst properties, the level of conversion, operating conditions and properties of the feedstock affect H_2 consumption during hydrotreating (Castañeda et al., 2011). Therefore, the determination of H_2 consumption is important for economic and technical issues. Pilot plant studies consider chemical H_2 consumption and dissolved H_2 only; studies at pilot scale can generally obtain accurate values by performing twenty experiments (Lee et al., 2008). Hydrogen is present in the liquid and gas streams of the process. Thus, the overall mass balance for hydrogen takes the following form:

$$G_1 \times H_{2G_1} + L_1 \times H_{2L_1} = G_2 \times H_{2G_2} + L_2 \times H_{2L_2} \quad (2.1)$$

where: G_1 and G_2 are the gas inlet and outlet flow rates (m^3/h), respectively; H_{2G_1} and H_{2G_2} are the hydrogen concentrations in gas inlet and outlet streams, respectively (mol. %); L_1 and L_2 are the liquid inlet and outlet flow rates, respectively (m^3/h); H_{2L_1} and H_{2L_2} are the hydrogen concentration in feedstocks and products, respectively (mol. %). The hydrogen concentration in the liquid products takes into consideration unreacted dissolved H_2 as well as molecular H_2 added to the products due to reaction.

In general, there are five approaches to determine H_2 consumption during hydrotreating. These approaches are listed below.

1. Analysis of H_2 concentrations in gas streams.
2. Analysis of H_2 concentrations in liquid streams.
3. H_2 consumption data reported in the literature.
4. Stoichiometric H_2 consumption in each type of reaction.
5. Kinetic modeling.

2.7.1 Analysis of H_2 concentrations in gas and liquid streams

The analysis of H_2 contents in gas and liquids require the use of different analytical techniques e.g. elemental analysis or nuclear magnetic resonance (NMR) for analysis of liquids, and high-resolution gas chromatography for analysis of gases (Castañeda et al., 2011). The equations used for both methods are shown below.

$$H_2\text{consumption gas}\left(\text{N } {}^{m^3}H_2/_{m^3\text{ oil}}\right) = \frac{G_1 \times H_{2G_1} - G_2 \times H_{2G_2}}{L_1} \qquad (2.2)$$

$$H_2\text{consumption liquid}\left(\text{N } {}^{m^3}H_2/_{m^3\text{ oil}}\right) = \frac{L_1 \times H_{2L_1} - L_2 \times H_{2L_2}}{L_1} \qquad (2.3)$$

2.7.2 H_2 consumption data reported in literature

The values reported in the literature can be used for a rapid estimation of H_2 consumption; values for each hydrotreating reaction are shown in Table 2.5 and these values differ between each other.

2.7.3 Stoichiometric H_2 consumption in hydrotreating reactions

Hydrogen consumption can be calculated based on the stoichiometry of each hydrotreating reaction. Lee et al. (2008) developed a method based on the stoichiometric H_2 consumption during hydrotreating of a mixture of 62 vol. % straight-run heavy gas oil, 10 vol. % coker light gas oil and 28 vol. % FCC light cycle oil for the production of diesel taking into account HDS, HDN, HDO, HGO (olefins saturation in terms of bromine number) and HDA reactions. Hydrogen consumption obtained by this method was 158.5 N m^3 H_2/m^3 oil. The method presented a standard deviation of 20.7 N m^3 H_2/m^3 oil in comparison with the gas streams analysis. Meanwhile, the analysis of the liquid streams presented a lower deviation (8.7 N m^3 H_2/m^3 oil). Lee et al. (2008) method is shown below.

$$\begin{aligned} H_2\text{consumption}\left(\text{N } m^3\ H_2/_{m^3\ \text{oil}}\right) = {} & 0.0252\ sg_f\left[S_f - \frac{S_p\, sg_p}{sg_f}\, Y_p\right] + 0.08\, sg_f\left[N_f - \frac{N_p\, sg_p}{sg_f}\, Y_p\right] \\ & + 0.05\, sg_f\left[O_f - \frac{O_p\, sg_p}{sg_f}\, Y_p\right] + 1.4\left[Br_f - \frac{Br_p\, sg_p}{sg_f}\, Y_p\right] \\ & + 3.3\, sg_f\left[PNA_f - \frac{PNA_p\, sg_p}{sg_f} Y_p + 3\left[MA_f - \frac{MA_p\, sg_p}{sg_f}\, Y_p\right]\right] \end{aligned} \tag{2.4}$$

where: S, N, O, Br, PNA, and MA are the sulfur, nitrogen, oxygen, bromine number, polynuclear aromatics, and mononuclear aromatics contents in wppm, respectively; S_g is the specific gravity; Y is the total liquid product yield. The subscripts f and p represent the feed and products, respectively.

Stratiev et al. (2009) reported a similar method for hydrogen consumption of HDS, HDN HGO, and HDA reactions during hydrotreating of different feedstocks. The method is shown in equations 2.5-2.9. Castañeda et al. (2011) compared experimental H_2 consumption with different methods reported in the literature; this work noticed that hydrogen consumption calculated by Lee et al.(2008) and Stratiev et al. (2009) methods worked relatively well with middle fractions obtained during hydrotreating. In contrast, the methods presented a variation of up to 29.2 % when applied to heavy gas oil.

$$H_2\text{consumption}\left(\text{N } {}^{m^3}H_2/_{m^3\text{ oil}}\right) = H_2HDS + H_2HDN + H_2HDA + H_2HGO \quad (2.5)$$

$$H_2HDS = \left[3\left(S_f\frac{1000}{32} - S_p\frac{Y_p\,BT_p}{320}\right) + 2\left(S_f\frac{1000\,DBT_f}{32} - S_p\frac{Y_p\,DBT_p}{320}\right)\right]22.4\ \frac{\rho_f}{100} \quad (2.6)$$

$$H_2HDN = \left[5\left(\frac{N_f}{140} - \frac{Y_p}{100} - \frac{N_f}{140}\right)\right]22.4\ \frac{\rho_f}{100} \quad (2.7)$$

$$H_2HGO = \left[\left(O_f\ \frac{1000}{Mw_f} - O_p\frac{10Y_p}{Mw_p}\right)\right]\ 22.4\ \frac{\rho_f}{100} \quad (2.8)$$

$$\begin{aligned} H_2HDA = &\left[\left[2\left(PNA_f\ \frac{1000}{Mw_f} - PNA_p\ \frac{10\,Y_p}{Mw_p}\right) + 3\left(MA_f\ \frac{1000}{Mw_f} - MA_p\ \frac{10Y_p}{Mw_p}\right)\right]22.4\ \frac{\rho_f}{100}\right] \\ &+\left[\left[2\left(TriA_f\ \frac{1000}{Mw_f} - TriA_p\ \frac{10Y_p}{Mw_p}\right) + 2\left(TriA_f - TriA_p\ \frac{Y_p}{100}\right) + 2\left(DiA_f\frac{1000}{Mw_f} - \right.\right.\right. \\ &\left.\left.\left. DiA_p\ \frac{10Y_p}{Mw_p}\right) + 3\left(MA_f - MA_p\ \frac{10Y_p}{Mw_p}\right)\right]22.4\ \frac{\rho_f}{100}\right] \end{aligned} \quad (2.9)$$

where: H_2HDS, H_2HDN, H_2HGO, H_2HDA, are the amount of H_2 consumed in HDS, HDN, HGO, and HDA reactions, respectively. S, BT, DBT,N,O,PNA, MA,TriA, and DiA represent sulfur, benzothiophene, dibenzothiophene, nitrogen, olefins, polycyclic arenes, monoaromatics, tricyclic

arenes, dyciclic arenes, and monocyclic arenes contents, respectively (wt. %).ρ and Y is the density at 20 °C (gr/mL) and the liquid yield (volumetric fraction), respectively. f and p represent feed and products, respectively.

Hisamitsu et al. (1976) developed a method that only requires the characterization of the liquid streams and it is based on the decrease in aromatic content. This method also considers HDS and HDN reactions resulting in the prediction of theoretical H_2 consumption. This method is adequate when limited hydrocracking is present. This method is shown below (Hisamitsu et al., 1976; Mapiour et al., 2010).

$$H_2\text{consumption}\left(\text{m}^3\ \text{H}_2/\text{m}^3\ \text{oil}\right) = \frac{\left[(C_A)_f - (C_A)_p\right] \times \rho\ \text{feed}}{100 \times 2 \times 12} \times 22.4 + \left(\frac{\left[(S)_f - (S)_p\right] \times \rho\ \text{feed}}{100 \times 32}\right) \times 2 \times 22.4 + \left(\frac{\left[(N)_f - (N)_p\right] \times \rho\ \text{feed}}{100 \times 14}\right) \times 2 \times 22.4 \quad (2.10)$$

where: C_A, S, and N are the aromatic carbon, sulfur and nitrogen contents (wt. %) respectively; 22.4 is the number of standard liters is a mole of an ideal gas. The subscripts f and p represent the feed and products, respectively. It can be seen in the equation that H_2 consumption for sulfur and nitrogen conversions is multiplied by two. This represents the hydrogen required to form hydrocarbons during HDS and HDN, and the hydrogen content in the form of H_2S and NH_3 in the product.

2.7.4 Kinetic modelling

This method is developed by analyzing the rates of all the reactions that consume hydrogen during hydrotreating. Therefore, it can provide accurate te values of H_2 consumption. Papayannakos & Georgiou 1988 proposed a simple kinetic model without considering diffusion in the catalysts particles for HDS of an atmospheric residue in a trickle bed reactor at the following conditions: T = 350-430 °C; LHSV = 0.25-3 h^{-1}, P = 5 MPa. Co-Mo/Al_2O_3 commercial catalysts were used. They obtained the following equation from a differential mass balance based on an isothermal plug flow model:

$$(C_H)^{1-\alpha} - (C_{HT})^{1-\alpha} = (\alpha-1) \times \xi \times (1-\varepsilon) \times k_v \times (V_R/Q_L) \quad (2.11)$$

Where: C_H = remaining H_2 demand or concentration of the bonds which are bound to react with H_2 at reaction conditions (mol H_2/m^3 oil); α = reaction rate order; C_{HT} = concentration of all the bonds likely to react with H_2 before any treatment occurs (mol H_2/m^3 oil); ξ = Catalyst remaining relative activity; ε = Catalyst bed void fraction; k_v = Rate constant; V_R = Catalyst bed volume; and Q_L = Oil volumetric flow rate.

The authors obtained a total H_2 reaction rate order of two. Also, C_H is the subtraction of C_{HT} from the H_2 consumption measured experimentally (CON). Therefore, eq. 2.10 takes the form of the following:

$$\frac{1}{\xi} \times \frac{CON}{(C_{HT}-CON) \times C_{HT}} = (1-\varepsilon) \times k_v \times \frac{V_R}{Q_L} \quad (2.12)$$

The H_2 consumption obtained by the model was 10.7×10^3 mol H_2/m^3 oil compared to 8.6×10^3 mol H_2/m^3 oil, which is based on the °API of the residue. Moreover, they also confirmed that the value obtained by the model can approach experimental values by comparing it with H_2 consumption of a 99.2 % HDS of a vacuum residue with similar properties as that of the feedstock. The H_2 consumption obtained in the latter case was 11.5×10^3 mol H_2/m^3 oil.

2.7.5 Analysis of hydrogen consumption studies

Methods based on stoichiometry and kinetics shown above calculate chemical H_2 consumption during hydrotreating. The overall hydrogen consumption in the industry involves other factors such as mechanical losses due to the use of compressors, venting losses in case of purging the gas stream, and solution losses which are defined as the amount of hydrogen dissolved in the final product (Hisamitsu et al., 1976). Therefore, in the case of experimental or pilot plant studies, total H_2 consumption must consider chemical H_2 consumption and dissolved hydrogen. Castañeda et al. (2011) reported that the estimation of total H_2 consumption could have an error of about 6% if dissolved H_2 is not considered.

As was mentioned previously, H_2 consumption is a dependent variable. One of the main factors affecting this variable is feedstock properties. Industries that work with hydrotreating units are concerned in the amount of hydrogen needed in the process due to the high costs and importance of this reactant. When refineries process one specific type of feedstock, the overall H_2 balance will not show significant changes; however, when different feedstocks with different properties need to be treated, the industry may overestimate the usage of reactant causing economic losses. Furthermore, under usage of hydrogen may cause operational problems and possible shutdown of the unit.

The models found in literature can be used for quick estimations, however, when more precision is needed these are not of great use e.g., the models were inaccurate to predict H_2 consumption for feeds that were not used in the development of such models as it was mentioned previously. Also, the use of some models may be difficult e.g. models based on the stoichiometric H_2 consumption on each type of reaction require detailed characterization of feedstocks and products.The development of regression models based on process conditions for feedstocks with varying composition and properties may contribute with important data to perform corrections in H_2 global mass balances of refineries.

2.8 Vapor-liquid equilibrium in hydrotreating process

The study of vapor-liquid interactions can contribute to the improvement of process design and catalyst formulations (Chávez et al., 2014; Chen et al., 2011). Reaction rates are dependent on the amount of hydrogen dissolved into the liquid which certainly will be affected by several factors such as H_2 consumption, levels of conversion, feedstock properties, temperature, pressure, and liquid and gas flowrates. The general parameters of concern are H_2 partial pressure, feed vaporization, and dissolved H_2 (Mapiour et al., 2010). Vapor-liquid equilibrium is explained by a series of laws and principles that are briefly reviewed in this section.

The principle of equilibrium in vapor-liquid interaction is similar to reversible chemical reactions; Gibbs energy (G) always tends to remain constant (G=0). Suppose there is an ideal mixture of decane and hydrogen in a flash operation, increasing temperature will increase the molar composition of decane in the gas phase modifying the partial pressure of each component

and forcing more hydrogen to dissolve in the liquid phase to force the system back into equilibrium (Mapiour et al., 2010; Skogestad, 2009).Three laws for ideal mixtures are the basis for this example. These laws are displayed in Table 2.6.

Hydrocarbons and hydrotreating products (H_2S, NH_3) are not ideal under hydroprocessing conditions; therefore, calculation of vapor-liquid equilibria requires the use of equations of state developed for non-ideal mixtures. Peng-Robinson is widely used to predict the behavior of hydrocarbons mixtures-hydrogen at high temperature and pressures (Lal et al., 1999). The modification of this model developed by Stryjek and Vera (PRSV) can improve the prediction of the equilibrium when there is the presence of polar compounds in the system (Ghosh, 1999).

2.8.1 Inlet and outlet hydrogen partial pressure

Hydrogen partial pressure improves hydrotreating conversions by increasing the concentration of hydrogen in the liquid which will diffuse into the catalyst prior to reaction (Fogler, 1999). Optimal levels of H_2 partial pressure will contribute to hydrotreating economically and will prevent the formation of coke; excessive levels of H_2pp will have no significant impact on hydrotreating activities (Speight, 1999). Many studies have analyzed the effect of H_2pp on hydrotreating conversions. The general trend is that H_2pp improves hydrogenation reactions (Girgis & Gates, 1991); this means that HDA and HDN conversions will increase with increasing H_2pp. In the case of HDS, H_2pp also improves the conversion; however, the effect is less significant than in the other two reactions (Fang, 1999).

In the hydrotreating process, outlet H_2pp is lower than inlet H_2pp due to the following factors: the presence of other gases in the system (H_2S, NH_3, C_1-C_4), H_2 consumption, feed vaporization and dissolved hydrogen. The study of outlet H_2pp during hydrotreating may be more relevant than inlet H_2pp because it represents the average conditions in the catalyst bed and the last opportunity of the catalyst to react with the feedstock (Mapiour, 2009). However, studies on the effect of outlet H_2pp on hydrotreating reactions and processing conditions are not readily available in the literature.

Table 2.6 Laws explaining liquid-gas interaction for ideal mixtures

Author	Description	Equation
Dalton	The partial pressure of a specific component is proportional to the mole fraction of the component multiplied by the system pressure.	$P = P_1+P_2+P_3....Pn$ $Pn = X_n \times P$ where: P=total pressure Pn= partial pressure of component n n_x=mole fraction of component n
Henry	The amount of a gas dissolved in a liquid is proportional to the partial pressure of the gas in the system.	$H = \frac{n_N}{\lambda \rho_L}$ where: H = Henry's coefficient n_N = molar gas volume at standard conditions λ = solubility coefficient; and ρL = density of the liquid at process conditions
Raoult	The partial pressure of a specific component is proportional to the vapor pressure of the component multiplied by its mole fraction in the liquid phase.	$y_i \times P = x_i \times P_i^{sat}(T)$ where: y_i = mole fraction of component i in the gas phase P = total pressure x_I = mole fraction of component i in the liquid phase $P_i^{sat}(T)$ = vapor pressure of component i

McCulloch & Roeder (1976), studied the effect of processing conditions on H_2pp (inlet and outlet) at the following process conditions: T = 343-380 °C, P = 500-545 psi, and G/O= 600-1200 scf/bbl. The feedstock properties were the following: density = 0.87g/cm^3, average boiling point = 296 °C, and molecular weight of 224 g/mole. The authors provided a method to calculate inlet and outlet H_2pp and studied the effect of process conditions on outlet H_2pp; they determined that temperature increased feed vaporization and H_2/oil ratio had a positive effect on outlet H_2pp only. Mapiour et al. (2010), studied how process conditions interact with feed vaporization,

dissolved H_2, H_2 consumption and H_2pp during hydrotreating of bitumen-derived heavy gas oil (HGO) at the following conditions: T = 360-400 °C, LHSV = 0.65-2 h^{-1}, and P = 7-11 MPa. The authors found out that temperature had a positive effect on feed vaporization and a slight negative effect on dissolved H_2. Increasing H_2pp leads to higher H_2 dissolution and H_2 consumption, and higher flow rates increased the amount of vaporized feed and dissolved H_2. This work did not find any correlation between H_2pp and feed vaporization. Therefore, experiments with lighter feeds could give an insight of how feed vaporization interacts with H_2pp.

2.8.2 Calculation of hydrogen partial pressure

Hydrogen partial pressure can be calculated by performing vapor-liquid equilibrium simulations on HYSYS software. The procedure to calculate H_2pp is mentioned in Mapiour (2009) and it was adapted from McCulloch & Roeder (1976). The procedure is summarized below.

First, the feedstock properties were entered in HYSYS. The feed can be simulated using the following properties: boiling point distribution, density, and sulfur and nitrogen content; the feedstock will approach more to reality when more properties are included. Several thermodynamic models have been used to develop vapor-liquid equilibria calculations for the interaction of hydrogen and hydrocarbons. Peng-Robinson (PR) thermodynamic model is widely used for these high pressure and high temperature systems (Lal et al., 1999); however, since there is the presence of polar compounds (H_2S and NH_3) on the gas outlet stream, PRSV model may improve the prediction of vapor-liquid equilibria (Ghosh, 1999).

Second, use a flash unit in the simulation environment. Input temperature, pressure, and gas and liquid flow rates of each component. Inlet hydrogen partial pressure calculation requires hydrogen and feedstock streams data only. The outlet hydrogen partial pressure calculation takes into consideration the consumption of H_2 and the properties and flow rates of the gases formed during the process (H_2S, NH_3, and light hydrocarbons). Once the simulation is performed, feed vaporization and hydrogen solubility can be calculated with the data provided by the simulation.

2.8.3 Dissolved hydrogen

Dissolved hydrogen is proportional to the hydrotreating reactions rates; therefore, the study of this variable is important for an improvement in the design of hydrotreating units. Different

works related to reactor simulation and modeling have found out that when VLE are considered, the models improve the prediction of hydrotreating conversions (Akgerman & Netherland, 1986; Chen et al., 2011). Most of the studies related to dissolved hydrogen have been performed with simple hydrocarbons; however, data of real hydrotreating feedstocks at high pressures and temperatures is not readily available in the literature (Chávez et al., 2014; Lal et al., 1999). The solubility of hydrogen is affected by temperature, pressure, and boiling point distribution (BPD) of petroleum fractions (Riazi & Roomi, 2007). Many authors reported the following: as temperature and pressure increase, the mole fraction of hydrogen in the liquid also increases. In the case of petroleum fractions with higher boiling point distribution, the solubility of H_2 in the latter tends to resemble dissolved H_2 in lighter fractions at high temperatures (Cai et al., 2001; Florusse et al., 2003; Lal et al., 1999).

3 EXPERIMENTAL

This chapter describes the experimental setup and procedure. Also, it describes the steps that were taken to carry the different phases of the study and the instruments used to characterize feed and products.

3.1 Materials

Commercial Ni-Mo/γ-alumina catalyst (C424) employed in this work was provided by Criterion Catalysts. Silicon carbide and glass beads were supplied by Fisher Scientific, Edmonton, Canada. Butanethiol was purchased from Sigma-Aldrich Canada. Helium and hydrogen gases were bought from Praxair, Saskatoon, Canada. Light gas oils were supplied by Syncrude Research Centre, Edmonton, Canada. The properties of the light gas oils are displayed in Table 3.1.

Table 3.1 Properties of feedstocks

Property	KLGO	HLGO	VLGO	PHTHGO
Density (g/cm^3)	0.901	0.877	0.894	0.912
Sulfur content (wt. %)	3.800	0.697	1.338	0.236
Nitrogen content (wt. %)	0.120	0.139	0.026	0.147
Aromatics content (wt. %)	28.9	24.1	20.3	29.1
Hydrogen-to-carbon ratio (H/C)	0.126	0.148	0.144	-
Boiling point distribution (°C)	162.9-484.2	200.4-647.1	158.3-446.7	163.3-583.1

* Hydrogen-to-carbon ratio for VLGO was taken from Yui, 2008

3.2 Experimental setup

The experimental setup is shown in Figure 3.1 and consists on a 304 stainless steel micro-reactor (inner diameter of 14mm and length of 240mm), a hydrogen mass flow controller to regulate the amount of H_2 going into to the system, an electrical furnace with temperature control, a water scrubber to remove ammonium sulfide, a high pressure separator, a back pressure regulator, a bubble flow meter connected to the gas outlet, and a sodium hydroxide scrubber connected to the gas outlet to prevent release of hydrogen sulfide to the environment.

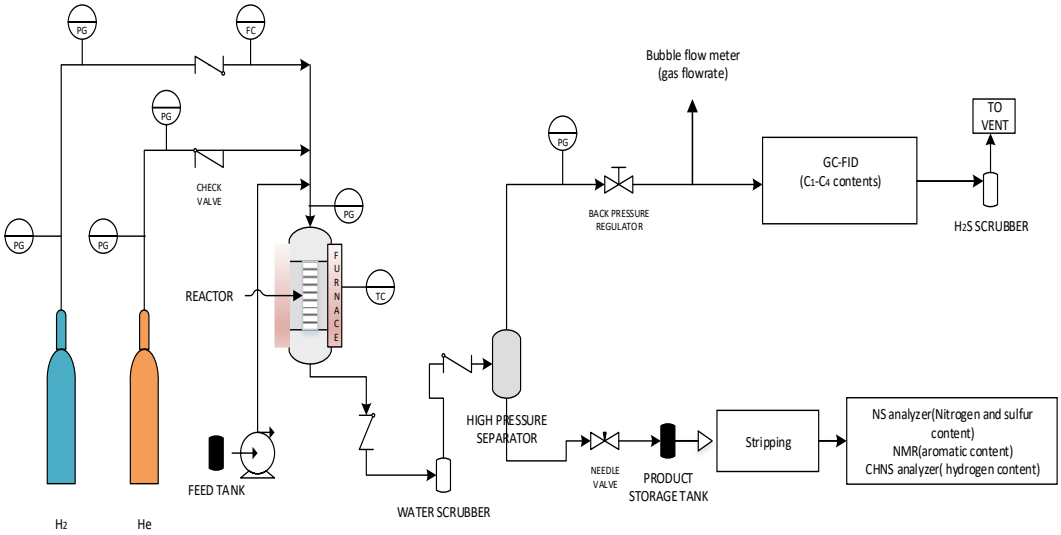

Figure 3.1 Experimental setup (PG: pressure gauge; FC: mass flow controller; TC: temperature controller)

3.3 Experimental procedure

Before catalyst loading, the NiMo/γAl_2O_3 catalyst has to be dried at 200 °C for three hours. Then, the reactor is loaded considering its division into three sections: bottom, middle and top. The top section in the upper part of the catalyst bed has one layer of 3 mm of glass beads and several layers of silicon carbide: 25, 10 and 10 mm height of 16, 46 and 60 mesh, respectively. The catalyst bed in the middle part consists of 90 mesh silicon carbide and 5 mL of catalyst mixed uniformly. The catalyst bed will have a height of around 10 cm. Finally, the bottom section is arranged similarly to the top section in reverse direction (Mapiour, 2009; Owusu-Boakye, 2005).

After loading the reactor, the pressure in the system was maintained at 8.96 MPa for 24 h to ensure a leakage free system. Subsequently, the reactor temperature was increased to 100 °C and sulfidation of the catalyst began by pumping 100 mL of butanethiol solution (2.9 vol. % in heating oil) at a flow rate of around 2.5 mL/min to wet the catalyst. Then, H_2 was introduced at H_2/oil ratio of 600 m^3/m^3 and flow rate was reduced to achieve LHSV = $1h^{-1}$. The temperature of the catalyst bed was then gradually increased to 193 °C and maintained for 24 h. Then, the temperature was again increased gradually to 343 °C and maintained for another 24 h. Following sulfidation, the catalyst was precoked by treating LGO at 370 °C for a period of 5 days; pressure, LHSV, and H_2/oil ratio were maintained constant. Samples were collected every 12 hours, stripped with nitrogen, and then analyzed for nitrogen, sulfur and aromatics conversions (Botchwey et al., 2003).

3.4 Experimental plan

3.4.1 Phase I - Development of H_2 consumption regression models during hydrotreating of gas oils

Experimental runs were designed based on a central composite design (CCD) methodology in MINITAB 7.0 software. CCD is used to build quadratic models with the objective to optimize process variables and study the interaction between and within variables and specific responses. CCD consists of one central point (repeated six times to improve accuracy), two axial points (2n), and two cube points (2^n) in which n are the number of the experimental variables (Lazic, 2004). In case of having three input variables, the number of experimental runs to be carried are twenty as shown in equation 3.1.

$$N= 2^n+2n+6 = 20 \quad (3.1)$$

The experimental variables and their ranges for this study are the following: T = 353-387 °C, P = 8.27-10.12 MPa, and LHSV = 0.7-2.3 h^{-1}; H_2 /oil ratio was maintained constant at 600 Nm^3 H_2/m^3 oil. The experimental design consists of twenty runs in which six are repeated to improve the model accuracy. The experimental matrix for VLGO, HLGO, KLGO, and PHTHGO feedstocks employed in this work is displayed in Table 3.2.

Hydrogen consumption was measured by analyzing the H_2 content in gas and liquid streams. Then, these data were compared with an approach developed by Hisamitsu et al. (1976). The best method (between gas and liquid) was selected to perform statistical analysis and build H_2 consumption regression models for each feedstock based on process conditions. Then, a composite model was developed by the statistical analysis of a new set of data. This set of data was obtained for calculating total H_2 consumption of this mixture by assuming equal volumetric flow rate of each of four streams: VLGO, HLGO, KLGO, and PHTHGO in the gas oil mixture. The prediction of the composite model was tested with a mixture of LGOs within the range of conditions provided by the CCD. The conditions were the following: T = 365 and 375 °C, P = 9.31 MPa, LHSV = 1.2 h^{-1}, and H_2/oil ratio = 600 m^3/m^3. The response of the model was also compared with values reported by Edgar (1993), and models developed by Hisamitsu et al. (1976) and Lee et al. (2008). These models available in the literature predict chemical H_2 consumption only; therefore, dissolved H_2 was calculated and added to obtain the total H_2 consumption. Dissolved H_2 was calculated by VLE simulations in HYSYS 2006. In addition, data of H_2 inlet pp, H_2 outlet pp, and feed vaporization obtained from the simulation was employed to study the effects of process conditions on these variables and the correlation between these variables. It is important to note that for the control experiment, the calculation of these four parameters was done by taking an average of hydrogen consumption.

3.4.2 Phase II - Effects of process conditions on HDS, HDN, and HDA conversions during hydrotreating of gas oils and optimization of process conditions

HDS, HDN, and HDA conversions were calculated for each experimental run in Table 3.2. For each experimental run, two samples were taken every 12 hours for reproducibility, and when conditions changed there was a stabilization period of 24 hours. Also, to ensure that catalyst deactivation did not occur, hydrotreating conversions were compared between the first and last three experiments carried at the central conditions. Then, statistical analysis was carried out to study interactions between and within hydrotreating conversions and process conditions, and develop regression models. The regression models were employed to find the best sets of conditions to process each feedstock.

Table 3.2 Experimental matrix

Run	T (^{0}C)	P (MPa)	LHSV (h^{-1})	HDS, HDN, HDA (%); H_2 consumption (Nm^3 H_2/m^3 oil)			
				VLGO	HLGO	KLGO	PHTHGO
1	370	8.96	1.5				
2	380	9.65	2				
3	387	8.96	1.5				
4	370	8.96	1.5				
5	360	9.65	2				
6	370	10.12	1.5				
7	360	9.65	1				
8	370	8.96	2.3				
9	380	9.65	1				
10	370	7.80	1.5				
11	353	8.96	1.5				
12	380	8.27	1				
13	360	8.27	1				
14	370	8.96	1.5				
15	360	8.27	2				
16	370	8.96	0.7				
17	380	8.27	2				
18	370	8.96	1.5				
19	370	8.96	1.5				
20	370	8.96	1.5				

3.5 Characterization of feedstocks and products

3.5.1 Boiling point distribution

Simulated distillation to calculate boiling point distribution was carried out in a Varian CP 3800 gas chromatographer (GC) coupled to a Varian CP8400 autosampler for injection. The basic principle of this analysis is to separate the components of the mixture based on their boiling points. The volatilized sample is carried by He (mobile phase) at 30mL/min through a capillary column in which the components of the sample are separated based on their partition time. The column has the following dimensions: length: 10 m; diameter: 0.53 mm; nominal film thickness: 0.88 mm. The temperature of the oven and detector were 380 °C and 375 °C, respectively. Following separation, the components are analyzed by a flame ionization detector (FID) which combust the gasses in the presence of H_2 (35 mL/min) and air (400 mL/min) releasing specific ions that are proportional to the concentration of the species in the gas mixture (Owusu-Boakye, 2005).

3.5.2 Nitrogen and sulfur analysis

Nitrogen and sulfur analysis were carried in an Antek 9000model: 9000NS. The nitrogen contents were analyzed by a combustion/chemiluminescence technique following ASTM 4629 procedure. The nitrogen groups are oxidized to nitric oxide (NO) at temperatures higher than 1000°C. Then, these groups react with ozone to produce metastable nitrogen dioxide species (NO_2*). When the latter species begin to decay, they emit energy in the form of light (chemiluminescence) which is detected by a photomultiplier at a specific wavelength (Owusu-Boakye, 2005).

The sulfur contents were analyzed by a combustion/fluorescence technique following ASTM 5463 procedure. When the sulfur contents of the sample are oxidized they are converted into sulfur dioxide (SO_2). The latter is then excited by UV light to produce an unstable SO_2^*. When SO_2^* starts to decay into its stable form, there is an emission of fluorescence which is detected by a photomultiplier (Mapiour, 2009). The chemistry of nitrogen and sulfur analysis is shown below.

$$R\text{-}N + R\text{-}S + O_2 \rightarrow CO_2 + H_2O + NO + SO_2 \quad (3.2)$$

$$SO_2 + hv' \rightarrow SO_2 + hv'' \quad (3.3)$$

$$NO + O_3 \rightarrow NO_2^* \rightarrow NO_2 + hv \quad (3.4)$$

The sulfur and nitrogen contents are calculated based on the following equation:

$$C_x(ppm) = \frac{(I - Y)}{S \times M^* \times K_g} \quad (3.5)$$

where: C_x is the concentration of sulfur or nitrogen species; I is the average integrated detector response for test specimen solution (counts); Y is the y-intercept of standard curve (counts); S is the slope of standard curve (counts/mg); M^* is the mass of test specimen solution injected; and K_g is the gravimetric dilution factor (g/g).

3.5.3 Analysis of aromatics content

Total aromatics content was analyzed by ^{13}C nuclear magnetic resonance spectroscopy at 500MHz in Fourier transform mode. The conditions for the analysis were inversed gate decoupling, sweep width of 27.7 kHz and a pulse delay of 4 seconds. Analysis of each sample took around 1.5 h for 2000 scans (Owusu-Boakye, 2005).

^{13}C has two orbital spins (½ and -½) in the presence of an external magnetic field. The latter has to be strong to obtain a valuable energy difference between these two spins. The samples for this analysis are placed in a special glass and radio frequencies (RF) are broadcasted through a coil that is situated around the glass. Each chemical species will absorb the RF to a different extent; therefore, the variation between the incoming and out coming frequencies allow the analysis of the composition of the sample. Tetramethylsilane is used as a standard to obtain a chemical shift to differentiate between saturated carbon (0-50ppm) and aromatic carbon (100-150 ppm) (Owusu-Boakye, 2005). The aromatic contents can be calculated by the following equation:

$$C_{Ar} = \frac{I_{Ar}}{I_{Ar} + I_{Sat}} \times 100 \quad (3.6)$$

where: C_{Ar} is the aromatics content; I_{Ar} is the the integral of total aromatics; I_{sat} is the integral of total saturates.

3.5.4 Measurements of hydrogen content

Hydrogen contents in liquid products and feedstocks were analyzed with an elemental analyzer. Samples are combusted at 1000 °C in excess of oxygen to form carbon dioxide and water; these products are then taken out from the combustion chamber by helium and passed through a copper metal to remove the oxygen that was not consumed during combustion. Finally, the compounds are quantified by a TCDs (thermal conductivity detectors).

3.5.5 Analysis of light hydrocarbons

The gas stream produced during hydrotreating was collected in a tedlar bag and then analyzed in a 7890A gas chromatograph. The instrument contains a complex valve system to carry the sample through five packed columns and one capillary column. In addition, the equipment contains a flame ionization detector (FID) for light hydrocarbons and a thermal conductivity detector (TCD) for hydrogen. Gas chromatography was used to measure the amount of feed cracked during hydrotreating in the form of C_1-C_4.

4 RESULTS AND DISCUSSION

4.1 Development of hydrogen consumption regression models during hydrotreating of gas oils

4.1.1 Hydrogen global mass balance

The global hydrogen mass balance (see equation 2.1) was calculated based on the hydrogen content in both gas and liquid streams. The global mass balances were calculated for KLGO and HLGO in the experiments carried at LHSV = 1 h^{-1} and LHSV = 2h^{-1} shown in the experimental matrix (Table 3.2). The mass balance for these experiments was in the range of 95.2-99.7 %. The data and results of the hydrogen mass balances are displayed in the appendices.

4.1.2 Experimental hydrogen consumption

H_2 consumption was determined by the analysis of H_2 content in liquid and gas streams at laboratory conditions; the laboratory average conditions were the following: T =23 °C and P = 96.0 kPa. The experimental data of H_2 consumption by gas analysis were transformed to normal conditions (T = 20 °C and P = 101.325 kPa) using equation 4.1 and will be reported as N m^3 H_2 / m^3 oil.

$$V_N = V \times \frac{P}{P_N} \times \frac{T_N}{T} \qquad (4.1)$$

where: V, P, and T are H_2 consumption, pressure, and temperature at laboratory conditions in m^3 H_2 / m^3 oil, kPa, and K, respectively. The subscript N represents normal laboratory conditions.

The major source of experimental error for the determination of H_2 consumption by gas and liquid analyses was related to to the gas flow rates and hydrogen concentrations, respectively.

Gas flow rates measured by a bubble flow meter presented an error of ± 3 mL/min which translated into a standard deviation of ± 2.1 N m^3 H_2/m^3 oil for H_2 consumption by gas analysis; flow rate measurement was carried out six times for each experimental run. In the case of H_2 consumption by liquid analysis, H_2 concentrations of liquids determined by the elemental analyzer varied significantly and the standard deviation of H_2 consumption by liquid analysis was ± 27 N m^3 H_2/ m^3 oil; H_2 concentrations were measured 2 times for each experimental run. The liquid analysis could have been inaccurate for the following reasons: H_2 tendency to escape from the products during stripping, the experimental setup could have retained some liquid in the section above the separator, and the elemental analyzer had issues to carry the samples to the combustion section.

H_2 consumption results based on gas and liquid analyses were compared with a method reported in the literature which determines H_2 consumption based on changes in the aromatics content; it is well known that most of the hydrogen is consumed by HDA. For instance, Owusu-Boakye (2005), removed 10.8 wt. % of aromatics in comparison with 1.68% of sulfur from an LGO blend at the following conditions: T (340-390 °C), P (6.9-12.4 MPa), LHSV (0.5-2.0 h^{-1}), and H_2/oil= 500 m^3 / m^3 . The method used for the comparison was shown in section 2.7.3 and it was adapted from Hisamitsu et al. (1976). The comparisons were performed with the experiments and feedstocks used for the H_2 global mass balances; the comparisons are shown in Figure 4.1 for HLGO and Figure 4.2 for KLGO.

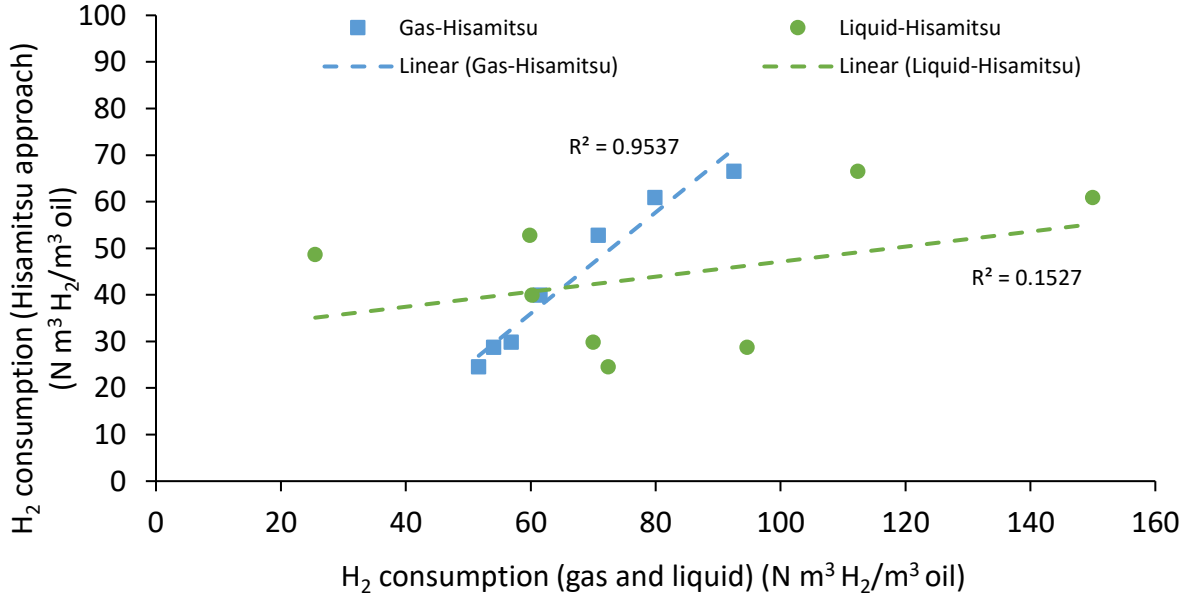

Figure 4.1 Comparison of methods to calculate H_2 consumption for HLGO

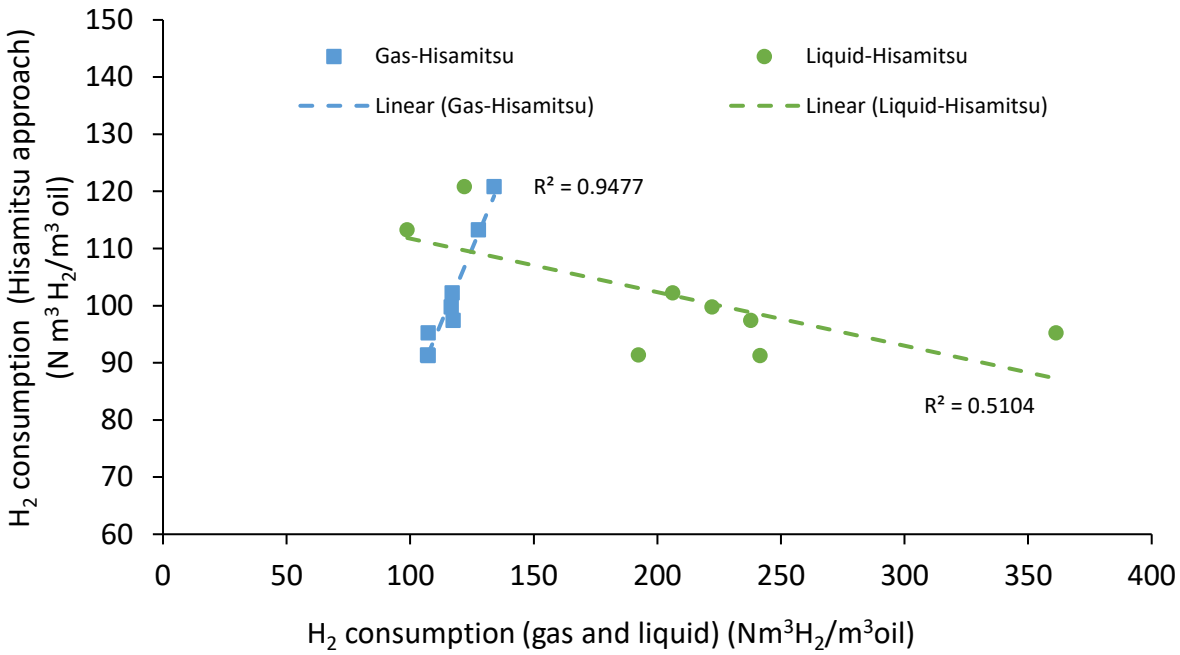

Figure 4.2 Comparison of methods to calculate H_2 consumption for KLGO

The data points shown in Figures 4.1 and 4.2 describe the relationships for H_2 consumption determined in the present study with gas analysis-Hisamitsu approach and liquid analysis-Hisamitsu approach. It can be seen in Figures 4.1 and 4.2 that the coordinates of the axes do not match for either of the correlations which means that these methods provide different predictions of H_2 consumption. However, there is a better agreement between gas analysis from the present study with Hisamitsu approach.

Based on the comparison between H_2 consumption methods and the standard deviations associated with gas and liquid analysis, the data and statements from this point forward regarding H_2 consumption are based on the gas analysis. Normal hydrogen consumption for the experiments given by the CCD are shown in Table 4.1 and there is a standard deviation of ±1.4 N m^3 H_2/m^3 oil between the control experiments.

Table 4.1 H_2 consumption by gas analysis during hydrotreating of VLGO, HLGO, KLGO, and PHTHGO

Run	T (^{0}C)	P (MPa)	LHSV (h^{-1})	H_2 consumption (N m^3 H_2 / m^3 oil)			
				VLGO	HLGO	KLGO	PHTHGO
1	370	8.96	1.5	89.8	67.1	123.1	48.9
2	380	9.65	2	80.5	68.1	117.5	29.9
3	387	8.96	1.5	80.5	62.3	105.1	51.6
4	370	8.96	1.5	87.9	68.5	127.2	47.5
5	360	9.65	2	93.2	54.1	107.3	26.6
6	370	10.12	1.5	90.9	74.3	115.8	46.4
7	360	9.65	1	103.1	79.9	117.0	27.1
8	370	8.96	2.3	87.5	60.6	101.8	34.7
9	380	9.65	1	90.3	92.6	127.6	40.6
10	370	7.80	1.5	59.9	63.0	113.2	43.8
11	353	8.96	1.5	94.8	56.3	86.0	35.4
12	380	8.27	1	81.0	70.8	134.0	36.0
13	360	8.27	1	98.3	61.5	107.0	23.9
14	370	8.96	1.5	88.8	70.2	124.5	49.1
15	360	8.27	2	91.1	51.7	113.1	26.3
16	370	8.96	0.7	92.2	81.4	131.2	50.3
17	380	8.27	2	77.1	56.9	116.6	33.6
18	370	8.96	1.5	87.7	69.4	125.6	46.9
19	370	8.96	1.5	89.1	69.0	126.1	48.3
20	370	8.96	1.5	87.2	69.5	125.2	48.4

Hydrogen consumption is affected by feedstock properties as shown in Figure 4.3. KLGO had maximum H_2 consumption among the feedstocks due to highest sulfur content and along with PHTHGO, these feeds had a higher content of aromatics than the other feeds. In case of VLGO and HLGO, it can be seen that VLGO consumed more H_2 than HLGO. Even though HLGO has higher aromatics content than VLGO, the latter may result in having less aromatics content in its products. Moreover, VLGO feedstock contains around 2 times more sulfur content than HLGO. PHTHGO feed consumed less H_2 in comparison with the others due to the pre-treatment of the feed which could have saturated most of the polyaromatics content. Thus, majorly leaving monoaromatics in the PHTHGO feed; it is well known that monoaromatics are more stable than polyaromatics and are hardly saturated at normal hydrotreating conditions.Furthermore, PHTHGO has less sulfur content that the other three feedstocks. In general, H_2 consumption had the following order: KLGO>VLGO>HLGO>PHTHGO.

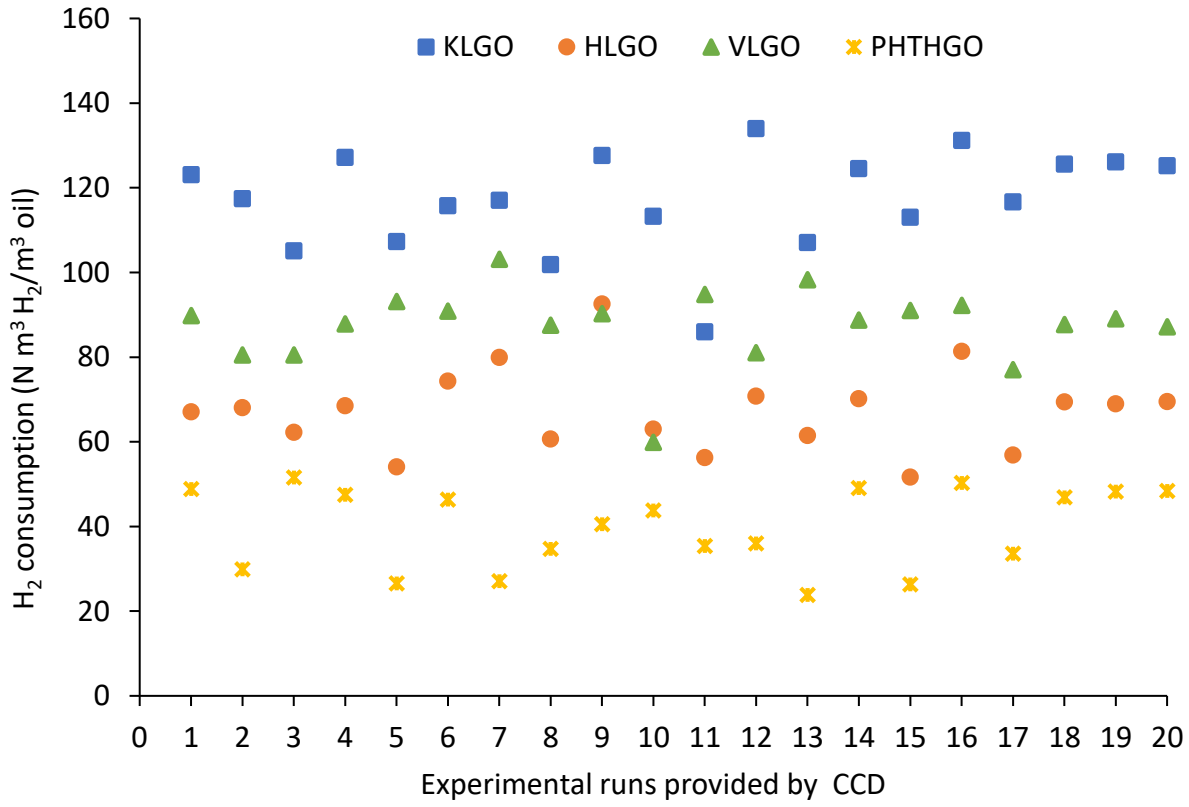

Figure 4.3 H_2 consumption comparison among feedstocks

4.1.3 Hydrogen consumption regression models

Statistical analysis was performed to develop regression models for H_2 consumption based on hydrotreating process variables. The experimental data of H_2 consumption was submitted to a test of significant factors. This test defines that a single factor or interaction between and within factors is significant when the p-value is lesser than 0.05 at a 95% confidence level. Then, the models were evaluated by an R^2 test which describes the variability of the model with respect to the experimental data. R^2 values range from 0 to 1; as R^2 approaches 1, the experimental data representation improves; this value increases along with the number of predictors. On the other hand, adjusted R^2 (Adj R^2) only improves if the variables or interactions are significant in the response of the model. Therefore, adjusted R^2 (Adj R^2) is most commonly used (Lazic, 2004). It is important to mention that the models presented in this work were obtained from different trials in which the factors or interactions were either eliminated or included to achieve the best value of Adj R^2. Furthermore, the models also considered T, P, or LHSV single terms if there was any interaction within or between these variables.The p-value test for H_2 consumption is shown in Table 4.2 and the empirical models for each feed are shown in Table 4.3.

Table 4.2 p-value test; H_2 consumption during hydrotreating of VLGO, HLGO, KLGO and PHTHGO

Factor or interaction	**p-value of factor or interaction**			
	VLGO	**HLGO**	**KLGO**	**PHTHGO**
T	<0.01	<0.01	<0.01	0.03
P	<0.01	<0.01	-	-
LHSV	0.05	<0.01	<0.01	-
$(T)^2$	-	<0.01	<0.01	0.03
$(P)^2$	0.01	-	-	-
$(LHSV)^2$	-	-	-	0.02
T * P	-	-	-	-
T * LHSV	-	-	-	-
P*LHSV	-	0.01	-	-

Table 4.3 H_2 consumption regression models for VLGO, HLGO, KLGO and PHTHGO

Feed	Model	R^2	Adj R^2
VLGO	H_2 consumption (N m^3 H_2/m^3 oil) = -377 - 0.59×T + 147.5×P - 5.68×LHSV - 7.81× (P^2)	0.77	0.71
HLGO	H_2 consumption (N m^3 H_2/m^3 oil) = -4822 + 25.12×T + 22.14×P+ 70.1×LHSV - 33.44×10^{-3} × (T^2) - 9.61× (P×LHSV)	0.92	0.89
KLGO	H_2 consumption (N m^3 H_2/m^3 oil) = -11349 + 61.5×T -11.79×LHSV - 8.23×10^{-2} × (T^2)	0.77	0.72
PHTHGO	H_2 consumption (N m^3 H_2/m^3 oil) = -6811 + 32.9×T + 144.7×P + 51.4×LHSV - 43.8×10^{-3} ×(T^2) - 8.03×(P^2) - 18.94×($LHSV^2$)	0.63	0.47

The experimental data of H_2 consumption for all the feeds was used to build a general model; it was assumed that in case of a mixture, each feed contributes to the total H_2 consumption in the same proportion. The statistical analysis of the combined data results in the model shown in equation 4.2. This composite model has an Adj R^2 of 0.98 and a standard error of ± 1.02 N m^3 H_2/m^3 oil.

$$H_2\text{consumption}\left(\text{N } {}^{m^3H_2}\!/_{m^3\text{oil}}\right) = -5837 + 28.85\times T + 96.5\times P + 132.8\times LHSV - 3.82\times 10^{-2}\times\left(T^2\right) - 4.74\times(P^2) - 3.27\times(LHSV^2) - 0.24\times(T\times LHSV) - 4.97\times(P\times LHSV) \quad (4.2)$$

The composite model (equation 4.2) was tested experimentally and compared with models and values reported in the literature. The feedstock for the experiments was a mixture of VLGO, KLGO, and HLGO at the same volumetric proportion. Two experiments at conditions not provided by the CCD were performed for this purpose. The conditions were the following: T = 365 °C and 375 °C, P = 9.31 MPa, LHSV = 1.2h^{-1}, and H_2/oi l= 600 N m^3/m^3. The mixture had a density of 0.88 gr/cm^3, 1.56 % sulfur, 0.107 % nitrogen, and 23.95 % aromatics. The hydrotreating conversions and dissolved H_2 during hydrotreating of the mixture are shown in Table 4.4.

Table 4.4 HDS, HDN, and HDA conversions, and H_2 consumption during hydrotreating of LGOs mixture.

Exp. Run	Experimental conditions			HDS (%)	HDN (%)	HDA (%)	Dissolved H_2 (N m^3 H_2/m^3 oil)
	T(°C)	P(MPa)	LHSV(h^{-1})				
1	365	9.31	1.2	94.0	95.9	28.5	10.7
2	375	9.31	1.2	96.1	97.7	26.5	9.8

The experimental H_2 consumption of the mixture was compared with the three models and values reported in the literature. Hisamitsu et al. (1976) and Lee et al. (2008) models were shown in section 2.7.3; meanwhile, Edgar(1993) published the following H_2 consumption data for each hydrotreating reaction: HDS=13.4 N m^3 H_2/m^3 oil per each 1 wt. % removed; HDN= 57.9 Nm^3 H_2/m^3 oil per each 1 wt. % removed; HDA= 4.81 N m^3 H_2/m^3 oil per each 1wt. % removed. The usage of the model developed by Lee et al. (2008) was made based on the following assumptions: HDO, olefins saturation and saturation of monoaromatics were not taken into account. Also, the density of the products was equal to the density of the feed, and liquid product yield was equal to 1. To improve the prediction of the models obtained from the literature, dissolved hydrogen during hydrotreating of VLGO, KLGO, and HLGO calculated on HYSYS was added to the chemical H_2 consumption. The comparison is shown in Table 4.5 and it can be noted that the regression model was able to predict H_2 consumption more precisely than the other three models.

Table 4.5 Comparison between H_2 consumption models for hydrotreating of petroleum fractions

		H_2 consumption (Nm^3H_2/m^3 oil)			
Exp. Run	**Experimental H_2 consumption (Nm^3 H_2/m^3 oil)**	**Composite regression model**	**Edgar (1993)**	**Hisamitsu et al. (1976)**	**Lee et al. (2008)**
1	101.3	85.2	68.1	76.4	68.8
2	100.2	88.1	64.3	71.7	67.4

4.2 Effects of temperature, pressure, and LSHV on hydrotreating conversions and optimization of process conditions during hydrotreating of gas oils

In this section, the effects of processing variables on hydrotreating conversions were studied for VLGO, HLGO, KLGO and PHTHGO for the experimental runs provided by CCD. After carrying the experiments, regression models were developed to estimate the best sets of conditions to process each feedstock; giving maximum HDS, HDN, and HDA conversions.

4.2.1 Effects of temperature, pressure, and LSHV on HDA conversions

Hydrodearomatization (HDA) reaction consumes more hydrogen than HDS and HDN during hydrotreating. Therefore, the effects of process conditions on this reaction were examined first. The experimental data of HDA conversions for each feed is shown in Table 4.6 and the standard deviation for HDA conversions was in the range of ±0.3-1.0%; catalyst deactivation was not observed. The conversion of the data point in which maximum conversion was achieved for each feedstock into the amount of aromatics removed from each feed gives the following results: KLGO= 11.4%; VLGO=10.3%; HLGO=9.0%; PHTHGO= 6.1%. These results confirm the H_2 consumption trend indicated in section 4.1.2.

The statistical analysis and regression models for HDA conversions are shown in Tables 4.7 and 4.8, respectively. It can be noted that the regression analysis shows no interaction between process variables; therefore, the analysis of the effects of process conditions on HDA was carried out by analyzing the experimental data at the following conditions: T = 353,370, and 387 °C; P = 7.80, 8.96, and 10.12 MPa; LHSV = 0.7, 1.5, and 2.3 h^{-1} as shown in Figures 4.4-4.6.

Table 4.6 HDA conversions during hydrotreating of VLGO, HLGO, KLGO, and PHTHGO

Run	T (^{0}C)	P (MPa)	LHSV (h^{-1})	HDA (wt. %)			
				VLGO	HLGO	KLGO	PHTHGO
1	370	8.96	1.5	42.5	27.8	32.0	19.2
2	380	9.65	2	40.1	26.0	29.8	10.9
3	387	8.96	1.5	34.3	20.8	24.9	20.4
4	370	8.96	1.5	43.4	28.6	32.6	19.9
5	360	9.65	2	46.3	12.9	27.8	10.6
6	370	10.12	1.5	46.1	31.8	32.5	20.1
7	360	9.65	1	50.8	33.8	32.2	9.1
8	370	8.96	2.3	42.2	21.3	22.9	13.7
9	380	9.65	1	42.2	37.4	36.4	14.4
10	370	7.80	1.5	27.1	23.0	29.6	19.8
11	353	8.96	1.5	47.9	15.5	25.5	13.3
12	380	8.27	1	37.5	28.4	39.4	13.0
13	360	8.27	1	47.7	20.1	27.5	8.8
14	370	8.96	1.5	43.7	27.4	31.8	18.9
15	360	8.27	2	45.7	10.3	29.3	10.2
16	370	8.96	0.7	45.7	34.9	38.5	20.9
17	380	8.27	2	36.4	13.5	31.0	12.2
18	370	8.96	1.5	42.6	28.9	31.5	19.0
19	370	8.96	1.5	43.1	28.3	32.7	19.6
20	370	8.96	1.5	42.9	28.5	32.8	19.5

Table 4.7 p-value test for HDA conversions during hydrotreating of VLGO, HLGO, KLGO and PHTHGO

Factor or interaction	p-value of factor or interaction			
	VLGO	**HLGO**	**KLGO**	**PHTHGO**
T	<0.01	<0.01	<0.01	-
P	<0.01	<0.01	-	-
LHSV	-	<0.01	<0.01	-
$(T)^2$	-	<0.01	<0.01	<0.01
$(P)^2$	-	-	-	-
$(LHSV)^2$	-	-	-	-
T * P	-	-	-	-
T * LHSV	-	-	-	-
P*LHSV	-	-	-	-

Table 4.8 HDA regression models for VLGO, HLGO, KLGO, and PHTHGO

Feed	**Model**	**R^2**	**Adj R^2**
KLGO	HDA (%) = -2613 + 14.21×T - 6.43×LHSV - $1.90\times10^{-2}\times(T^2)$	0.66	0.60
HLGO	HDA (%) = -5320 + 28.46×T + 5.59×P - 11.7×LHSV – $3.81\times10^{-2}\times (T^2)$	0.90	0.87
VLGO	HDA (%) = 155.8 - $4.19\times10^{-2}\times$T + 4.63×P	0.78	0.74
PHTHGO	HDA (%) =-3593 + 17.7×T + 51.6×P + 99×LHSV – $23.2\times10^{-2}\times (T^2)$ - 2.57× (P^2) - 8.64× $(LHSV^2)$ - 0.01× (T×P) - 0.18× (T×LHSV) – 0.94× (P×LHSV)	0.65	0.33

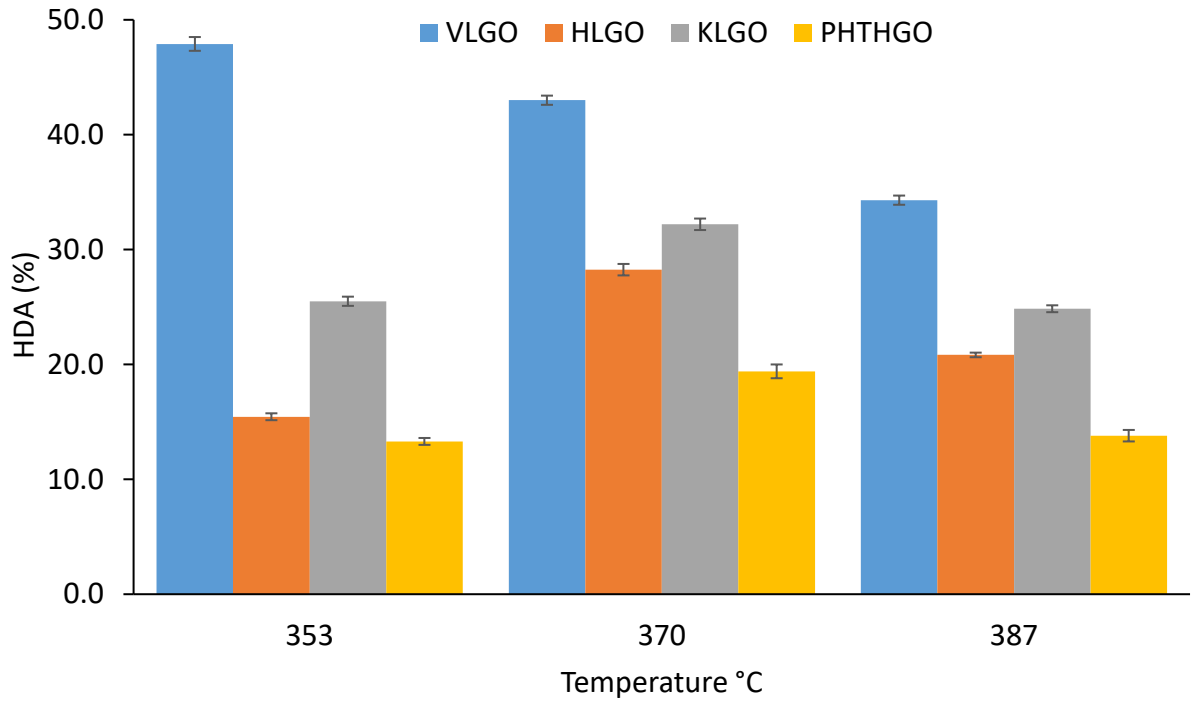

Figure 4.4 Effects of temperature on HDA conversions during hydrotreating of VLGO, HLGO, KLGO, and PHTHGO. Pressure and LHSV constant at 8.96 MPa and 1.5 h^{-1},

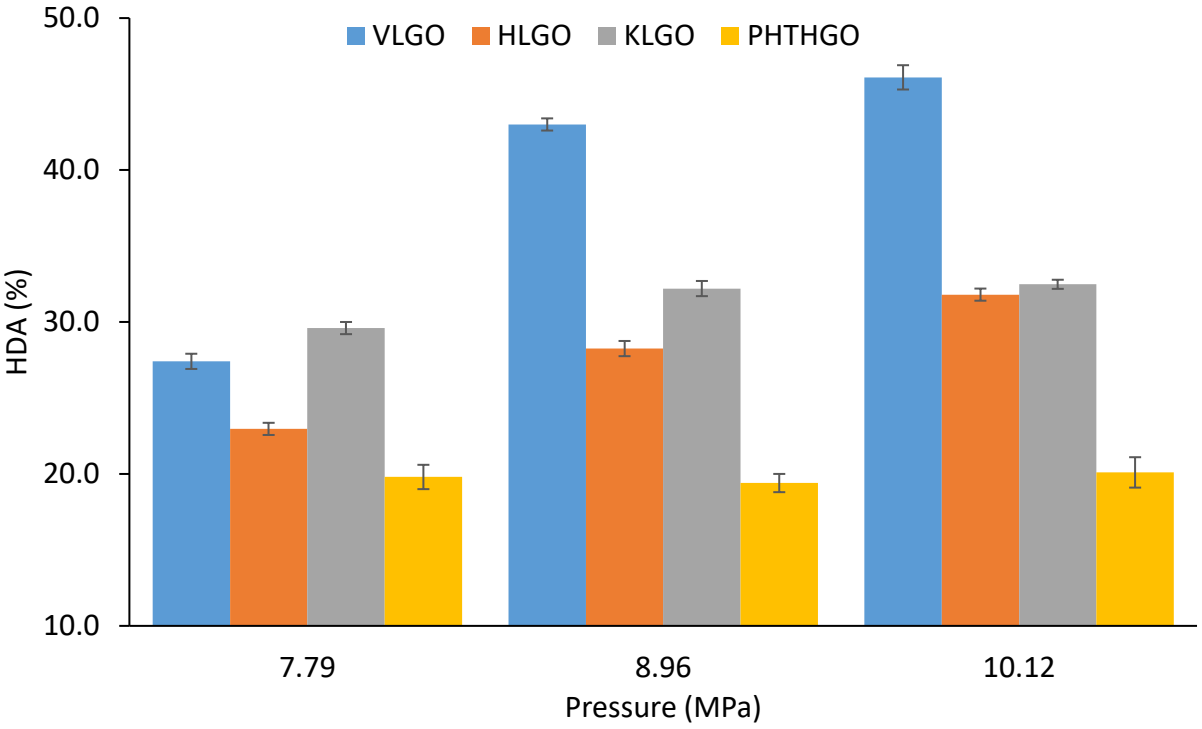

Figure 4.5 Effects of pressure on HDA conversions during hydrotreating of VLGO, HLGO, KLGO, and PHTHGO. Temperature and LHSV constant at 370 °C and 1.5 h^{-1}, respectively

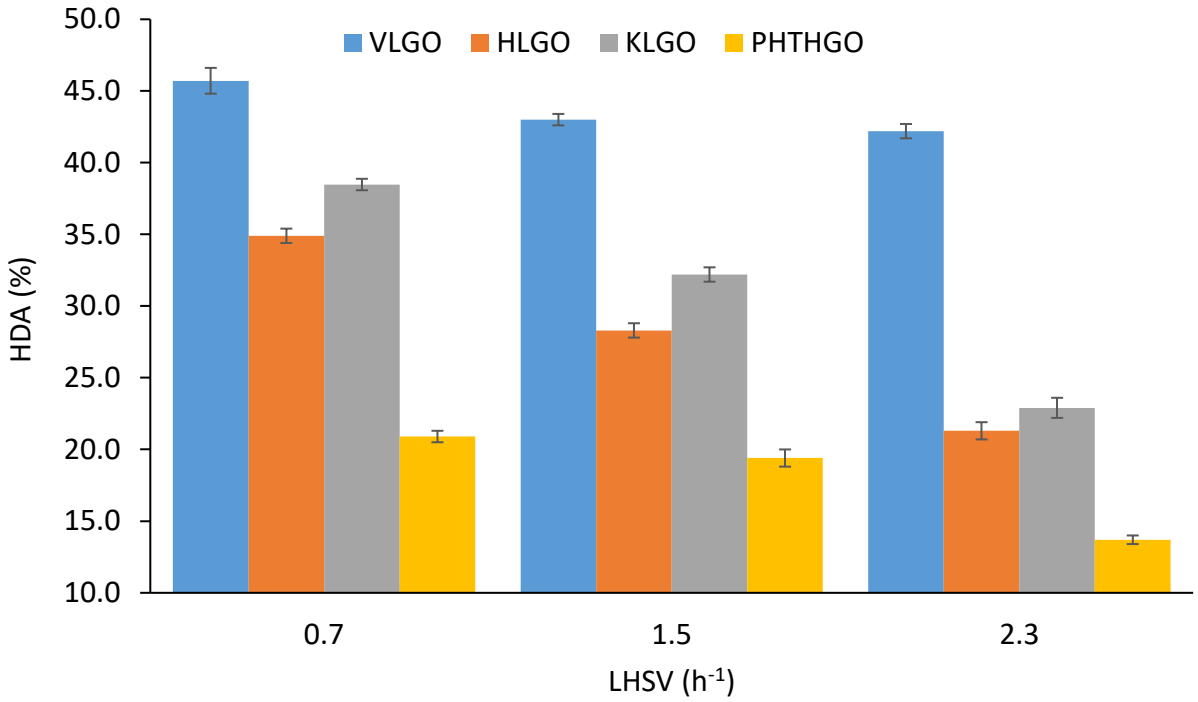

Figure 4.6 Effects of LHSV on HDA conversions during hydrotreating of VLGO, HLGO, KLGO, and PHTHGO. Temperature and pressure constant at 370 °C and 8.96 MPa, respectively.

HDA is a reaction limited at high temperatures due to the reversibility nature of hydrogenation (Gary et al., 2007). The equilibrium will shift in such a way that the reaction will produce more aromatic compounds instead of producing saturation (Owusu-Boakye et al., 2006). Temperature limits can be observed for each feedstock in Figure 4.4. Owusu-Boakye et al. (2006) found out that the optimum temperature to carry HDA during hydrotreating of an LGO blend was 379°C. Meanwhile, Chandra-Mouli & Dalai (2009) noted that this negative effect of temperature on HDA conversions began at 300°C when processing pre-hydrotreated LGO with an aromatics content of 16.4 % wt. Specific temperature limits will be reported in the optimization section of this work.

In case of LHSV, it can be observed in Figure 4.6 that increasing LHSV led to a decrease in HDA conversions for all the feedstocks. Mapiour et al. (2010) found a similar trend during hydrotreating of heavy gas oil under similar conditions. In contrast, when statistical analysis was performed, LHSV did not show a significant effect on HDA conversions for VLGO and PHTHGO. Mann et al. (1987) also found out that residence time had a non-significant effect on HDA

conversions during hydrotreating of coker naphtha at the following conditions: T = 300-450 °C, P = 4.24-12.51 MPa, and LHSV= 0.5-4 h^{-1}.

The role of pressure on HDA conversions for this study is discussed below. It can be seen in Figure 4.5 that increasing pressure did not show an improvement on HDA of KLGO at 8.96-10.12 MPa and in case of PHTHGO, increasing pressure did not improve aromatics saturation at any of the conditions employed in this work. These effects may be due to the aromatic groups present in these feeds. KLGO originates from coking processes in which big amounts of aromatics compounds and olefins are produced (Aoyagi et al., 2003). Furthermore, coking processes vacuum residue which may contain high contents of monoaromatics. These compounds may not be completely saturated at the conditions employed in this work. In case of PHTHGO, the primary hydrotreating process could have saturated most of the polyaromatics compounds which result in a lower HDA efficiency for this study. On the other hand, pressure had a positive effect on HDA conversions during hydrotreating of HLGO and VLGO; HDA is favored by high H_2pp due to the hydrogenation mechanism taken by aromatic compounds.

4.2.2 Effects of temperature, pressure, and LSHV on HDS of gas oils

The experimental data for HDS for each feedstock is shown in Table 4.9 and the standard deviation for HDS conversions was in the range of ±0.3-1.5%. The effects of process conditions on HDS were studied in two forms. First, the independent or single effects of temperature, pressure, and LSHV on HDS conversions were studied by analyzing the experimental data at the following conditions: T = 353,370, and 387 °C; P = 7.80, 8.96, and 10.12 MPa; LHSV = 0.7, 1.5, and 2.3 h^{-1}; the graphical representation of independent effects of process conditions on HDS conversions is presented as final sulfur content in products (sulfur removal) in terms of ppm for a better visuality of the trends; the standard deviation in terms of ppm was ± 3.3-418 ppm. Second, in case of interaction between variables provided by the regression models, Minitab software was used to develop graphs that show the corresponding interactions. The statistical analysis and regression models for HDS conversions are shown in Tables 4.10 and 4.11, respectively.

Table 4.9 HDS conversions during hydrotreating of VLGO, HLGO, KLGO, and PHTHGO

Run	T (^{0}C)	P (MPa)	LHSV (h^{-1})	HDS (wt. %)			
				VLGO	HLGO	KLGO	PHTHGO
1	370	8.96	1.5	96.0	88.2	97.3	65.3
2	380	9.65	2	92.0	89.7	98.0	68.9
3	387	8.96	1.5	97.6	90.7	98.9	79.8
4	370	8.96	1.5	95.5	87.8	96.8	64.5
5	360	9.65	2	88.9	87.5	93.4	51.6
6	370	10.12	1.5	96.1	91.4	97.4	66.8
7	360	9.65	1	97.8	92.7	93.8	66.0
8	370	8.96	2.3	93.0	85.3	96.2	54.6
9	380	9.65	1	96.3	94.4	96.8	79.6
10	370	7.80	1.5	95.5	87.1	97.5	64.8
11	353	8.96	1.5	95.2	85.0	93.9	48.1
12	380	8.27	1	97.5	93.1	97.9	76.8
13	360	8.27	1	98.8	90.8	95.9	68.8
14	370	8.96	1.5	96.4	89.1	96.3	64.4
15	360	8.27	2	92.2	86.4	95.3	50.1
16	370	8.96	0.7	97.6	89.9	98.1	66.7
17	380	8.27	2	94.6	89.4	96.3	65.0
18	370	8.96	1.5	96.1	88.5	98.2	64.8
19	370	8.96	1.5	96.9	88.8	97.1	65.2
20	370	8.96	1.5	97.2	87.8	98.3	64.9

Table 4.10 p-value test for HDS activities during hydrotreating of VLGO, HLGO, KLGO, and PHTHGO

Factor or interaction	p-value of factor or interaction			
	VLGO	**HLGO**	**KLGO**	**PHTHGO**
T	0.02	<0.01	<0.01	<0.01
P	-	0.04	-	-
LHSV	<0.01	<0.01	-	<0.01
$(T)^2$	-	-	-	-
$(P)^2$	-	-	-	-
$(LHSV)^2$	-	-	-	-
T * P	-	-	0.04	-
T * LHSV	<0.01	-	-	-
P*LHSV	-	-	-	-

Table 4.11 HDS regression models for VLGO, HLGO, KLGO, and PHTHGO

Feed	Model	R^2	Adj R^2
KLGO	HDS (%) = -270 + 3.25×T - 53.50×P - 19.90×LHSV - $58.70\times10^{-4}\times (T^2)$ + 0.136× (T×P) + 2.10× (P×LHSV)	0.70	0.55
HLGO	HDS (%) = 32.80 + 0.14×T + 1.25×P - 3.77×LHSV	0.71	0.66
VLGO	HDS (%) = 199.20 - 0.26×T - 81.20×LHSV + 0.21 × (T×LHSV)	0.73	0.67
PHTHGO	HDS (%) = -208.70 + 0.78×T - 11.12× LHSV	0.90	0.89

The processing variables affect gas oils to different extents depending on their composition and properties. An increase in temperature improved sulfur removal for all the feedstocks as it can be seen in Figure 4.7. Similarly, the temperature was a significant factor in the statistical analysis for all the feedstocks as shown in Table 4.10. This general trend has been observed by many works related to hydrotreating of several petroleum fractions (Yui & Chan, 1992; Bej et al., 2007). Yui & Chan (1992) reported that during hydrotreating of coker naphtha with a NiMo catalyst at T = 140-280 °C, P = 3-5 MPa, LHSV = 1-2 h^{-1} and G/O=600 m^3/m^3, HDS conversions increased with an increase in temperature. In addition, the authors found that pressure did not have any significant effect on HDS conversions.

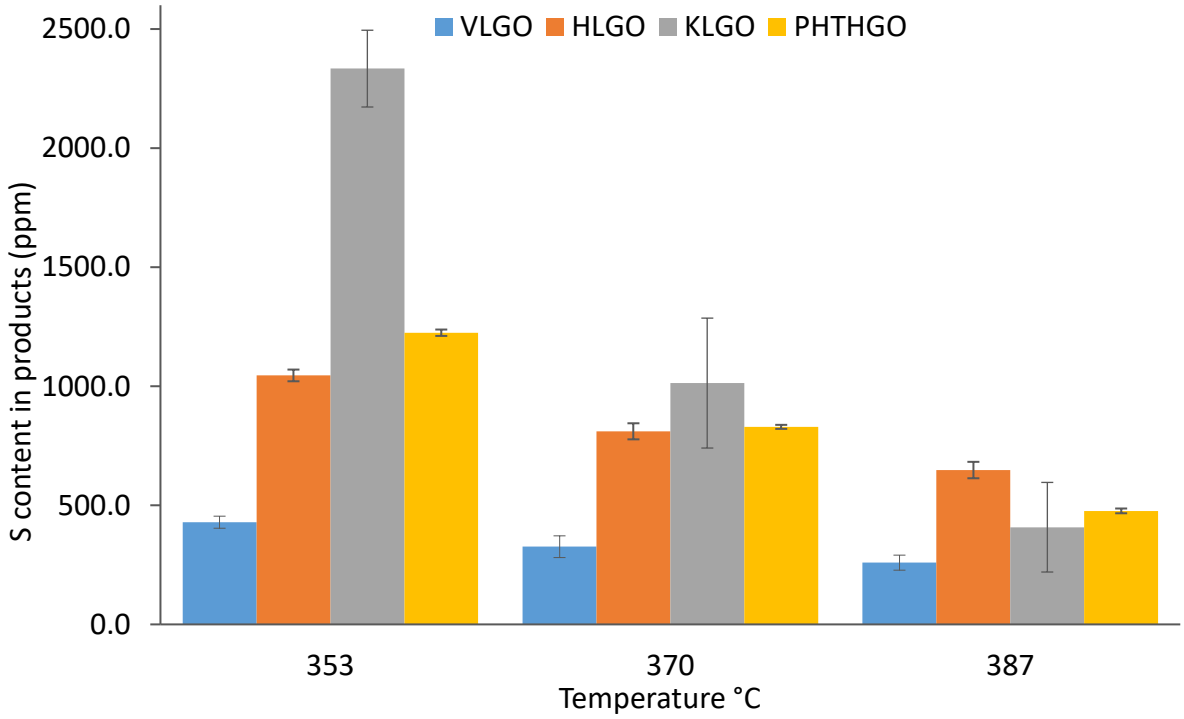

Figure 4.7 Effects of temperature on sulfur removal during hydrotreating of VLGO, HLGO, KLGO, and PHTHGO. Pressure and LHSV constant at 8.96 MPa and 1.5 h^{-1}, respectively

Figure 4.8 shows that the positive effect of pressure on sulfur removal was only clear for HLGO. The latter statement is also supported by the p-value test. In case of KLGO, the statistical analysis shows a significant interaction between pressure and temperature on HDS conversions.

This effect is shown graphically in Figure 4.9. The surface plot in Figure 4.9 (a) shows that changes in both temperature and pressure at constant LHSV had an impact on HDS conversions. These plots may be difficult to read; therefore, it is advised to include an interaction plot which is shown in Figure 4.9 (b); interaction terms are significant when the trend lines of an interaction plot are not parallel. Girgis & Gates (1991) stated that HDS reaction may proceed by two mechanisms: direct scission of the C-S bond by hydrogenolisis, or hydrogenation of an unsaturated bond followed by hydrogenolisis, the former reaction is reversible. This means that the removal of sulfur for KLGO could have been limited by hydrogenation due to the temperature limits that are shown in Figure 4.9. Moreover, NiMo catalyst is reported to achieve high hydrogenation activities (Aoyagi et al., 2003; Knudsen et al., 1999).

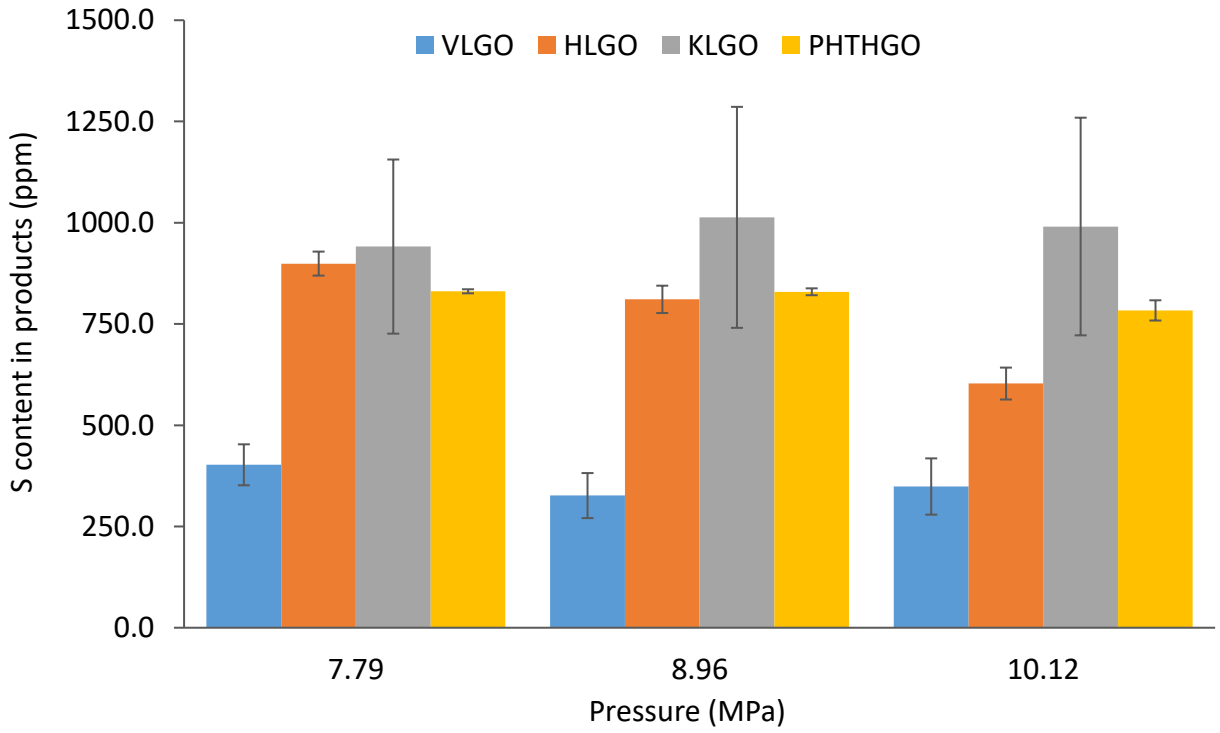

Figure 4.8 Effects of pressure on sulfur removal during hydrotreating of VLGO, HLGO, KLGO, and PHTHGO. Temperature and LHSV constant at 370 °C and 1.5 h^{-1}, respectively

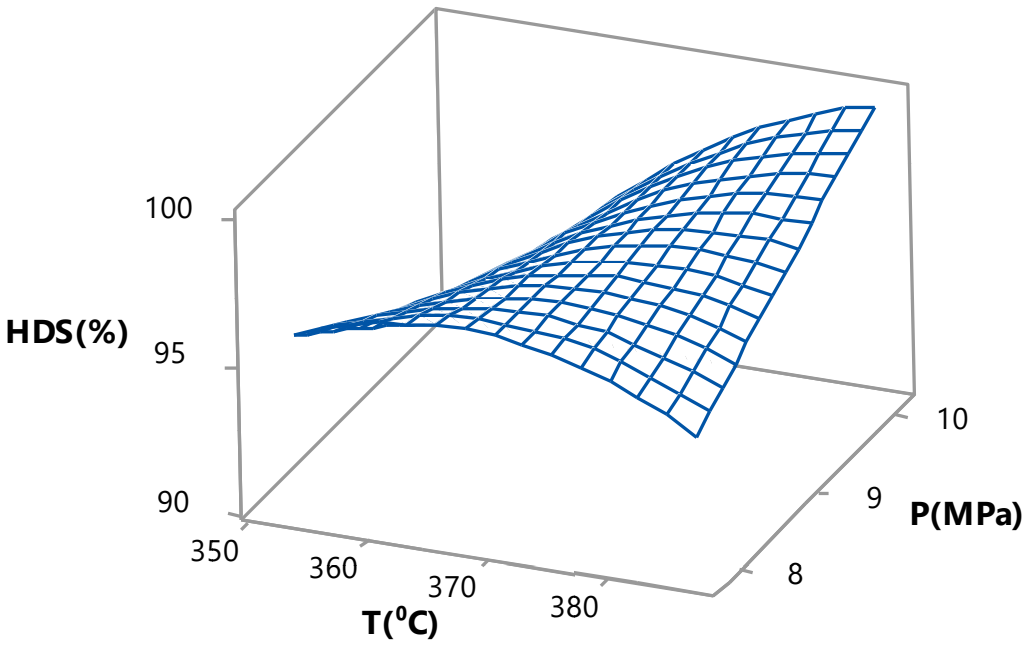

(a)

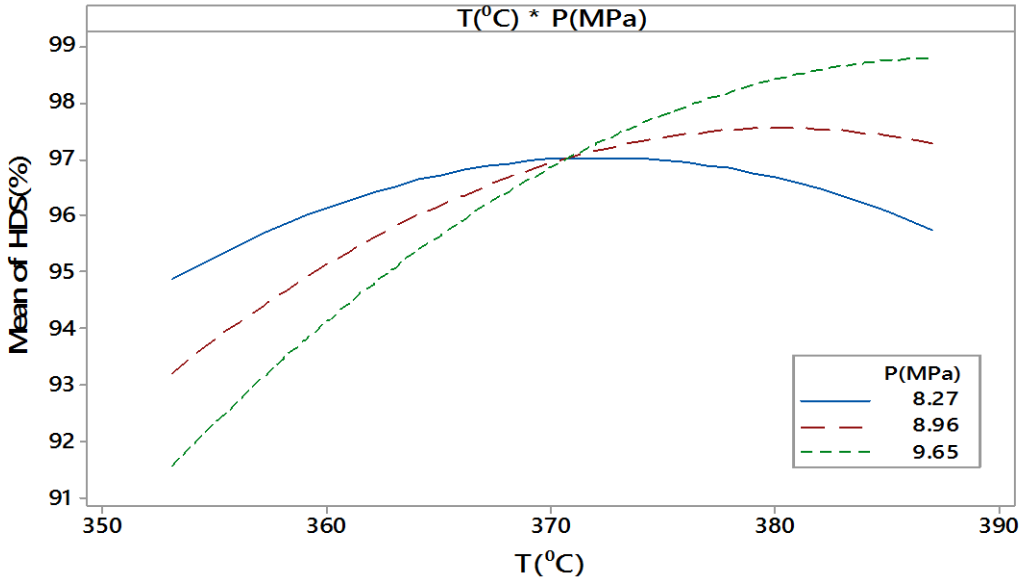

(b)

Figure 4.9 Surface plot (a) and Interaction plot (b) of effects of temperature and pressure on HDS conversions at LHSV = 1.5 h^{-1} for KLGO

In case of LHSV, Figure 4.10 shows that any increase in LHSV had a negative effect on the sulfur removal for all the feeds. This effect is due to less residence time of the reactants in the reactor (Bej et al., 2007; Botchwey et al., 2003). Moreover, the regression analysis displayed in Table 4.10 indicates that temperature and LHSV had a joint effect on HDS conversions for VLGO. According to Figure 4.11, HDS is taking place in excess at LHSV= 1 h^{-1}; therefore, any further increase in temperature has a negative effect on HDS conversions. Meanwhile, at higher LHSV, the temperature continues to have a positive effect on HDS because the reaction is not being limited by equilibrium. The regression analysis also indicates that LHSV did not have any effect on HDS conversions for KLGO; however, Figure 4.10 shows the contrary. It is important to note that the trends provided by the models are not completely accurate; the models have an Adj R^2 in the following range: 0.55-0.89.

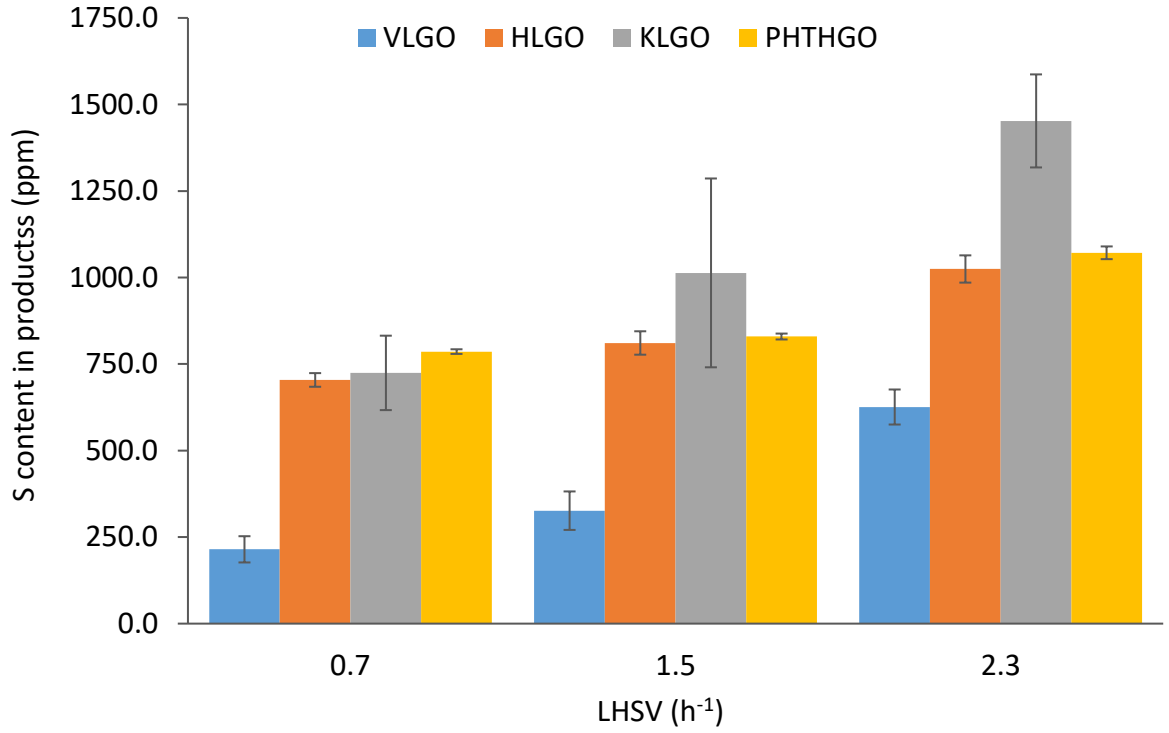

Figure 4.10 Effects of LHSV on sulfur removal during hydrotreating of VLGO, HLGO, KLGO, and PHTHGO. Temperature and pressure constant at 370 °C and 8.96 MPa,

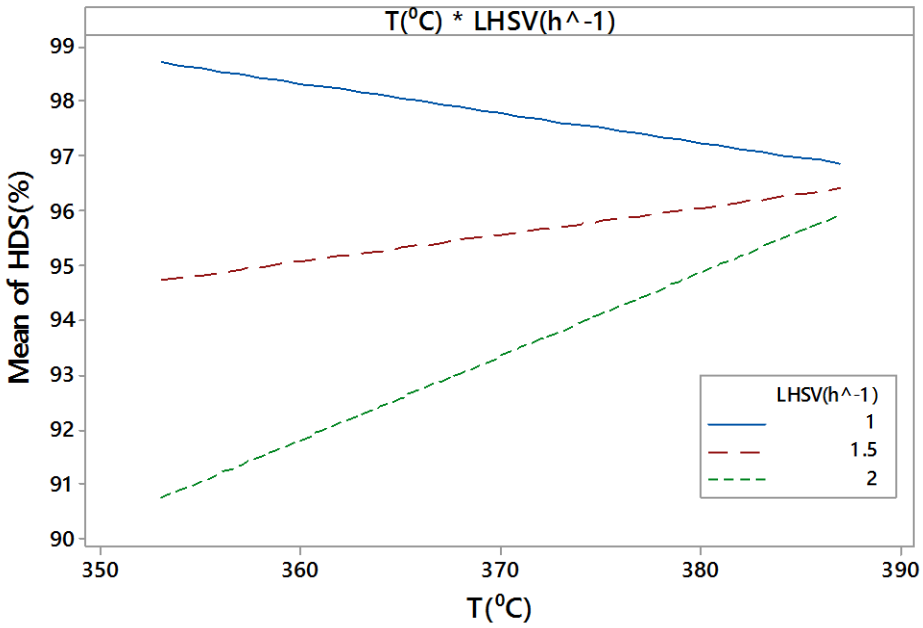

Figure 4.11 Interaction plot of the effects of temperature and LHSV on HDS conversions during hydrotreating of VLGO. Pressure constant at 8.96 MPa

4.2.3 Effects of temperature, pressure, and LSHV on HDN conversions

The experimental data for HDN conversions during hydrotreating of each feedstock is shown in Table 4.12 and the standard deviation for HDN conversions was in the range of ±0.3-1.2%. The statistical analysis and regression models for HDN conversions are shown in Tables 4.13 and 4.14. Similar to HDS conversions, the independent effects of process conditions on HDN were studied with the experimental data at the same conditions as mentioned in section 4.2.2. Meanwhile, the interactions between process variables were studied by analyzing the trends provided by the HDN regression models.

Table 4.12 HDN conversions during hydrotreating of VLGO, HLGO, KLGO, and PHTHGO

Run	T (^{0}C)	P (MPa)	LHSV (h^{-1})	HDN (wt. %)			
				VLGO	HLGO	KLGO	PHTHGO
1	370	8.96	1.5	96.1	90.8	92.7	68.4
2	380	9.65	2	99.5	88.3	96.4	67.3
3	387	8.96	1.5	99.4	96.9	98.2	69.8
4	370	8.96	1.5	96.8	92.3	93.5	66.9
5	360	9.65	2	98.5	89.2	85.1	65.2
6	370	10.12	1.5	99.6	93.4	96.3	68.7
7	360	9.65	1	99.9	94.9	94.7	69.0
8	370	8.96	2.3	94.2	84.9	84.6	65.0
9	380	9.65	1	99.9	97.9	98.3	73.1
10	370	7.80	1.5	93.5	90.2	88.2	66.2
11	353	8.96	1.5	95.2	83.4	82.4	65.4
12	380	8.27	1	99.9	97.0	98.1	70.1
13	360	8.27	1	98.3	90.7	92.9	67.6
14	370	8.96	1.5	96.9	90.9	93.1	66.6
15	360	8.27	2	89.7	85.2	75.0	64.5
16	370	8.96	0.7	99.1	96.5	98.0	72.1
17	380	8.27	2	96.5	88.0	87.4	65.4
18	370	8.96	1.5	96.2	91.6	92.8	67.4
19	370	8.96	1.5	97.0	91.1	92.9	67.0
20	370	8.96	1.5	96.8	92.0	93.9	67.1

Table 4.13 p-value test for HDN conversions during hydrotreating of VLGO, HLGO, KLGO, and PHTHGO

Factor or interaction	p-value of factor or interaction			
	VLGO	HLGO	KLGO	PHTHGO
T	<0.01	<0.01	<0.01	<0.01
P	<0.01	<0.01	<0.01	<0.01
LHSV	<0.01	<0.01	<0.01	0.04
$(T)^2$	-	-	<0.01	-
$(P)^2$	-	-	-	-
$(LHSV)^2$	-	-	<0.01	0.01
T * P	<0.01	-	-	-
T * LHSV	0.02	-	<0.01	0.02
P*LHSV	<0.01	-	<0.01	-

Table 4.14 HDN regression models for VLGO, HLGO, KLGO, and PHTHGO

Feed	Model	R^2	Adj R^2
KLGO	HDN (%) = -1462 + 8.09×T + 25.50×P - 194.40×LHSV - 1.05 × (T^2) - 0.75× (P^2) - 2.72× $(LHSV^2)$ - 4.74×10^2× (T×P) + 0.37× (T×LHSV) + 6.18× (P×LHSV)	0.99	0.98
HLGO	HDN (%) = -527 + 1.66×T + 48.50×P + 61.20×LHSV - 12.68×10^{-2}× (T×P) - 0.19× (T×LHSV)	0.91	0.88
VLGO	HDN (%) = -267 + 1.07×T + 45.90×P - 94.10×LHSV - 0.13× (T×P) + 0.16× (T×LHSV) + 3.70× (P×LHSV)	0.93	0.90
PHTHGO	HDN (%) = 139.1 - 0.195×T + 17.58×P + 23.90×LHSV + 1.70× $(LHSV^2)$ + 50.7×10^{-3}× (T×P) - 0.09× (T×LHSV)	0.97	0.96

In general, HDN conversions improve with increasing temperature and pressure. Meanwhile, any decrease on the residence time will affect HDN conversions negatively (Girgis & Gates, 1991). As it can be observed in Figures 4.12-4.14, HDN conversions for all the feedstocks followed this general trend. In addition, the interaction between processing variables affected HDN conversions for VLGO, KGLO, and PHTHGO. Figures 4.15 and 4.16 show that changes in temperature and pressure were more significant at higher values of LHSV to compensate the lesser residence time. Pressure and temperature effects for KLGO shown in Figure 4.15 plateau at high levels of conversion. This means that the reaction passes through a maximum due to equilibrium limitations; HDN takes place by hydrogenation followed by C-N bond scission (Angelici, 1997).

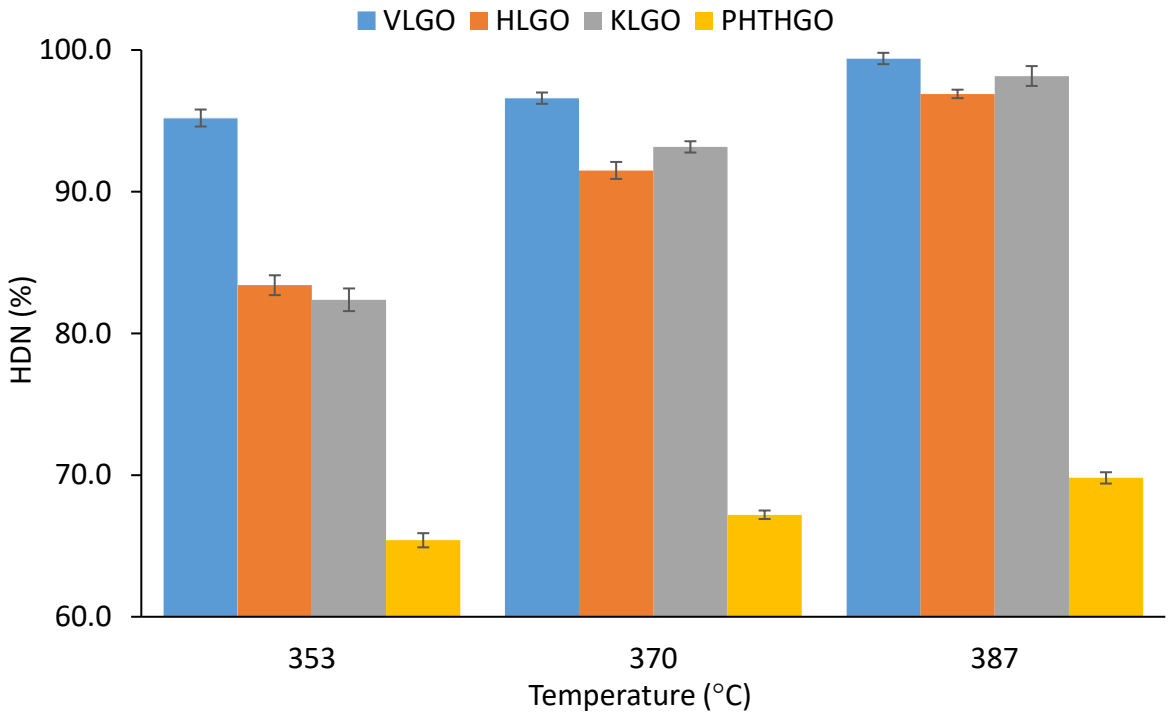

Figure 4.12 Effects of temperature on HDN conversions during hydrotreating of VLGO, HLGO, KLGO, and PHTHGO. Pressure and LHSV constant at 8.96 MPa and 1.5 h^{-1},

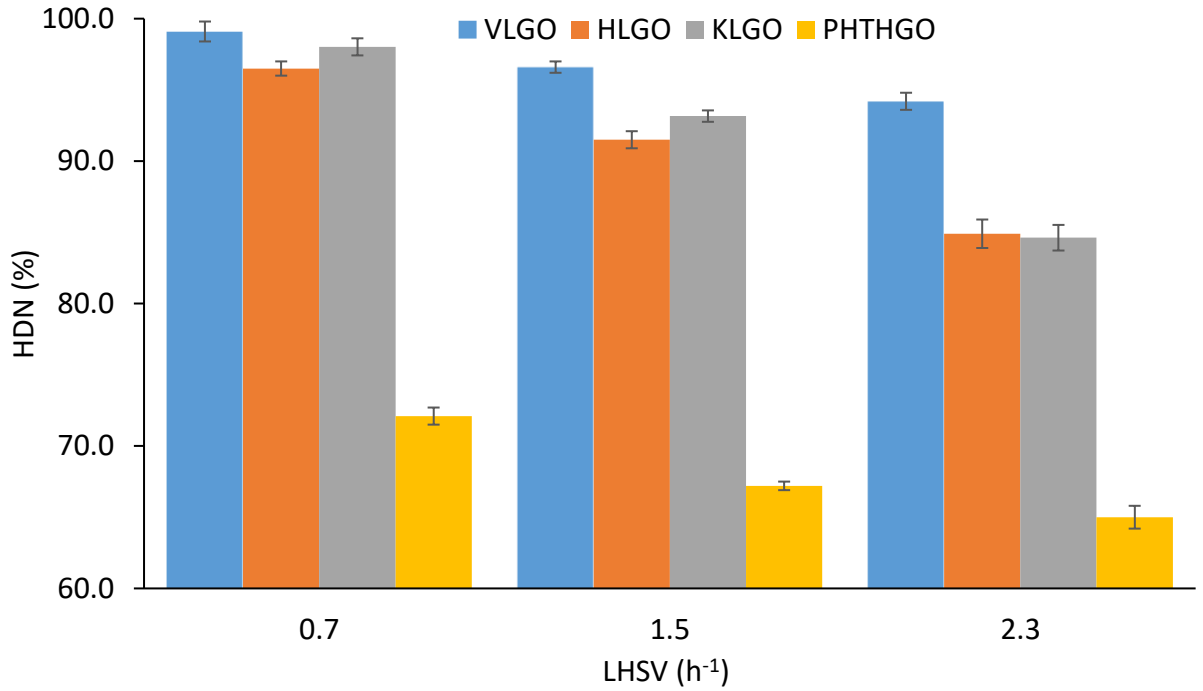

Figure 4.13 Effects of LHSV on HDN conversions during hydrotreating of VLGO, HLGO, KLGO, and PHTHGO. Temperature and pressure constant at 370 °C and 8.96 MPa, respectively

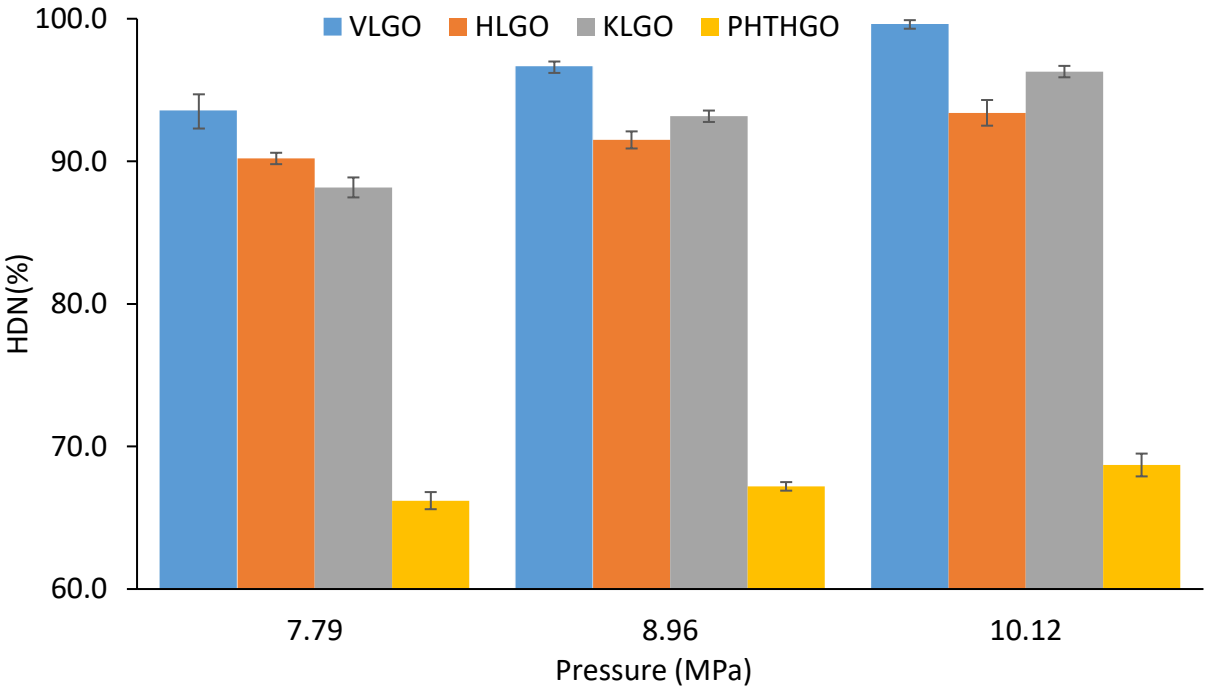

Figure 4.14 Effects of pressure on HDN conversions during hydrotreating of VLGO, HLGO, KLGO, and PHTHGO. Temperature and LHSV constant at 370 °C and 1.5 h^{-1}, respectively

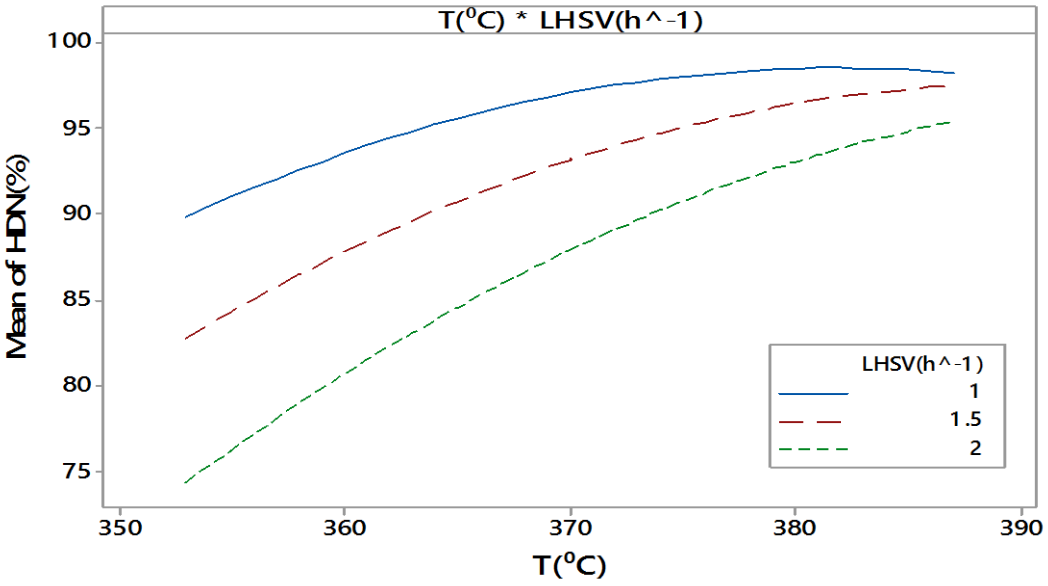

(a)

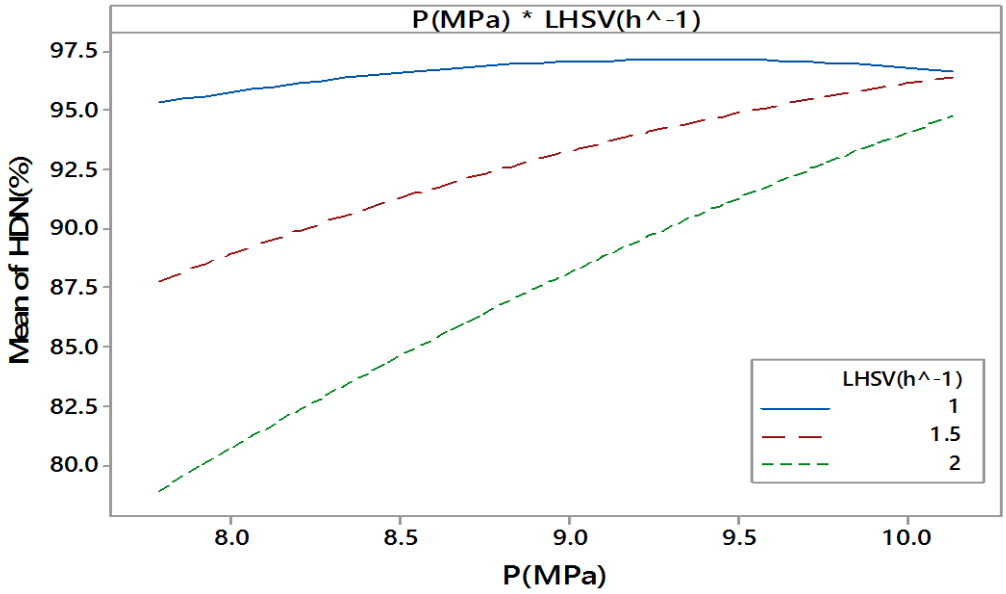

(b)

Figure 4.15 Interaction plots of (a) effects of temperature and LHSV on HDN conversions for KLGO at constant P (8.96 MPa), and (b) effects of pressure and LHSV on HDN conversions for KLGO at constant T (370 °C)

The interaction between pressure and LHSV for VLGO is supposed to reach a limit similar to KLGO; however, Figure 4.16 shows that the products achieved lower nitrogen content at higher values of LHSV. This discrepancy may be due to the predictability power of the models. The model for KLGO has an adjusted R^2 value of 0.98 in comparison with 0.90 for VLGO which gives and an indication that the trends represented by the KLGO model are more reliable. Moreover, the experimental data shows conversions as high as 99.9 % and 99.5 % when the reaction proceeds at LHSV = 1 h^{-1} and LHSV = 2 h^{-1}, respectively; however, the model predicted higher conversion at higher LHSV. In case of PHTHGO, HDN did not reach a temperature limit; therefore, higher residence time had a negative effect on HDN activities as shown in Figure 4.17.

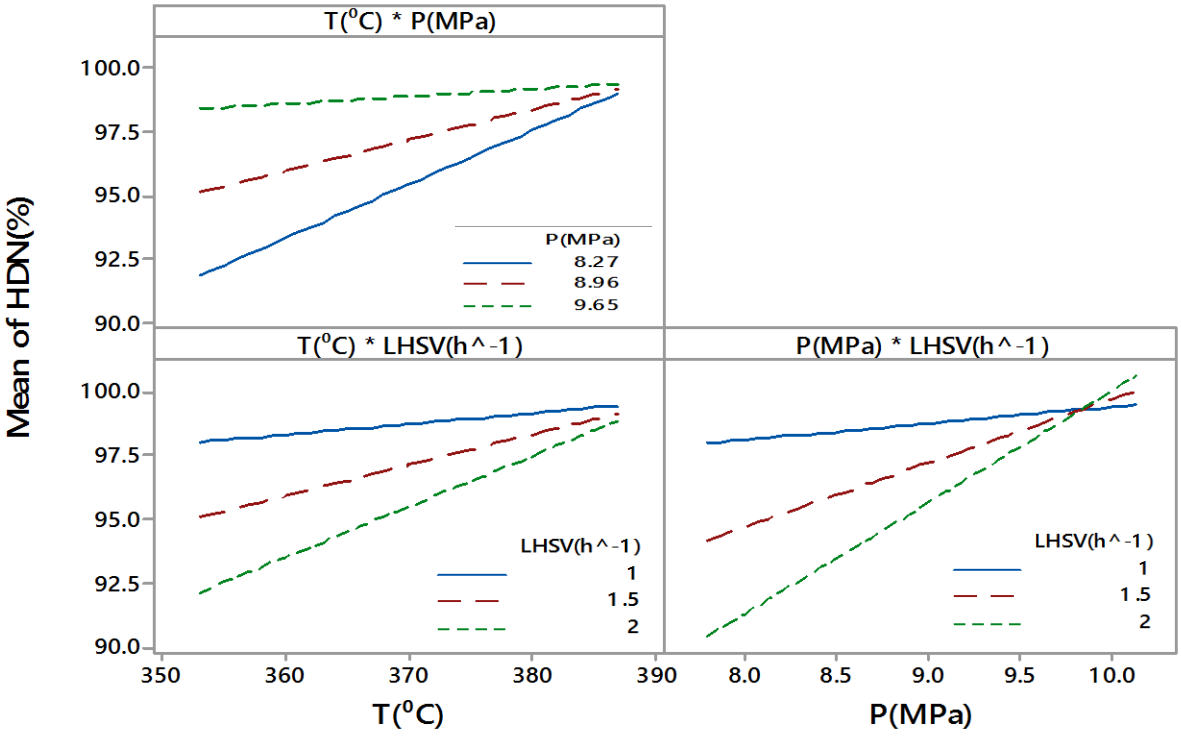

Figure 4.16 Interaction plots of the effects of pressure, temperature, and LHSV on HDN conversions for VLGO

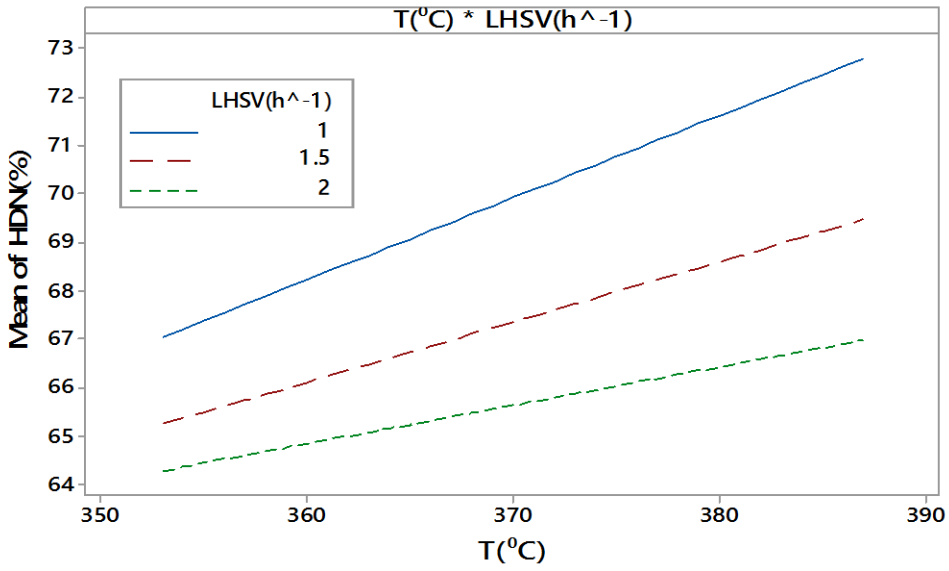

Figure 4.17 Interaction plot of the effects of temperature and LHSV on HDN conversions at constant P (8.96 MPa) for PHTHGO

4.2.4 Summary of the effects of process conditions on hydrotreating conversions for gas oils

Table 4.15 shows the impact for four different feedstocks of the overall effects of process conditions and the combination of these conditions on hydrotreating process given by the regression models. It can be noticed that even though all the fractions are considered light gas oils, each one is affected by different combinations of process variables and interactions.

Table 4.15 Overall effects of process conditions and interactions on hydrotreating conversions provided by the models

Feed	**Reactions**	**T**	**P**	**LHSV**	**T^2**	**P^2**	**$LHSV^2$**	**T× P**	**T× LHSV**	**P× LHSV**
VLGO	HDA	↓	↑	-	-	-	-	-	-	-
	HDS	↑	-	↓	-	-	-	-	↑	-
	HDN	↑	↑	↓	-	-	-	↓	↑	↑

HLGO	HDA	↑	↑	↓	↓	-	-	-	-	-
	HDS	↑	↑	↓	-	-	-	-	-	-
	HDN	↑	↑	↓	-	-	-	-	-	-
KLGO	HDA	↑	-	↓	↓	-	-	-	-	-
	HDS	↑	-	-	-	-	-	↑	-	-
	HDN	↑	↑	↓	↓	-	↓	-	↑	↑
PHTHGO	HDA	-	-	-	↓	-	-	-	-	-
	HDS	↑	-	↓	-	-	-	-	-	-
	HDN	↑	↑	↓	-	-	↑	-	↓	-

* ↑ represents positive effect, ↓ represents negative effect, − represents non-significant effect.

4.2.5 Optimization of process conditions during hydrotreating of gas oils

Based on the experimental data, the best conditions to achieve maximum HDS, HDN, and HDA conversions are shown below in Tables 4.16-4.18.

Table 4.16 Optimum conditions for HDS conversions during hydrotreating of VLGO, HLGO, KLGO, and PHTHGO based on experimental data

Feedstocks	**Process variables**			**HDS (%)**	**Final sulfur content (ppm)**
	T (°C)	**P (MPa)**	**LHSV (h^{-1})**		
VLGO	360	8.27	1	98.8	160.6
HLGO	380	9.65	1	94.4	390.3
KLGO	387	8.96	1.5	98.9	418.0
PHTHGO	387	8.96	1.5	79.8	476.7

Table 4.17 Optimum conditions for HDN conversions during hydrotreating of VLGO, HLGO, KLGO, and PHTHGO based on experimental data

Feedstocks	Process variables			HDN (%)	Final nitrogen content (ppm)
	T (°C)	P (MPa)	LHSV (h^{-1})		
VLGO	360	9.65	1	99.9	0.26
HLGO	380	8.27	1	97.0	41.7
KLGO	380	9.65	1	98.3	20.4
PHTHGO	380	9.65	1	73.1	395.4

Table 4.18 Optimum conditions for HDA conversions during hydrotreating of VLGO, HLGO, KLGO, and PHTHGO based on experimental data

Feedstocks	Process variables			HDA (%)	Final aromatics content (%)
	T (°C)	P (MPa)	LHSV (h^{-1})		
VLGO	360	9.65	1	50.8	10.0
HLGO	380	9.65	1	37.4	15.1
KLGO	380	8.27	1	39.4	17.5
PHTHGO	370	8.96	0.7	20.9	23.0

The advantage of developing regression models for hydrotreating conversions is the possibility to predict the best combination of process conditions to treat each feedstock within the range of conditions employed. As it was mentioned previously, HDA consumed more H_2 than the other reactions during hydrotreating; therefore, the optimization of HDA alone was carried out. The results of the HDA optimization for each feed are shown in Table 4.19. Maximizing HDA implies that the process conditions for the other reactions will not be optimum. Due to the latter, the optimization was carried including the other two reactions. The results are shown in Table 4.20

and two constraints were included to achieve reasonable results (HDS and HDN conversions could not be higher than 99.9%). The optimization based on the regression models was carried out by a tool in Minitab software called Minitab response optimizer.

Table 4.19 Optimum process conditions for HDA alone during hydrotreating VLGO, HLGO, KLGO, and PHTHGO based on the regression models

Feedstocks	Process variables			HDA (%)
	T (°C)	P (MPa)	LHSV (h^{-1})	
VLGO	353	10.12	0.7	56.8
HLGO	374	10.12	0.7	44.4
KLGO	374	10.12	0.7	38.5
PHTHGO	372	9.02	1.4	19.8

Table 4.20 Optimum process conditions to carry out hydrotreating of VLGO, HLGO, KLGO, and PHTHGO based on the regression models

Feedstocks	Process variables			Hydrotreating conversions		
	T (°C)	P (MPa)	LHSV (h^{-1})	HDS (%)	HDN (%)	HDA (%)
VLGO	353	9.37	0.9	99.9	99.9	51.2
HLGO	383	10.12	0.9	94.6	99.9	37.5
KLGO	372	7.79	0.7	99.9	99.9	37.9
PHTHGO	379	9.44	0.7	84.3	74.3	15.8

4.3 Effects of processing conditions on dissolved hydrogen, H_2 inlet partial pressure, H_2 outlet partial pressure, and feed vaporization during hydrotreating of gas oils.

Dissolved H_2 was obtained from VLE calculations in HYSYS software to improve the H_2 consumption prediction of the models from literature. In addition to this variable, H_2 pp and feed vaporization can also be obtained from the simulation. Therefore, the effects of process conditions on these variables are also studied in this section.

Variation of process conditions modifies vapor-liquid equilibrium during hydrotreating processes. Hydrogen partial pressure increases linearly with total system pressure; meanwhile, as temperature increases, inlet and outlet hydrogen partial pressure tend to decrease due to the production of H_2S, NH_3 and light hydrocarbons, hydrogen consumption, and the vaporization of the feed. Figure 4.18 shows that changes in hydrogen partial pressure were more significant for VLGO and KLGO. Simultaneously, these feedstocks achieved higher vaporization rates during the process as it can be seen in Figure 4.19. Due to the latter, it can be concluded that feed vaporization is having an effect on H_2pp. On the other hand, pressure had a negative impact on feed vaporization and the effect was prominent in lighter feeds as shown in Figure 4.20 due to equilibrium shifts; higher pressure increases the volume of gases in the system forcing the equilibrium towards the production of more liquid (Mapiour et al., 2010). In case of feed vaporization, this variable increased with increasing LHSV due to the presence of more feedstock in the system.

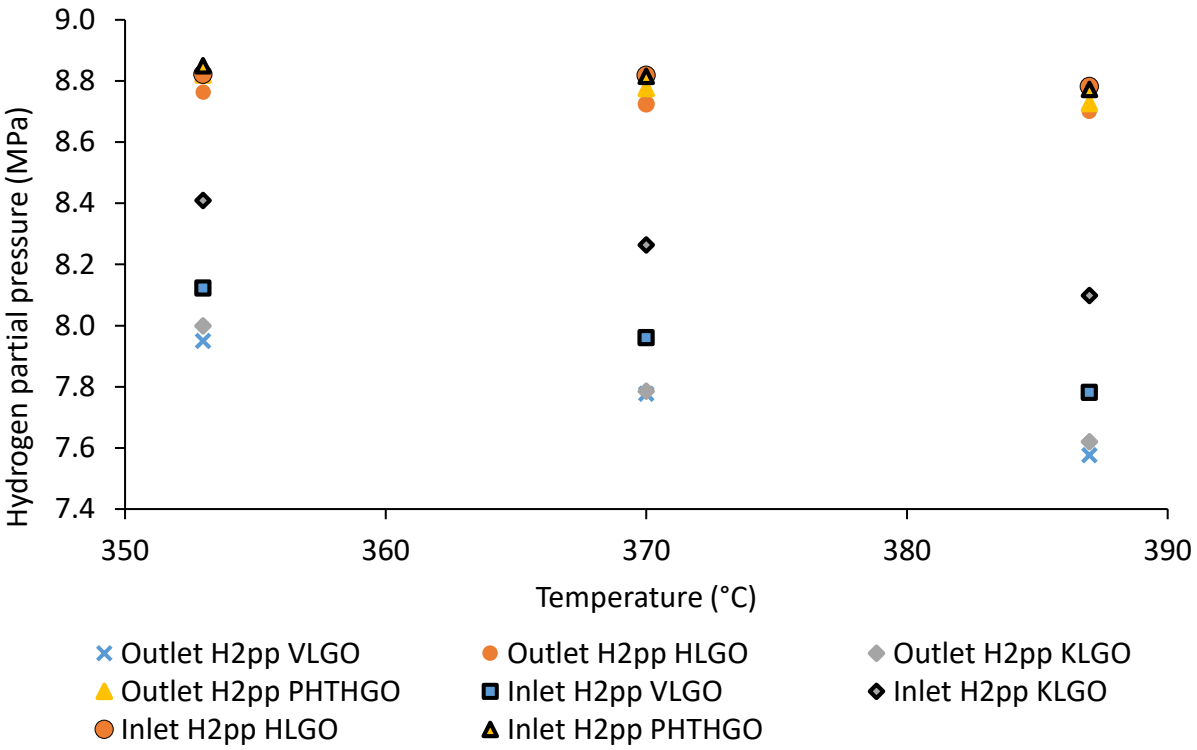

Figure 4.18 Effects of temperature on outlet and inlet H_2pp for VLGO, HLGO, KLGO, and PHTHGO. Pressure and LHSV constant at 8.96 MPa and 1.5 h^{-1}, respectively

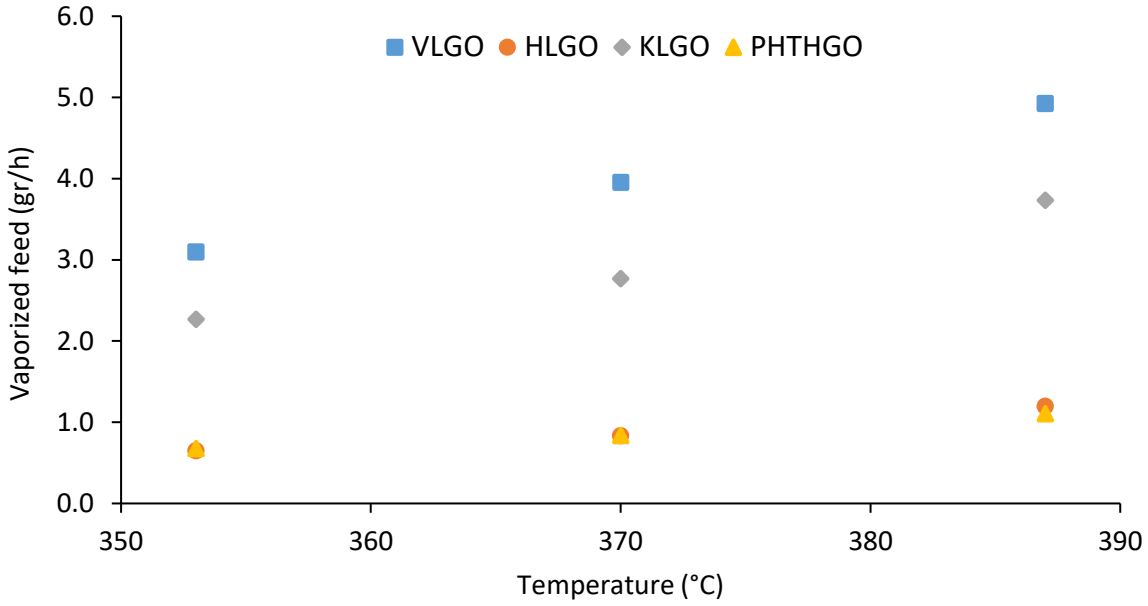

Figure 4.19 Effects of temperature on feed vaporization for VLGO, HLGO, KLGO, and PHTHGO. Pressure and LHSV constant at 8.96 MPa and 1.5 h^{-1}, respectively

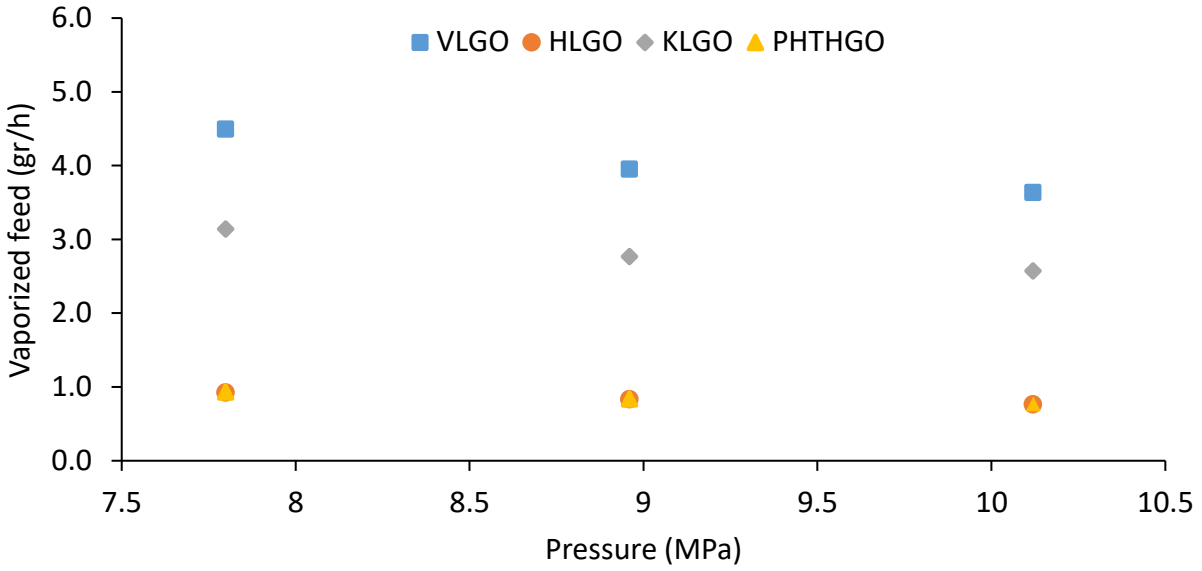

Figure 4.20 Effects of pressure on feed vaporization for VLGO, HLGO, KLGO, and PHTHGO. Temperature and LHSV constant at 370 °C and 1.5 h^{-1}, respectively

Another important parameter in vapor-liquid interactions during hydrotreating processes is dissolved hydrogen. This variable is important for modeling and design of hydrotreaters; however, data for hydrotreating feedstocks with varying properties is not readily available (Lal et al., 1999). The solubility of hydrogen is affected by temperature, pressure, and boiling point distribution of petroleum fractions (Riazi & Roomi, 2007). It can be seen in Figures 4.21 and 4.22 that dissolved hydrogen in terms of mole fraction increased with any increase in both temperature and pressure.

Increasing temperature increased feed vaporization which forces H_2 to dissolve in the liquid phase. Similarly, pressure had a positive effect on dissolved H_2. This effect is due to the direct proportionality between dissolved H_2 and H_2 partial pressure in Henry's law. Moreover, when hydrogen contacted heavier feedstocks (higher boiling point distribution) there was an increase in hydrogen solubility as shown in Figures 4.21 and 4.22 due to less H_2 feed vaporization of these feedstocks causing an increase in the liquid volume of the product. The amount of dissolved hydrogen decreased in the following order: HLGO>PHTHGO>KLGO>VLGO Finally, LHSV had no effect on the mole fraction of dissolved hydrogen due to maintaining H_2/oil ratio constant at 600 N m^3/m^3.

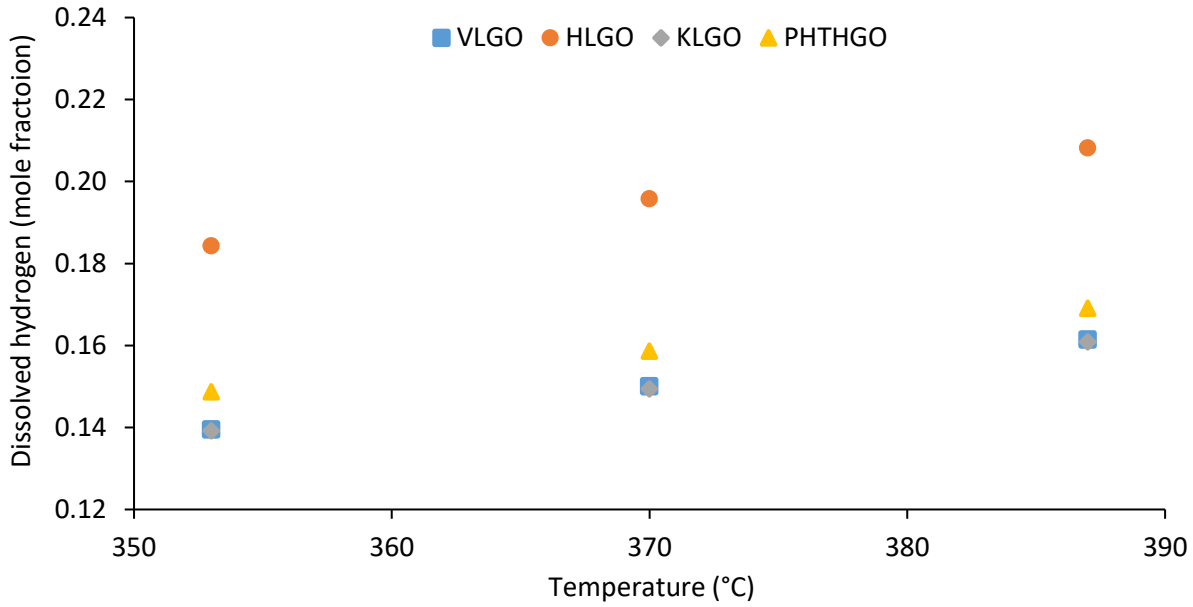

Figure 4.21 Effects of temperature on dissolved hydrogen for VLGO, HLGO, KLGO, and PHTHGO. Temperature and LHSV constant at 370 °C and 1.5 h^{-1}, respectively

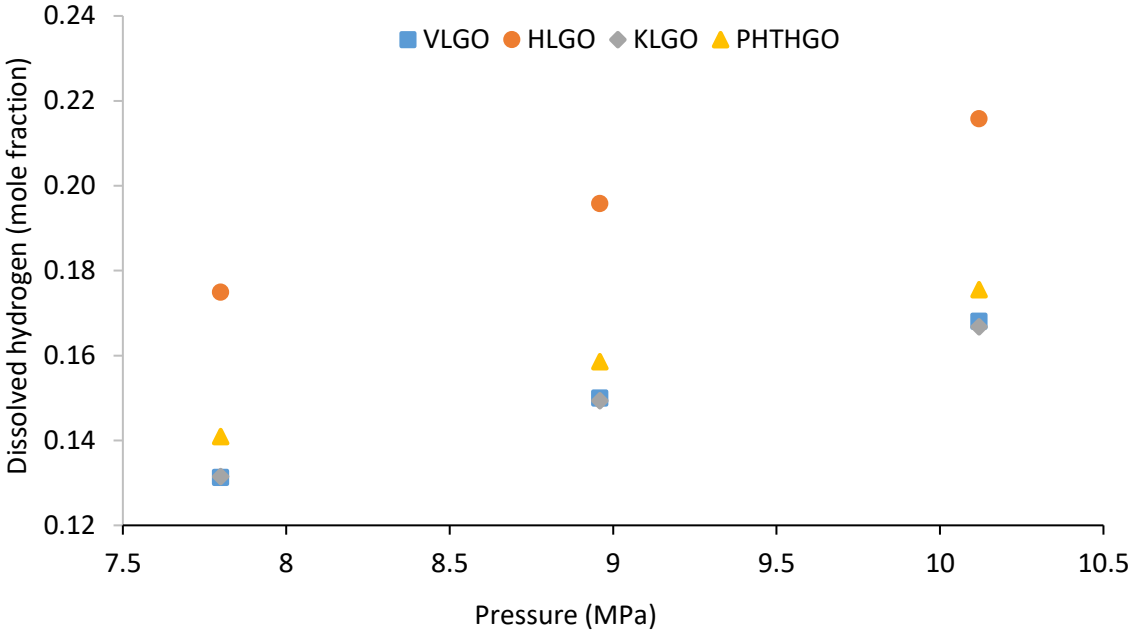

Figure 4.22 Effects of pressure on dissolved hydrogen for VLGO, HLGO, KLGO, and PHTHGO. Pressure and LHSV constant at 8.96 MPa and 1.5 h^{-1}, respectively

4.3.1 Effects of outlet H_2pp on feed vaporization, dissolved hydrogen and H_2 consumption during hydrotreating of VLGO, HLGO, KLGO, and PHTHGO.

Mapiour et al. (2010) reported that dissolved hydrogen and hydrogen consumption increases with increasing hydrogen outlet partial pressure during hydrotreating of bitumen-derived heavy gas oil. However, the interaction between these variables may vary by treating feedstocks with different composition and properties. Figure 4.23 shows that dissolved hydrogen increases along with an increase in outlet H_2pp due to pressure being responsible for forcing hydrogen to dissolve in the liquid. In case of hydrogen consumption, Figure 4.24 shows different trends for each feedstock. H_2 consumption during hydrotreating of KLGO and PHTHGO tends to remain relatively constant at higher outlet H_2pp. The latter can be explained by the effect of pressure on HDA conversions. Table 4.10 shows that the effect of pressure on HDA activities for these two feedstocks was insignificant. In the case of VLGO and HLGO, Figure 4.24 displays that hydrogen consumption is affected positively by outlet H_2pp due to the positive effects of pressure on HDA conversions for these two feedstocks. The effects of outlet H_2pp on feed vaporization during hydrotreating of VLGO, HLGO, KLGO and PHTHGO are shown in Figure 4.25. This figure shows that the interaction between these variables is not clear; however, there is more dispersion in case of VLGO and KLGO which are the feeds with higher vaporization rate.

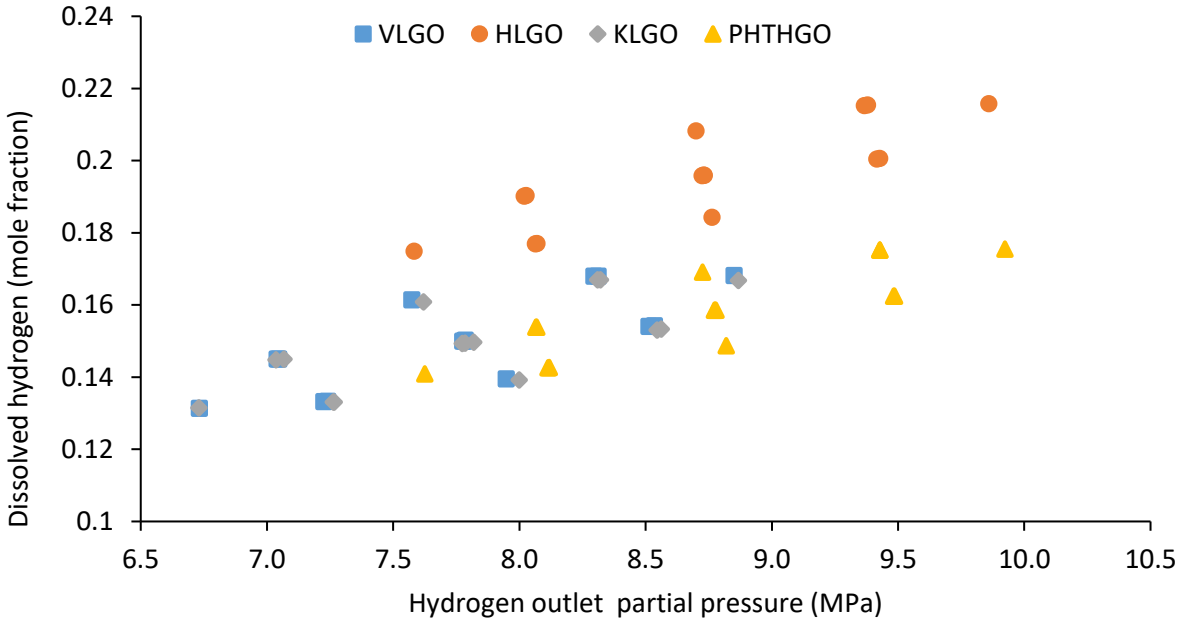

Figure 4.23 Effects of hydrogen outlet partial pressure on dissolved hydrogen for VLGO, HLGO, KLGO, and PHTHGO

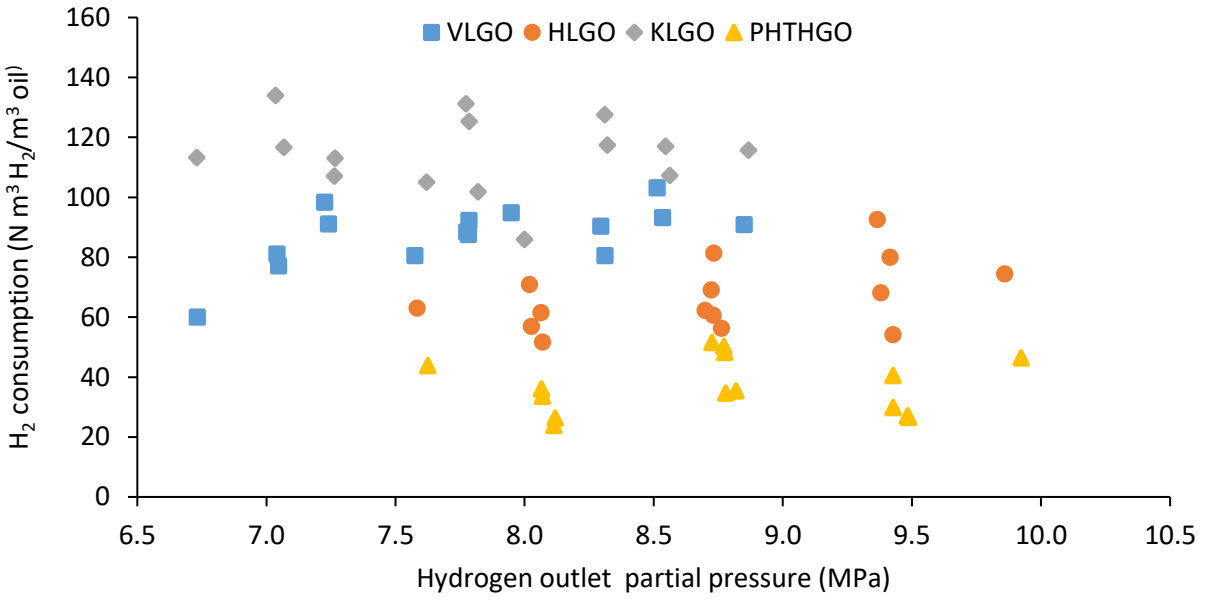

Figure 4.24 Effects of hydrogen outlet partial pressure on hydrogen consumption for VLGO, HLGO, KLGO, and PHTHGO

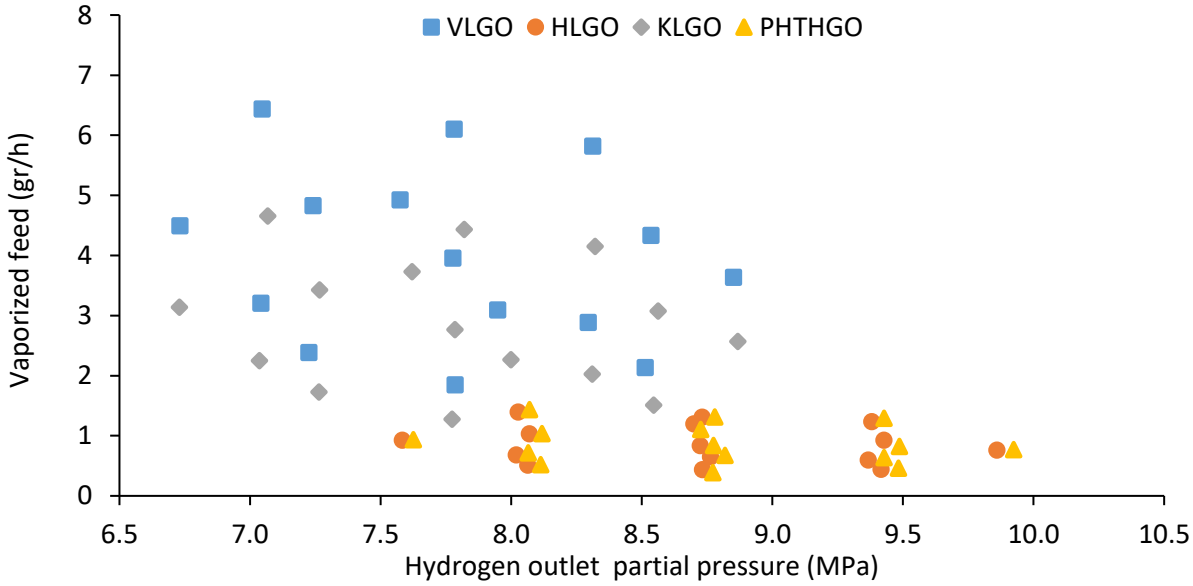

Figure 4.25 Effects of hydrogen outlet partial pressure on feed vaporization for VLGO, HLGO, KLGO, and PHTHGO

5 SUMMARY, CONCLUSIONS AND RECOMMENDATIONS

5.1 Summary

- **Phase I**
  - H_2 consumption was determined by the analysis of H_2 content in liquid and gas streams. These analyses were then compared with an approach developed by Hisamitsu et al. (1976) which determines H_2 consumption based on the decrease of the aromatic carbon content. The comparison showed a better correlation between the analysis of gas streams and the approach developed by Hisamitsu et al. (1976).
  - In general, H_2 consumption determined by the analysis of H_2 content in gas streams for each feedstock decreased in the following order: KLGO>VLGO>HLGO>PHTHGO. The H_2 consumption ranges for each feedstock were the following:
    - VLGO: 59.9-103.1 N m^3 H_2/m^3 oil.
    - HLGO:51.7-92.6 N m^3 H_2/m^3 oil.
    - KLGO: 86.0-134.0 N m^3 H_2/m^3 oil.
    - PHTHGO: 23.9-51.6 N m^3 H_2/m^3 oil.
  - The effects of process conditions on H_2 consumption (analysis of H_2 content in gas streams) were studied by statistical analysis for VLGO, HLGO, KLGO, and PHTHGO. Then, regression models of H_2 consumption based on process conditions were developed for each of these feedstocks.
  - The data of H_2 consumption of the 4 feedstocks was combined to obtain a new set of data. This set of data was obtained by assuming that in case of a mixture of VLGO, HLGO, KLGO, and PHTHGO, each of them will contribute to the total H_2 consumption of this mixture in the same proportion. The statistical analysis of this new set of data was used to develop a combined (composite) regression model.

- The combined regression model provided a better prediction of H_2 consumption than other models and values available in the literature. For example, the experimental run carried out for the mixture of LGOs at 375 °C showed an experimental H_2 consumption of 100.2 N m^3 H_2/m^3 oil. The correlation developed in this work predicted a H_2 consumption of 88.1 N m^3 H_2 / m^3 oil. Meanwhile, the H_2 consumption prediction by other models available in literature was in the following range: 64.3-71.7 N m^3 H_2 / m^3 oil. It is important to note that the values of H_2 consumption mentioned above consider chemical H_2 consumption (obtained by the models) and dissolved H_2. Dissolved H_2 was calculated in this work by using HYSYS;
- The mole fraction of dissolved hydrogen in the liquid product increased when temperature and pressure also increased. In addition, feedstocks with higher boiling point distribution presented higher hydrogen solubility.
- The effects of process conditions on H_2 partial pressure and feed vaporization; these two variables were also obtained in the HYSYS simulation.
- Increasing LHSV had a positive effect on feed vaporization and dissolved hydrogen in terms of mass.
- Changes in inlet and outlet H_2pp were more significant for VLGO and KLGO. These two feeds have higher vaporization rate than HLGO and PHTHGO.
- Changes in inlet and outlet H_2pp were more significant for VLGO and KLGO. These two feeds have higher vaporization rate than HLGO and PHTHGO.
- Increasing temperature improved the vaporization rate for all the feedstocks. In contrast, pressure had a negative effect on feed vaporization and the effect was more prominent in lighter feeds.
- Dissolved hydrogen increased at the same time outlet H_2pp increased for VLGO, HLGO, KLGO and PHTHGO.
- H_2 consumption appears to remain constant by increasing outlet H_2pp for KLGO and PHTHGO. On the other hand, increasing outlet H_2pp for VLGO and HLGO caused the process to consume more H_2.

- The correlation between outlet H_2pp and feed vaporization is not clear. However, it is important to note that by plotting these two variables together there is more dispersion for VLGO and KLGO in comparison with HLGO and PHTHGO.

- **Phase II**
  - The effects of process conditions on hydrotreating conversions were studied by the analysis of experimental data and the development of regression models for the different feedstocks treated in this work.
  - Increasing temperature had a positive effect on HDS conversions for VLGO, HLGO, KLGO and PHTHGO.
  - Pressure improved the efficiency of HDS for HLGO only. In addition, the interaction between pressure and temperature was significant on HDS conversions during hydrotreating of KLGO. HDS conversions for KLGO were limited by temperature and the effect of this variable was less prominent at higher levels of pressure.
  - Increasing LHSV had a negative effect on HDS conversions for VLGO, HLGO, KLGO, and PHTHGO. In the case of VLGO, the interaction between temperature and LHSV was significant and it shows that the reaction is taking place in excess at lower values of LHSV.
  - Increasing temperature and pressure had a positive effect on HDN conversions for VLGO, HLGO, KLGO and PHTHGO. On the other hand, increasing LHSV decreased HDN efficiency for every feedstock.
  - The statistical analysis for HDN conversions developed in this work provided the following interactions:
    - Changes in temperature and pressure were more significant at higher values of LHSV for KLGO due to the fact that the reaction took place in excess.
    - Similar to KLGO, the interactions between temperature-LHSV and pressure-LHSV for VLGO were more significant at higher values of LHSV. However, the interaction between pressure and LHSV shows that the products have less nitrogen content at higher values of LHSV which is not

logical. This discrepancy may be related to the following factors: the predictability of the HDN model for VLGO (Adj R^2 for VLGO is 8% lower than for KLGO) and the small differences between HDN conversions levels for VLGO (99.9 % and 99.5 % when HDN proceeds at LHSV = 1 h^{-1} and LHSV = 2 h^{-1}, respectively).

- The interaction between temperature and LHSV for PHTHGO show that the reaction does not reach a temperature limit; therefore, higher residence time had a negative effect on HDN conversions and the effect of temperature is more significant at lower values of LHSV.

- The experimental data for HDA conversions shows that this reaction is being limited by temperature for VLGO, HLGO, KLGO and PHTHGO.
- Increasing pressure had a positive effect on HDA conversions for VLGO and HLGO. On the other hand, pressure did not improve HDA for KLGO and PHTHGO at the conditions employed in this work; these two feeds might contain high amounts of monoaromatics which may require higher pressures for complete saturation.
- The experimental data shows that increasing LHSV had a negative effect on HDA conversions for VLGO, HLGO, KLGO, and PHTHGO. In contrast, the statistical analysis shows that LHSV did not show a significant effect on HDA for VLGO and PHTHGO.
- The best combinations of processing conditions to maximize HDA alone for each feedstock is provided below.
    - VLGO: T = 353 °C, P = 10.12 MPa, and LHSV = 0.7 h^{-1} to achieve the following HDA conversion: 56.8 %.
    - HLGO: T = 374 °C, P = 10.12 MPa, and LHSV = 0.7 h^{-1} to achieve the following HDA conversion: 44.4 %.
    - KLGO: T = 374 °C, P = 10.12 MPa, and LHSV = 0.7 h^{-1} to achieve the following HDA conversion: 38.5 %.
    - PHTHGO: T = 372 °C, P = 9.02MPa, and LHSV = 1.4h^{-1} to achieve the following HDA conversion: 19.8 %.

- The best combination of processing conditions to maximize HDS, HDN and HDA conversions are provided below.
    - VLGO: T = 353 °C, P = 9.37 MPa, and LHSV = 0.9 h^{-1} to achieve the following conversions: 99.9 %, 99.9 % and 51.2 % for HDS, HDN and HDA, respectively.
    - HLGO: T = 383 °C, P = 10.12 MPa, and LHSV = 0.9 h^{-1} to achieve the following conversions: 94.6 %, 99.9 % and 37.5 % for HDS, HDN and HDA, respectively.
    - KLGO: T = 372 °C, P = 7.79 MPa, and LHSV = 0.7 h^{-1} to achieve the following conversions: 99.9 %, 99.9 % and 37.9 % for HDS, HDN and HDA, respectively.
    - PHTHGO: T = 379 °C, P = 9.44 MPa, and LHSV = 0.7 h^{-1} to achieve the following conversions: 84.3 %, 74.3 % and 15.8 % for HDS, HDN and HDA, respectively.

5.2 Conclusions

The models of H_2 consumption for each feedstock under consideration as well as a composite model for all four feedstocks were developed. In conclusion, the composite regression model of H_2 consumption based on process conditions for different feedstocks (VLGO, HLGO, KLGO, and PHTHGO) gave better performance than similar correlations available in the literature. The prediction of H_2 consumption provided by the model showed the dependence of hydrogen consumption on process conditions.

Each of the four feedstocks used in this work required a different set of process conditions (T, P, and LHSV) to maximize HDS, HDN, and HDA conversions. Similarly, the effects of these conditions varied for each feedstock. Statistical models for HDS, HDN, and HDA were developed for these feedstocks based on the process optimization study which indicated the complexity of hydrotreating of various gas oils.

5.3 Recommendations

- Detailed characterization of the feedstocks and products related to specific sulfur, nitrogen, and aromatic groups may contribute to a better understanding of the differences between H_2 consumption during hydrotreating of each feedstock.
- This study can be used as a reference to perform further optimization of processing conditions; the common industrial operating conditions are not optimum for all the feedstocks employed in this work.

REFERENCES

Akgerman, A., & Netherland, D. (1986). Effect Of Equation of State on Prediction of Trickle Bed Reactor Model Performance. *Chemical Engineering Communications*, *49*(1–3), 133–143.

Ancheyta-Juárez, J., Aguilar-Rodríguez, E., Salazar-Sotelo, D., Betancourt-Rivera, G., & Leiva-Nuncio, M. (1999). Hydrotreating of straight run gas oil–light cycle oil blends. *Applied Catalysis A: General*, *180*(1–2), 195–205.

Ancheyta, J., Rana, M. S., & Furimsky, E. (2005). Hydroprocessing of heavy petroleum feeds: Tutorial. *Catalysis Today*.*109*(1), 3-15.

Ancheyta, J., & Speight, J. G. (2007). *Hydroprocessing of Heavy Oils and Residua*. Boca Raton, Florida: Taylor & Francis.

Angelici, R. J. (1997). An overview of modeling studies in HDS, HDN, and HDO catalysis. *Polyhedron*, *16*(18).

Aoyagi, K., McCaffrey, W. ., & Gray, M. R. (2003). Kinetics of Hydrocracking and Hydrotreating of Coker and Oilsands Gas Oils. *Petroleum Science and Technology*, *21*(5&6), 997–1015.

Banerkke, L. (2012). *Oil sands, Heavy oil & Bitumen: from Recovery to Refinery* (pp. 59-124). Tulsa,OK: Pennwell.

Bej, S. K., Dalai, A. K., & Adjaye, J. (2001). Comparison of Hydrodenitrogenation of Basic and Nonbasic Nitrogen Compounds Present in Oil Sands Derived Heavy Gas Oil. *Energy & Fuels*, *15*(2), 377–383.

Bej, S. K., Dalai, A. K., & Adjaye, J. (2007). Kinetics of hydrodesulfurization of heavy gas oil derived from oil-sands bitumen. *Petroleum Science and Technology, 20*(7-8), 867-877.

Botchwey, C., Dalai, A. K., & Adjaye, J. (2003). Product selectivity during hydrotreating and mild hydrocracking of bitumen-derived gas oil. *Energy and Fuels.17*(5), 1372-1381.

Cai, H. Y., Shaw, J. M., & Chung, K. H. (2001). Hydrogen solubility measurements in heavy oil and bitumen cuts. *Fuel, 80*(8), 1055-1063.

Castañeda, L. C., Muñoz, J. A. D., & Ancheyta, J. (2011). Comparison of approaches to determine hydrogen consumption during catalytic hydrotreating of oil fractions. *Fuel*, *90*(12), 3593–3601.

Chandra Mouli, K., & Dalai, A. K. (2009). Ring opening and kinetics study of hydrotreated LGO on Ni-Mo carbide supported on HY and H-Beta catalysts. *Applied Catalysis A: General*, *364*(1–2), 80–86.

Chávez, L. M., Alonso, F., & Ancheyta, J. (2014). Vapor-liquid equilibrium of hydrogen-hydrocarbon systems and its effects on hydroprocessing reactors. *Fuel*, *138*, 156(20).

Chen, J., Mulgundmath, V., & Wang, N. (2011). Accounting for vapor-liquid equilibrium in the modeling and simulation of a commercial hydrotreating reactor. *Industrial and Engineering Chemistry Research*, *50*(3), 1571-1579.

Chen, J., & Ring, Z. (2004). HDS reactivities of dibenzothiophenic compounds in a LC-finer LGO and H_2S/NH_3 inhibition effect. *Fuel*, *83*(3), 305–313.

Edgar, M. (1993). Hydrotreating Q&A. In *Paper presented at the NPRA Annual Meeting 1993*. San Antonio, Texas.

Fang, X. (1999). H_2 partial pressure on HDS and HDN of Shengli VGO. *Shiyou Xuebao*, *15*(5).

Florusse, L. J., Peters, C. J., Pamies, J. C., Vega, L. F., & Meijer, H. (2003). Solubility of Hydrogen in Heavy n-Alkanes: Experiments and SAFT Modeling. *AIChE Journal*, *(49)*12, 3260-3269.

Fogler, S. (1999). *Elements of Chemical Reaction Engineering* (3rd ed.). Lebanon, Indiana, USA: Prentice Hall.

Gary, H. ., Handewerk, E. ., & Kaiser, J. (2007). *Petroleum refining: Technology and economics*. (pp. 175-183) Boca Raton, Florida: Taylor & Francis.

Ghosh, P. (1999). Prediction of Vapor-Liquid Equilibria Using Peng-Robinson and Soave-Redlich-Kwong Equations of State. *Chemical Engineering & Technology*, *22*(5), 379–399.

Girgis, M. J., & Gates, B. C. (1991). Reactivities, Reaction Networks, and Kinetics in High-Pressure Catalytic Hydroprocessing. *Industrial & Engineering Chemistry Research*, *30*, 2021–2058.

Hisamitsu, T., Shite, Y., Maruyama, F., Yamane, M., Satomi, Y., & Ozaki, H. (1976). Studies on Hydrodesulfurization of Heavy Distillate. *Japan Petroleum Institute*, *18*(2), 146–152.

IEA. (2011). World Energy Outlook 2011. Retrieved from: http://www.iea.org/publications/freepublications/publication/WEO2011_WEB

Ishihara, A., Dumeignil, F., Lee, J., Mitsuhashi, K., Qian, E. W., & Kabe, T. (2005). Hydrodesulfurization of sulfur-containing polyaromatic compounds in light gas oil using noble metal catalysts. *Applied Catalysis A: General, 289*(2), 163-173.

Jones, D. S. ., & Pujado, P. P. (2006). *Handbook of Petroleum Processing*. (pp. 1-76) Netherlands: Springer.

Knudsen, K. G., Cooper, B. H., & Topsøe, H. (1999). Catalyst and process technologies for ultra low sulfur diesel. *Applied Catalysis A: General*, *189*, 205–215.

Lal, D., Otto, F. D., & Mather, A. E. (1999). Solubility of hydrogen in Athabasca bitumen. *Fuel, (78)*12, 1437-1447.

Lazic, Z. (2004). *Design of Experiments in Chemical Engineering: A Practical Guide*. Hoboken: Wiley.

Lee, C. K., Mcgovern, S. J., Silva, D., Luiz, E., Magalhaes, C., & Osowski, C. A. (2008). Study compares methods that measure hydrogen use in diesel hydrotreaters. *Oil & Gas Journal*, *106*(38).

Luck, F. (1991). A Review of Support Effects On the Activity and Selectivity of Hydrotreating Catalysts. *Bulletin Des Societes Chimiques Belges*, *100*(11–12), 781–800.

Mann, R. ., Sambi, I. ., & Khulbe, K. (1987). Catalytic Hydrofining of Heavy Gas Oil. *Ind. Eng. Chem. Res*, *26*(3), 410–410.

Mapiour, M. (2009). *Kinetics and Effects of H_2 Partial Pressure on Hydrotreating of Heavy Gas Oil*. University of Saskatchewan.

Mapiour, M., Sundaramurthy, V., Dalai, A. K., & Adjaye, J. (2010). Effects of hydrogen partial pressure on hydrotreating of heavy gas oil derived from oil-sands bitumen: Experimental and kinetics. *Energy and Fuels*, *24*(2), 772–784.

McCulloch, D. ., & Roeder, R. (1976). Find hydrogen partial pressure. *Hydrocarbon Processing*, *81*.

Mochida, I., & Choi, K. (2006). Current progress in catalysts and catalysis for hydrotreating. *Practical Advances in Petroleum Processing*, 257–296.

Owusu-Boakye, A. (2005). *Two-stage aromatics hydrogenation of bitumen-derived light gas oil*. University of Saskatchewan.

Owusu-Boakye, A., Dalai, A., Ferdous, D., & Adjaye, J. (2006). Experimental and Kinetics Studies of Aromatic Hydrogenation in a Two-Stage Hydrotreating Process using $NiMo/Al_2O_3$ and NiW/Al_2O_3 Catalysts. *The Canadian Journal of Chemical Engineering*, *84*, 572–580.

Papayannakos, N., & Georgiou, G. (1988). Kinetics of hydrogen consumption during catalytic hydrodesulphurization of a residue in a trickle-bed reactor. *Journal of Chemical Engineering of Japan(21)*3, 244-249.

Peramanu, S., Cox, B. ., & Pruden, B. . (1999). Economics of hydrogen recovery processes for the purification of hydroprocessor purge and off-gases. *International Energy Journal of Hydrogen, 24*(5), 405–424.

Ramachandran, R., & Menon, R. K. (1998). An Overview of Industrial Uses of Hydrogen. *International Journal of Hydrogen Energy,23*(7), 593–598.

Rana, M. S., Sámano, V., Ancheyta, J., & Diaz, J. A. I. (2007). A review of recent advances on process technologies for upgrading of heavy oils and residua. *Fuel, 86*(9), 1216-1231.

Riazi, M. R., & Roomi, Y. A. (2007). A method to predict solubility of hydrogen in hydrocarbons and their mixtures. *Chemical Engineering Science, 62*(23), 6649-6658.

Silvy, R. P. (2010). Refining catalyst market begins to recover in 2010. *Oil and Gas Journal, 108*(15), 40–43.

Skogestad, S. (2009). *Chemical and Energy Process Engineering*. Boca Raton, FL (Unites States): CRC press.

Speight, J. G. (1999). *Desulfurization of Heavy Oils and Residua* (2nd ed.). New York, NY (United States): CRC press.

Stanislaus, A., Marafi, A., & Rana, M. S. (2010). Recent advances in the science and technology of ultra low sulfur diesel (ULSD) production. *Catalysis Today, 153*(1), 1-68.

Stratiev, D., Tzingov, T., Shishkova, I., & Dermatova, P. (2009). Hydrotreating units chemical hydrogen consumption analysis: A tool for improving refinery hydrogen management. *44th International Petroleum Conference*, Bratislava, Slovak Republic, September 21-22, 2009, 1–14.

Sun, M., Nelson, A. E., & Adjaye, J. (2005). Adsorption and hydrogenation of pyridine and pyrrole on NiMoS: An ab initio density-functional theory study. *Journal of Catalysis*, *231*(1), 223-231.

Topsøe, H. (2007). The role of Co-Mo-S type structures in hydrotreating catalysts. *Applied Catalysis A: General, 322*, 3–8.

Yui, S. (2008). Producing quality synthetic crude oil from Canadian oil sands bitumen. *Journal of the Japan Petroleum Institute, 51*(1), 1-13.

Yui, S., & Chan, E. (1992). Hydrogenation of Coker Naphtha with NiMo catalyst. In K. Smith & Sandford E.C (Eds.), *Progress in Catalysis* (pp. 59–66). Amsterdam, Netherlands: Elsevier Science Publishers B.V.

APPENDICES

Appendix A: Experimental calibrations

A.1 Hydrogen mass flow meter calibration

The amount of hydrogen going into the system was calibrated prior to carry the experimental runs. Different set points in the mass flow controller were tested to achieve the required hydrogen flow rates. The flow rates of hydrogen were measured by a bubble flow meter placed after the back-pressure regulator as displayed in Figure 3.1. Also, the flow rates obtained at laboratory conditions were normalized using equation 5.2. The calibration curve of the mass flow meter is shown in Figure A.1.

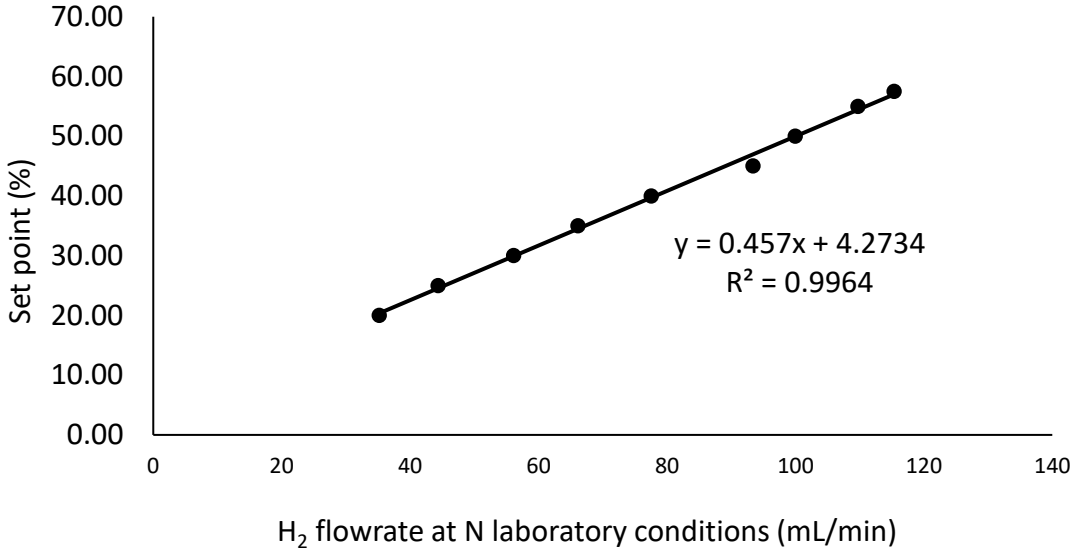

Figure A. 1 Calibration curve for H_2 mass flow meter

A.2. Temperature calibration

The temperature calibration of the reactor was carried out at different temperatures and distance points to build the axial temperature profile shown in Figure A.2. A thermocouple was placed in the center of the reactor and then moved upwards to obtain several temperature readings. The temperature controller calibration curve is shown in Figure A.3.

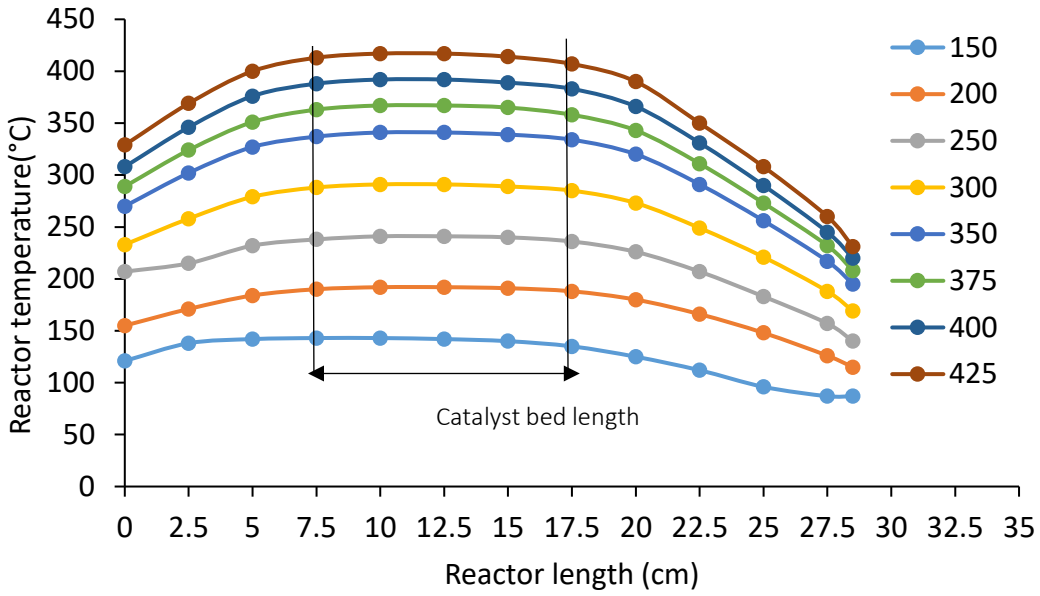

Figure A. 3 Axial temperature profile

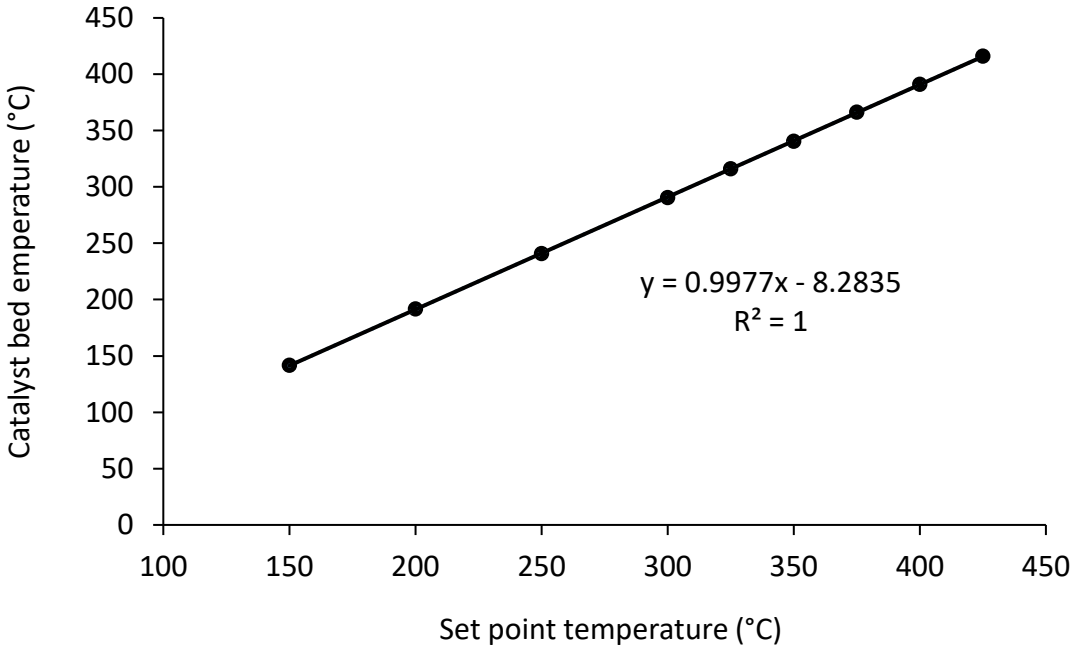

Figure A. 4 Temperature calibration curve

Appendix B: Additional experimental data

Table B. 1 Inlet and outlet hydrogen partial pressure, feed vaporization, and dissolved hydrogen during hydrotreating of VLGO

Run	T (^{0}C)	P (MPa)	LHSV (h^{-1})	H_2 inlet pp (MPa)	H_2 outlet pp (MPa)	Feed vaporization at outlet (g/h)	Dissolved H_2 at outlet (mol fraction)	Dissolved H_2 at outlet (m^3H_2/m^3 oil)
1	360	8.27	1	7.4	7.2	2.4	0.13	6.95
2	380	8.27	1	7.2	7.0	3.2	0.15	4.50
3	360	9.65	1	8.7	8.5	2.1	0.15	9.35
4	380	9.65	1	8.5	8.3	2.9	0.17	7.13
5	360	8.27	2	7.4	7.2	4.8	0.13	6.86
6	380	8.27	2	7.2	7.0	6.4	0.15	4.46
7	360	9.65	2	8.7	8.5	4.3	0.15	9.22
8	380	9.65	2	8.5	8.3	5.8	0.17	6.94
9	353	8.96	1.5	8.1	7.9	3.1	0.14	8.56
10	387	8.96	1.5	7.8	7.6	4.9	0.16	5.03
11	370	7.80	1.5	6.9	6.7	4.5	0.13	4.92
12	370	10.12	1.5	9.1	8.9	3.6	0.17	9.11
13	370	8.96	0.7	8.0	7.8	1.8	0.15	6.94
14	370	8.96	2.3	8.0	7.8	6.1	0.15	6.87
15	370	8.96	1.5	8.0	7.8	4.0	0.15	6.94

Table B. 2 Inlet and outlet hydrogen partial pressure, feed vaporization, and dissolved hydrogen during hydrotreating of HLGO

Run	T (^{0}C)	P (MPa)	LHSV (h^{-1})	H_2 inlet pp (MPa)	H_2 outlet pp (MPa)	Feed vaporization at outlet (g/h)	Dissolved H_2 at outlet (mol fraction)	Dissolved H_2 at outlet (m^3H_2/m^3 oil)
1	360	8.27	1	8.2	8.1	0.5	0.18	9.39
2	380	8.27	1	8.1	8.0	0.7	0.19	9.78
3	360	9.65	1	9.5	9.4	0.4	0.20	11.28
4	380	9.65	1	9.5	9.4	0.6	0.22	11.69
5	360	8.27	2	8.2	8.1	1.0	0.18	9.37
6	380	8.27	2	8.1	8.0	1.4	0.19	9.74
7	360	9.65	2	9.5	9.4	0.9	0.20	11.23
8	380	9.65	2	9.5	9.4	1.2	0.22	11.61
9	353	8.96	1.5	8.8	8.8	0.6	0.18	10.44
10	387	8.96	1.5	8.8	8.7	1.2	0.21	10.26
11	370	7.80	1.5	7.7	7.6	0.9	0.17	9.12
12	370	10.12	1.5	10.0	9.9	0.8	0.22	11.95
13	370	8.96	0.7	8.8	8.7	0.4	0.20	11.19
14	370	8.96	2.3	8.8	8.7	1.3	0.20	10.91
15	370	8.96	1.5	8.8	8.7	0.8	0.20	10.96

Table B. 3 Inlet and outlet hydrogen partial pressure, feed vaporization, and dissolved hydrogen during hydrotreating of KLGO

Run	T (^{0}C)	P (MPa)	LHSV (h^{-1})	H_2 inlet pp (MPa)	H_2 outlet pp (MPa)	Feed vaporization at outlet (g/h)	Dissolved H_2 at outlet (mol fraction)	Dissolved H_2 at outlet (m^3H_2/m^3 oil)
1	360	8.27	1	7.7	7.3	1.7	0.13	8.64
2	380	8.27	1	7.5	7.0	2.2	0.14	8.03
3	360	9.65	1	9.0	8.5	1.5	0.15	11.34
4	380	9.65	1	8.8	8.3	2.0	0.17	10.48
5	360	8.27	2	7.7	7.3	3.4	0.13	8.70
6	380	8.27	2	7.5	7.1	4.7	0.15	7.75
7	360	9.65	2	9.0	8.6	3.1	0.15	11.23
8	380	9.65	2	8.8	8.3	4.2	0.17	10.28
9	353	8.96	1.5	8.4	8.0	2.3	0.14	9.99
10	387	8.96	1.5	8.1	7.6	3.7	0.16	8.07
11	370	7.80	1.5	7.1	6.7	3.1	0.13	7.51
12	370	10.12	1.5	9.4	8.9	2.6	0.17	11.80
13	370	8.96	0.7	8.3	7.8	1.3	0.15	9.55
14	370	8.96	2.3	8.3	7.8	4.4	0.15	9.17
15	370	8.96	1.5	8.3	7.8	2.8	0.15	9.47

Table B. 4 Inlet and outlet hydrogen partial pressure, feed vaporization, and dissolved hydrogen during hydrotreating of PHTHGO

Run	T (^{0}C)	P (MPa)	LHSV (h^{-1})	H_2 inlet pp (MPa)	H_2 outlet pp (MPa)	Feed vaporization at outlet (g/h)	Dissolved H_2 at outlet (mol fraction)	Dissolved H_2 at outlet (m^3H_2/m^3 oil)
1	360	8.27	1	8.1	8.1	0.5	0.14	8.95
2	380	8.27	1	8.1	8.1	0.7	0.15	9.37
3	360	9.65	1	9.5	9.5	0.5	0.16	10.89
4	380	9.65	1	9.5	9.4	0.6	0.18	11.30
5	360	8.27	2	8.1	8.1	1.0	0.14	8.95
6	380	8.27	2	8.1	8.1	1.4	0.15	9.36
7	360	9.65	2	9.5	9.5	0.8	0.16	10.89
8	380	9.65	2	9.5	9.4	1.3	0.18	11.27
9	353	8.96	1.5	8.8	8.8	0.7	0.15	10.01
10	387	8.96	1.5	8.8	8.7	1.1	0.17	10.16
11	370	7.80	1.5	7.7	7.6	0.9	0.14	8.72
12	370	10.12	1.5	10.0	9.9	0.8	0.18	11.66
13	370	8.96	0.7	8.8	8.8	0.4	0.16	9.76
14	370	8.96	2.3	8.8	8.8	1.3	0.16	9.72
15	370	8.96	1.5	8.8	8.8	0.8	0.16	9.75

Table B. 5 Mass balance calculations and data for VLGO

Experimental conditions			**GAS**				**LIQUID**					**MASS BALANCE**		
T(^{0}C)	P(MPa)	LHSV (h-1)	Gas outlet flowrate (mL/min)	H_2 concentration outlet (vol. %)	H_2 outlet mass flow rate (g/h)	H_2 inlet mass flow rate (gr/h)	Oil Inlet flowrate(gr/h)	H_2 inlet flowrate (gr/h)	Oil outlet flowrate (gr/h)	H_2 Concentration outlet (wt. %)	H_2 outlet flow rate (gr/h)	Left	Right	Mass balance closure (%)
360	1200	1	40.06	94.74	0.20	0.27	4.50	0.47	4.25	13.03	0.55	0.74	0.76	98.08
380	1200	1	37.56	93.97	0.19	0.27	4.50	0.47	4.55	11.52	0.52	0.74	0.71	96.03
380	1400	1	39.13	94.14	0.20	0.27	4.50	0.47	4.65	12.04	0.56	0.74	0.76	97.94
360	1400	1	38.15	94.76	0.19	0.27	4.50	0.47	4.50	11.44	0.51	0.74	0.71	95.18
360	1400	2	79.00	95.04	0.40	0.54	9.00	0.95	8.89	12.35	1.10	1.49	1.50	99.06
380	1400	2	78.33	94.44	0.40	0.54	9.00	0.95	8.90	11.68	1.04	1.49	1.44	96.76
380	1200	2	80.07	94.57	0.41	0.54	9.00	0.95	8.85	11.84	1.05	1.49	1.46	97.97
360	1200	2	78.18	94.89	0.40	0.54	9.00	0.95	8.85	11.82	1.05	1.49	1.44	97.08

Table B. 6 Mass balance calculations and data for HLGO

Experimental conditions			**GAS**				**LIQUID**					**MASS BALANCE**		
T(^{0}C)	P(MPa)	LHSV (h-1)	Gas outlet flowrate (mL/min)	H_2 concentration outlet (vol. %)	H_2 outlet mass flow rate (g/h)	H_2 inlet mass flow rate (gr/h)	Oil Inlet flowrate(gr/h)	H_2 inlet flowrate (gr/h)	Oil outlet flowrate (gr/h)	H_2 Concentration outlet (wt. %)	H_2 outlet flow rate (gr/h)	Left	Right	Mass balance closure (%)
360	1200	1	45.07	98.85	0.24	0.27	4.35	0.56	4.29	13.57	0.58	0.83	0.82	99.50
380	1200	1	44.33	98.63	0.24	0.27	4.35	0.56	4.28	13.60	0.58	0.83	0.82	98.94
380	1400	1	43.47	98.74	0.23	0.27	4.35	0.56	4.26	14.55	0.62	0.83	0.85	97.10
360	1400	1	42.44	98.51	0.23	0.27	4.35	0.56	4.26	14.18	0.60	0.83	0.83	99.65
360	1400	2	91.91	98.84	0.49	0.54	8.70	1.11	8.45	13.54	1.14	1.65	1.64	98.84
380	1400	2	91.13	98.68	0.49	0.54	8.70	1.11	8.48	13.48	1.14	1.65	1.63	98.48
380	1200	2	91.35	98.98	0.49	0.54	8.70	1.11	8.50	13.57	1.15	1.65	1.64	99.27
360	1200	2	88.90	98.92	0.49	0.54	8.70	1.11	8.47	13.42	1.14	1.65	1.62	98.10